Since 1959

Matter in Confinement:

Clusters, Microdroplets and Clean Water

Matter in confinement for sustainability

Thalappil Pradeep

Institute Professor, IIT Madras

https://pradeepresearch.org/

pradeep@iitm.ac.in

Co-founder

InnoNano Research Pvt. Ltd.
InnoDI Water Technologies Pvt. Ltd.
VayuJAL Technologies Pvt. Ltd.
Aqueasy Innovations Pvt. Ltd.
Hydromaterials Pvt. Ltd.
EyeNetAqua Pvt. Ltd.
Deepspectrum Analytics Pvt. Ltd.

Professor-in-charge

International Centre for Clean Water

MURTI Colloquium, GITAM University, December 19, 2024

Contents

Quantum Dots – Seeds of Nanoscience

KUNGL. VETENSKAPS-AKADEMIEN

THE ROYAL SWEDISH ACADEMY OF SCIENCES

THE NOBEL PRIZE IN CHEMISTRY 2023

The Royal Swedish Academy of Sciences has decided to award the Nobel Prize in Chemistry 2023 to

©Johan Jarnestad/The Royal Swedish Academy of Sciences

Moungi G. Bawendi
Massachusetts Institute of Technology (MIT), Cambridge, MA, USA

Louis E. Brus
Columbia University, New York, NY, USA

Alexei I. Ekimov
Nanocrystals Technology Inc., New York, NY, USA

'for the discovery and synthesis of quantum dots'

THE NOBEL PRIZE IN CHEMISTRY 2023

How small are these 'Quantum Dots'?

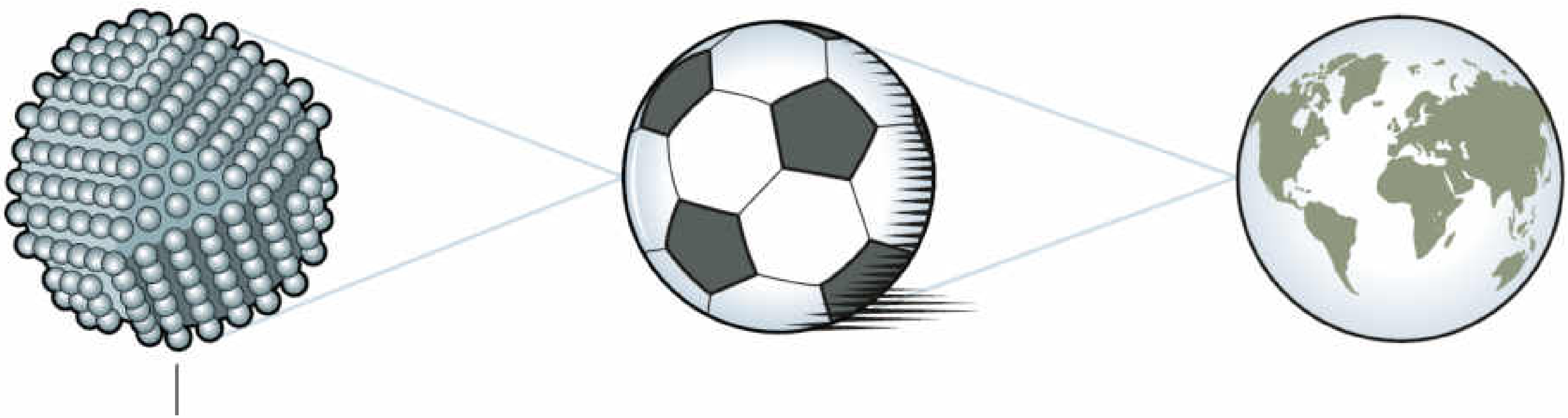

A quantum dot is a crystal that often consists of just a few thousand atoms. In terms of size, it has the same relationship to a football as a football has to the size of the Earth.

Remembering pioneers

THE NOBEL PRIZE IN CHEMISTRY 2023

Michael Faraday – Divided metals

Lord Kelvin – Melting depends on size?

Richard Feynman, Nobel Prize 1965 –
Plenty of room at the bottom

Robert F. Curl, Harold W. Kroto and Richard E. Smalley Nobel Prize 1996

Andre Geim and Konstantin Novoselov, Graphene, Nobel Prize 2010

Jean Pierre Sauvage, J. Fraser Stoddart, and Bernard Lucas Feringa, Molecular machines Nobel Prize 2016

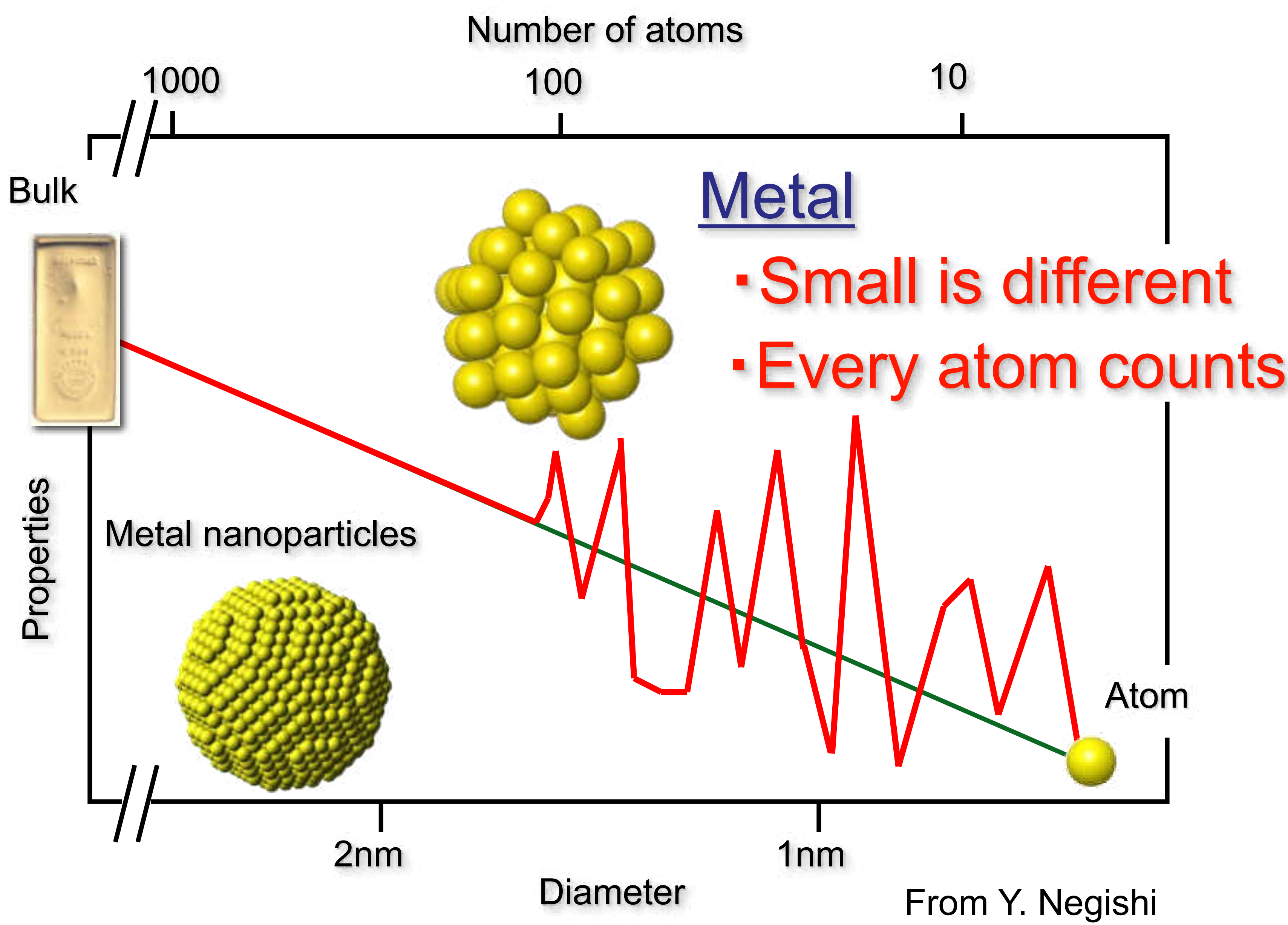

Number of atoms
1000
100
10
Bulk
Metal
·Small is different
·Every atom counts
Properties
Metal nanoparticles
Atom
2nm
1nm
Diameter
From Y. Negishi

New molecules and materials

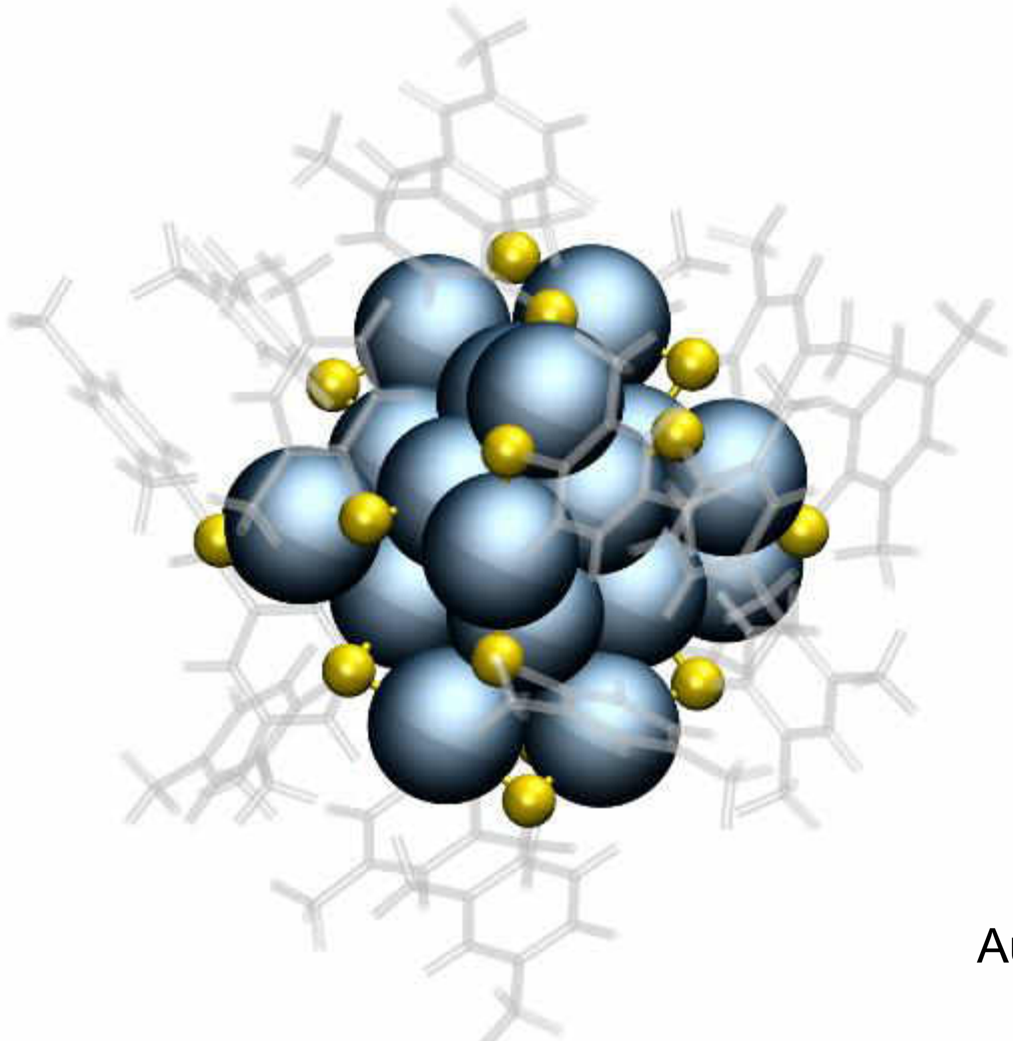

Au_{25}, Ag_{25}, Ag_{29}

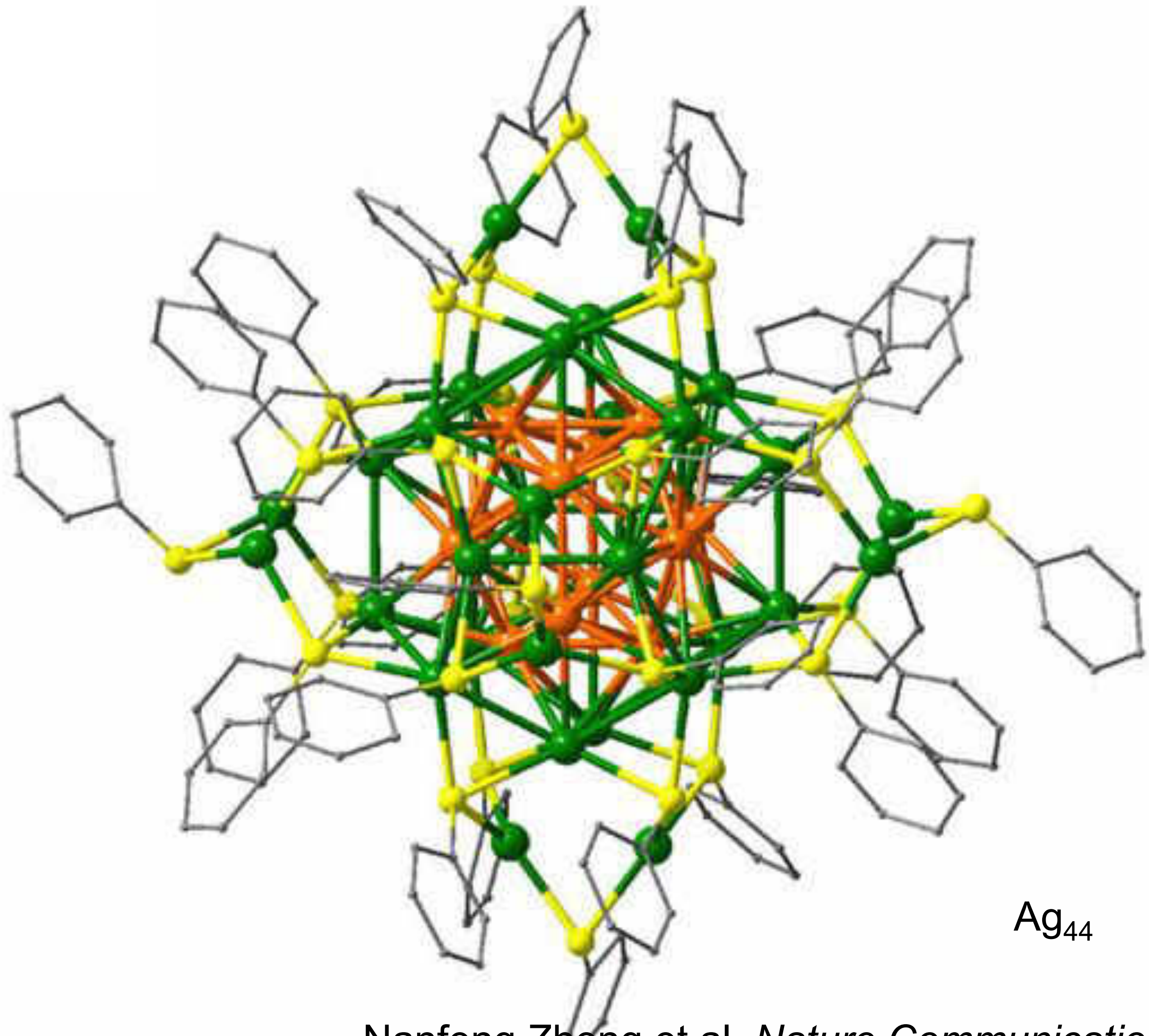

Ag_{44}

Nanfeng Zheng et al. *Nature Communications*, 2013

Terry Bigioni et al. *Nature* 2013

Atomically precise metal clusters as materials

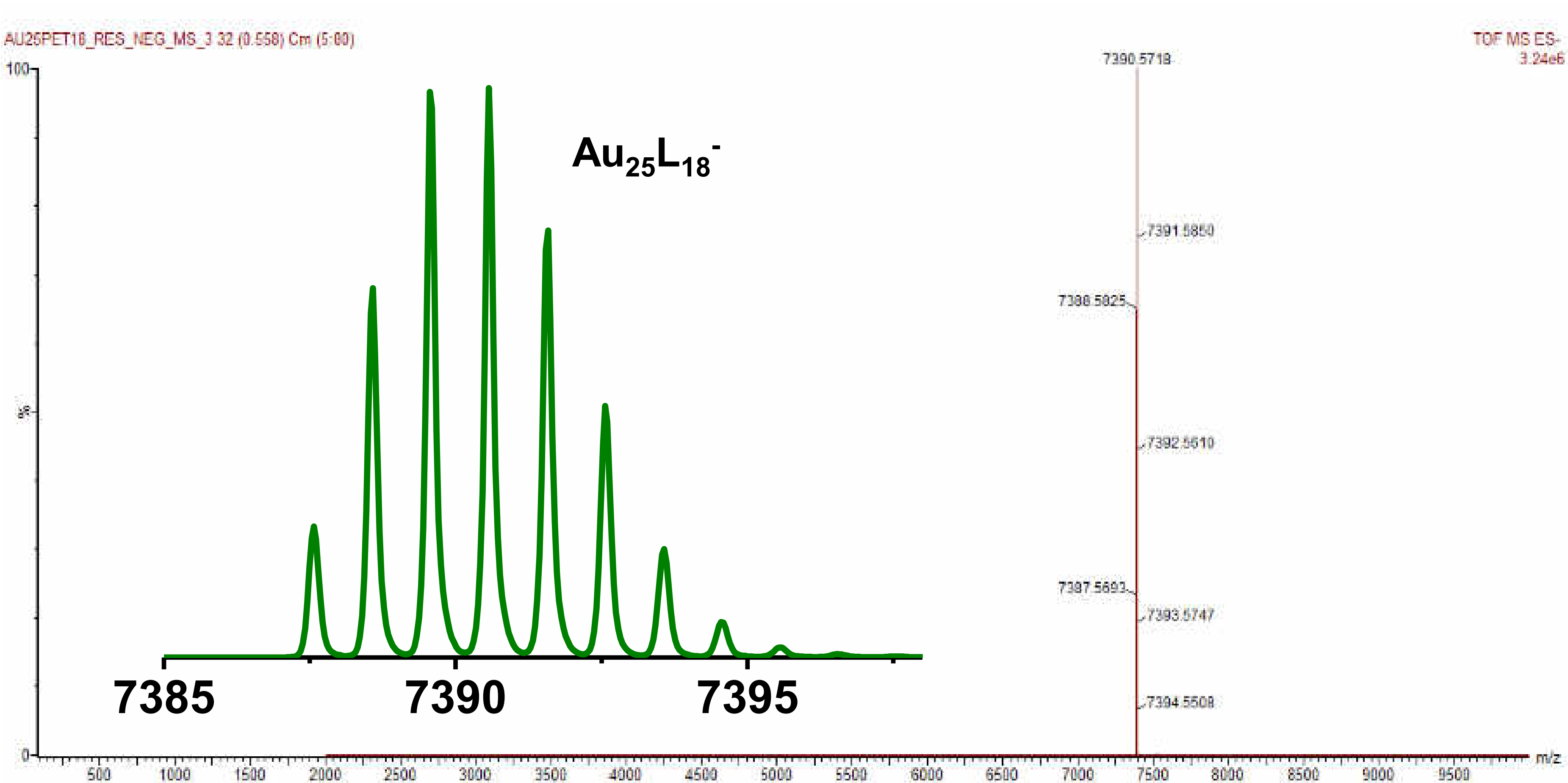

T. Pradeep et. al. *Acc. Chem. Res.* 2018; 2019.

They make high quality crystals

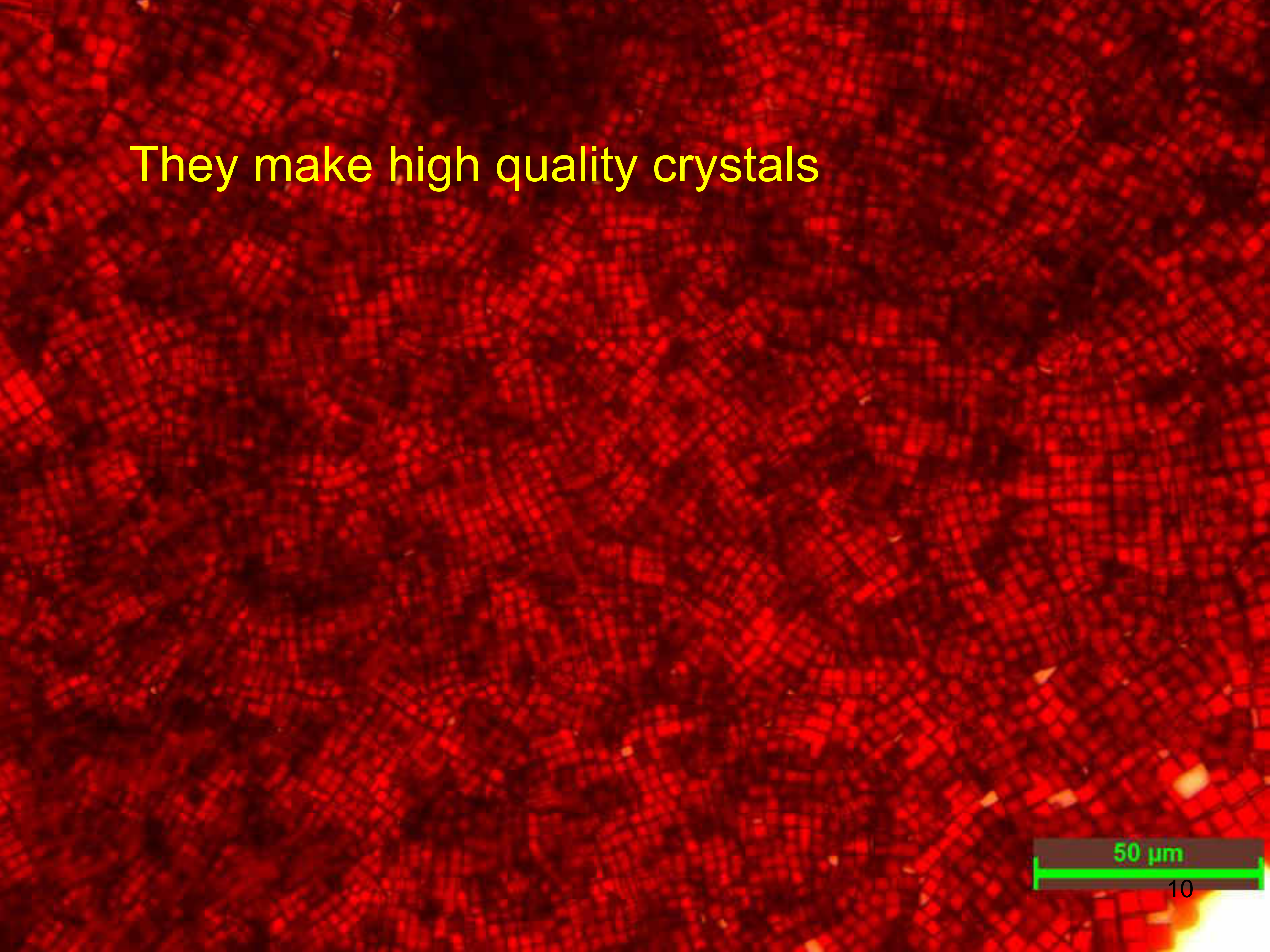

Molecular structure

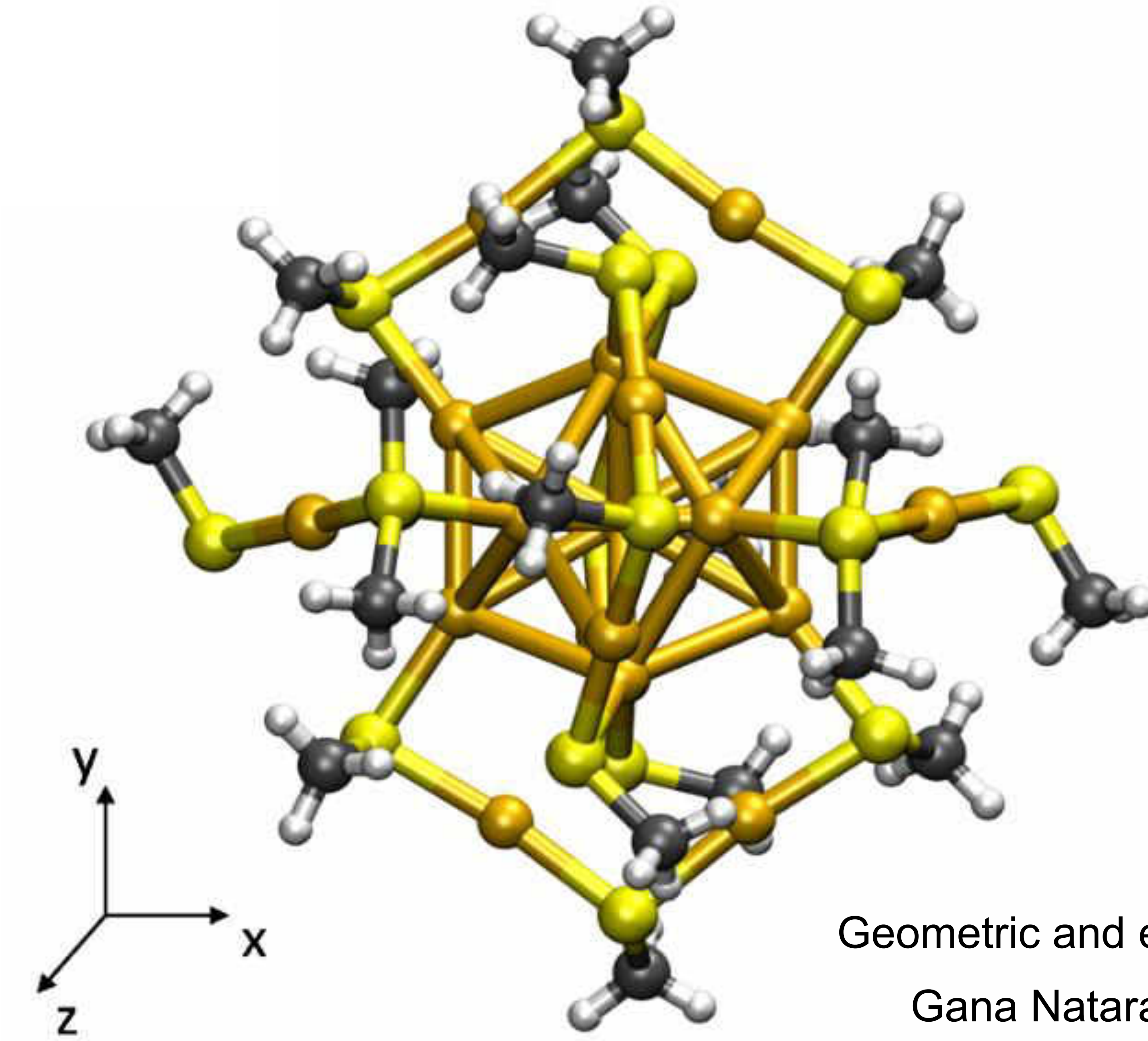


Synthetic methods

J. CHEM. SOC., CHEM. COMMUN., 1994 801

Synthesis of Thiol-derivatised Gold Nanoparticles in a Two-phase Liquid–Liquid System

Mathias Brust, Merryl Walker, Donald Bethell, David J. Schiffrin and Robin Whyman
Department of Chemistry, The University of Liverpool, PO Box 147, Liverpool, UK L69 3BX

Using two-phase (water–toluene) reduction of $AuCl_4^-$ by sodium borohydride in the presence of an alkanethiol, solutions of 1–3 nm gold particles bearing a surface coating of thiol have been prepared and characterised; this novel material can be handled as a simple chemical compound.

Colloidal solutions of metals have been known for a long time[1] and a large variety of preparative techniques is now available.[2,3] Depending on the preparative conditions, the particles have a tendency to agglomerate slowly, eventually lose their disperse character and flocculate. The removal of the solvent generally leads to the complete loss of the ability to reform a colloidal solution. Preparation of colloidal metals in a two-phase system was introduced by Faraday,[4] who reduced an aqueous gold salt with phosphorus in carbon disulfide and obtained a ruby coloured aqueous solution of dispersed gold particles. Combining this two phase approach with the more recent techniques of ion extraction and monolayer self-assembly with alkane thiols,[5] a one-step method for the preparation of an unusual new metallic material of derivatised nanometre-sized gold particles is described.

The strategy followed consisted in growing the metallic clusters with the simultaneous attachment of self-assembled thiol monolayers on the growing nuclei. In order to allow the surface reaction to take place during metal nucleation and growth, the particles were grown in a two-phase system. Two-phase redox reactions can be carried out by an appropriate choice of redox reagents present in the adjoining phases.[6] In the present case, $AuCl_4^-$ was transferred from aqueous solution to toluene using tetraoctylammonium bromide as the phase-transfer reagent and reduced with aqueous sodium borohydride in the presence of dodecanethiol ($C_{12}H_{25}SH$). On addition of the reducing agent, the organic phase changes colour from orange to deep brown within a few seconds. The overall reaction is summarized by eqns. (1) and (2), where the

$$AuCl_4^-(aq) + N(C_8H_{17})_4^+(C_6H_5Me) \rightarrow N(C_8H_{17})_4^+AuCl_4^-(C_6H_5Me) \quad (1)$$

$$mAuCl_4^-(C_6H_5Me) + nC_{12}H_{25}SH(C_6H_5Me) + 3me^- \rightarrow 4mCl^-(aq) + (Au_m)(C_{12}H_{25}SH)_n(C_6H_5Me) \quad (2)$$

source of electrons is BH_4^-. The conditions of the reaction determine the ratio of thiol to gold, i.e. the ratio n/m. The preparation technique was as follows. An aqueous solution of hydrogen tetrachloroaurate (30 ml, 30 mmol dm^{-3}) was mixed with a solution of tetraoctylammonium bromide in toluene (80 ml, 50 mmol dm^{-3}). The two phase mixture was vigorously stirred until all the tetrachloroaurate was transferred into

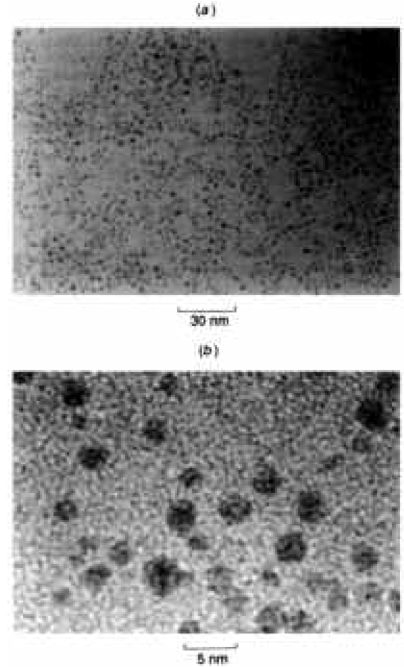

Fig. 1 TEM pictures of the thiol derivatised gold nanoparticles at (a) low and (b) high magnification

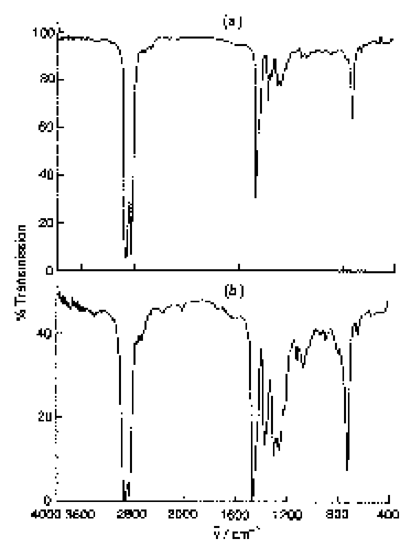

Fig. 2 IR spectra of (a) dodecanethiol and (b) nanoparticles prepared in the present work. The particles were deposited on an NaCl disc by evaporation of a drop of a toluene solution.

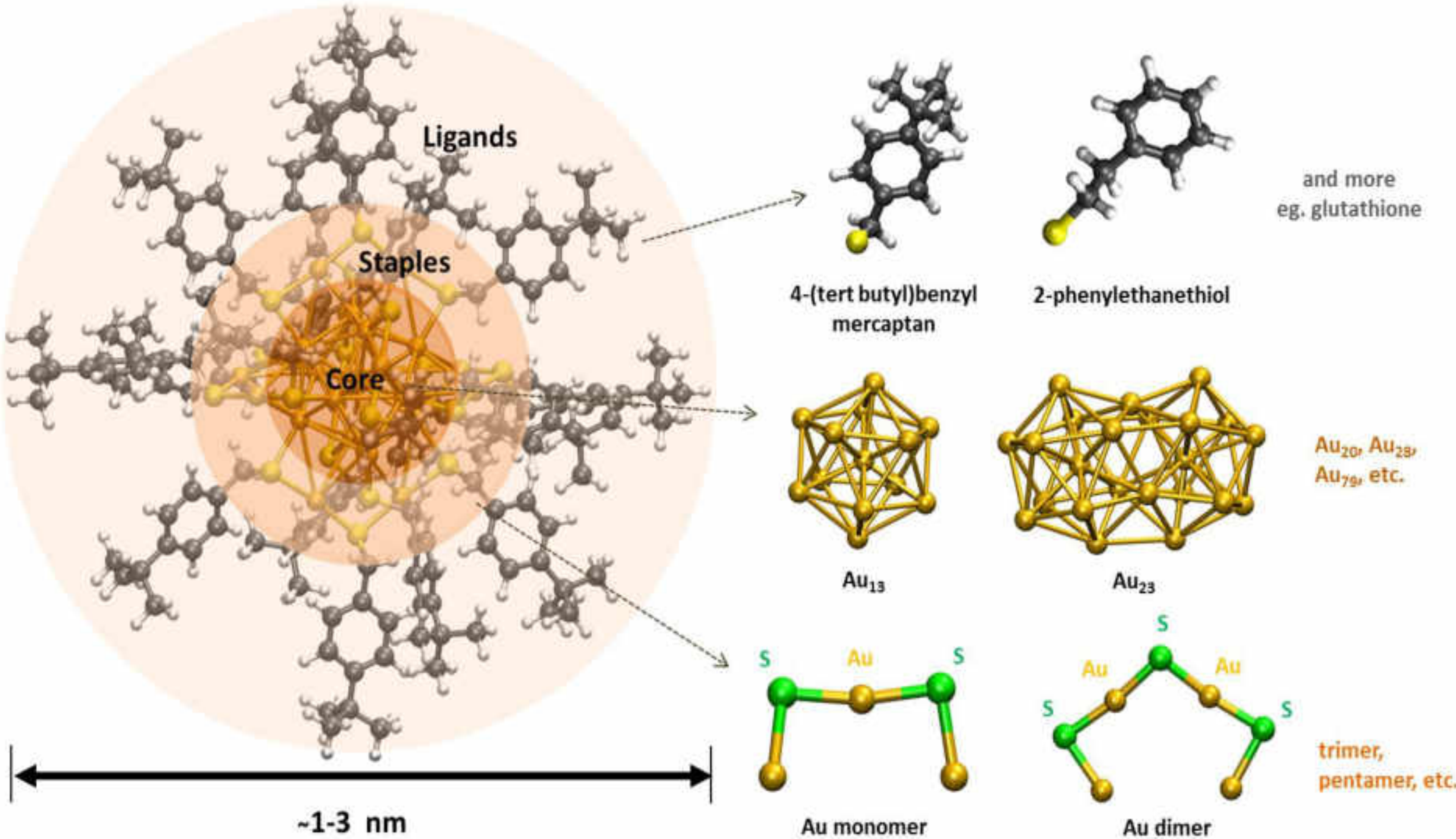

Ligands
Staples
Core
~1-3 nm
and more
eg. glutathione
4-(tert butyl)benzyl
mercaptan
2-phenylethanethiol
Au_{13}
Au_{23}
Au_{20}, Au_{28},
Au_{79}, etc.
S
Au
S
Au monomer
S
Au
Au
S
S
Au dimer
trimer,
pentamer, etc.

Evolution of noble metal clusters

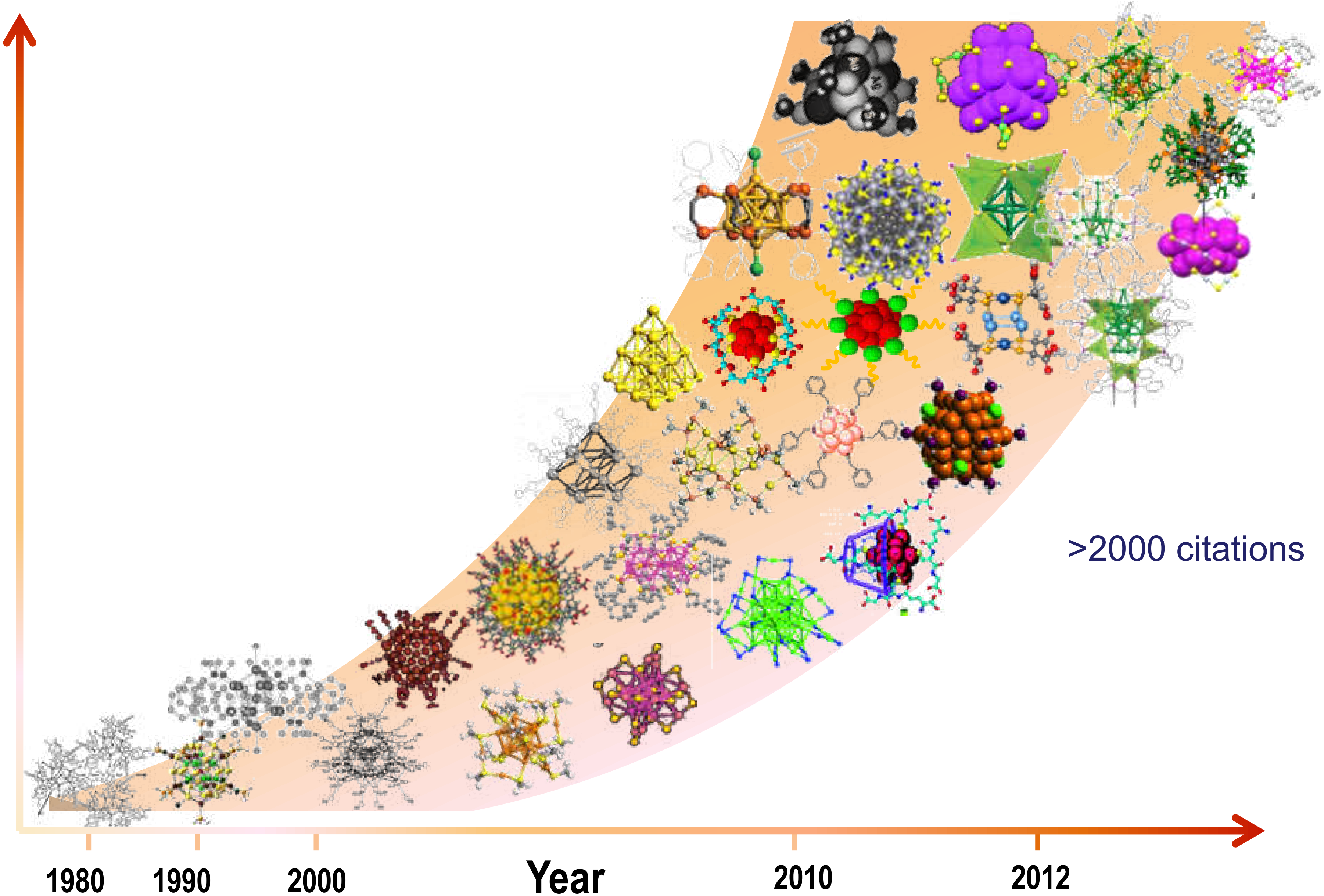

I. Chakraborty and T. Pradeep, *Chem. Rev.* 2017

Mass spectrometry and materials science

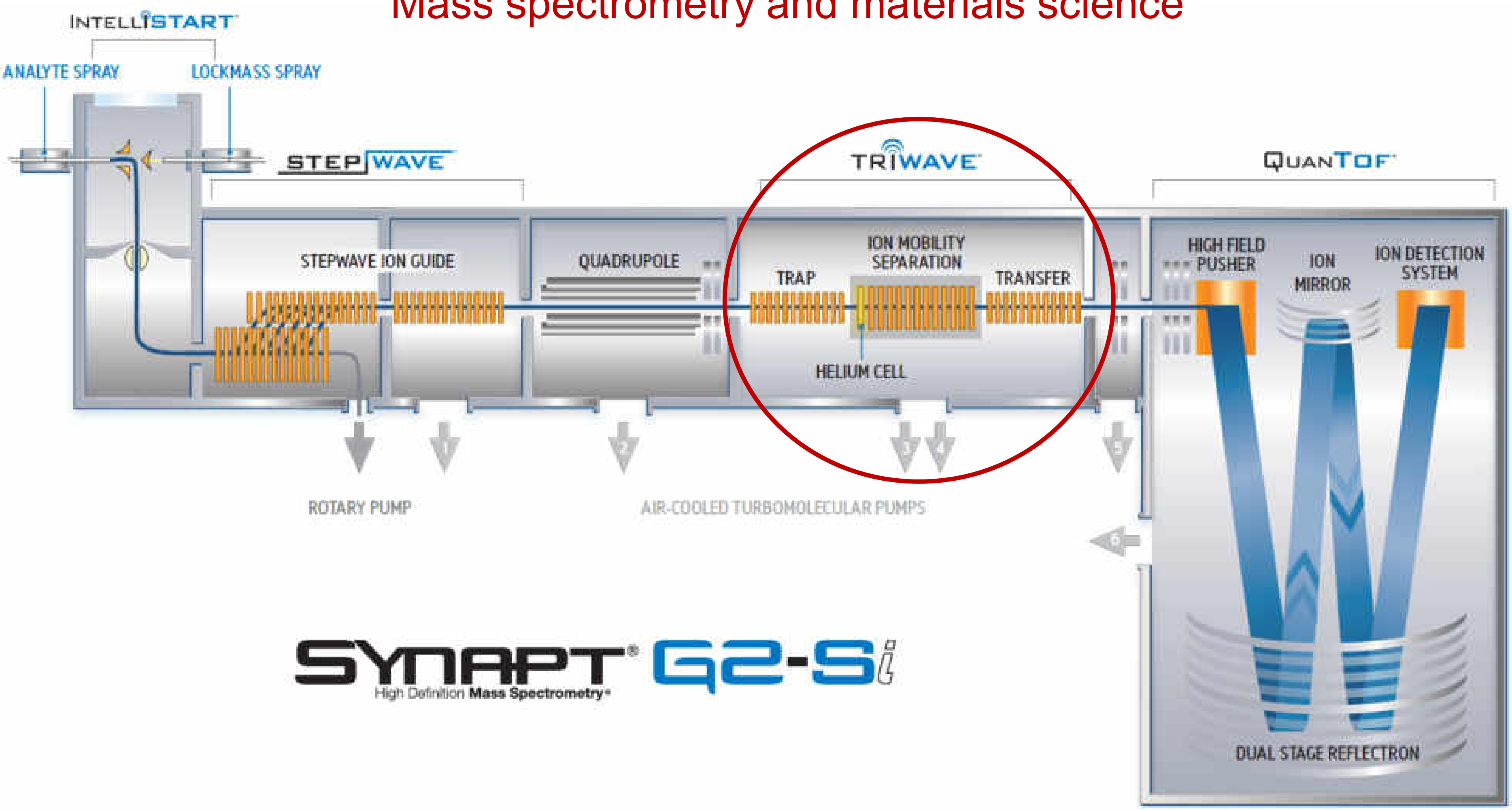

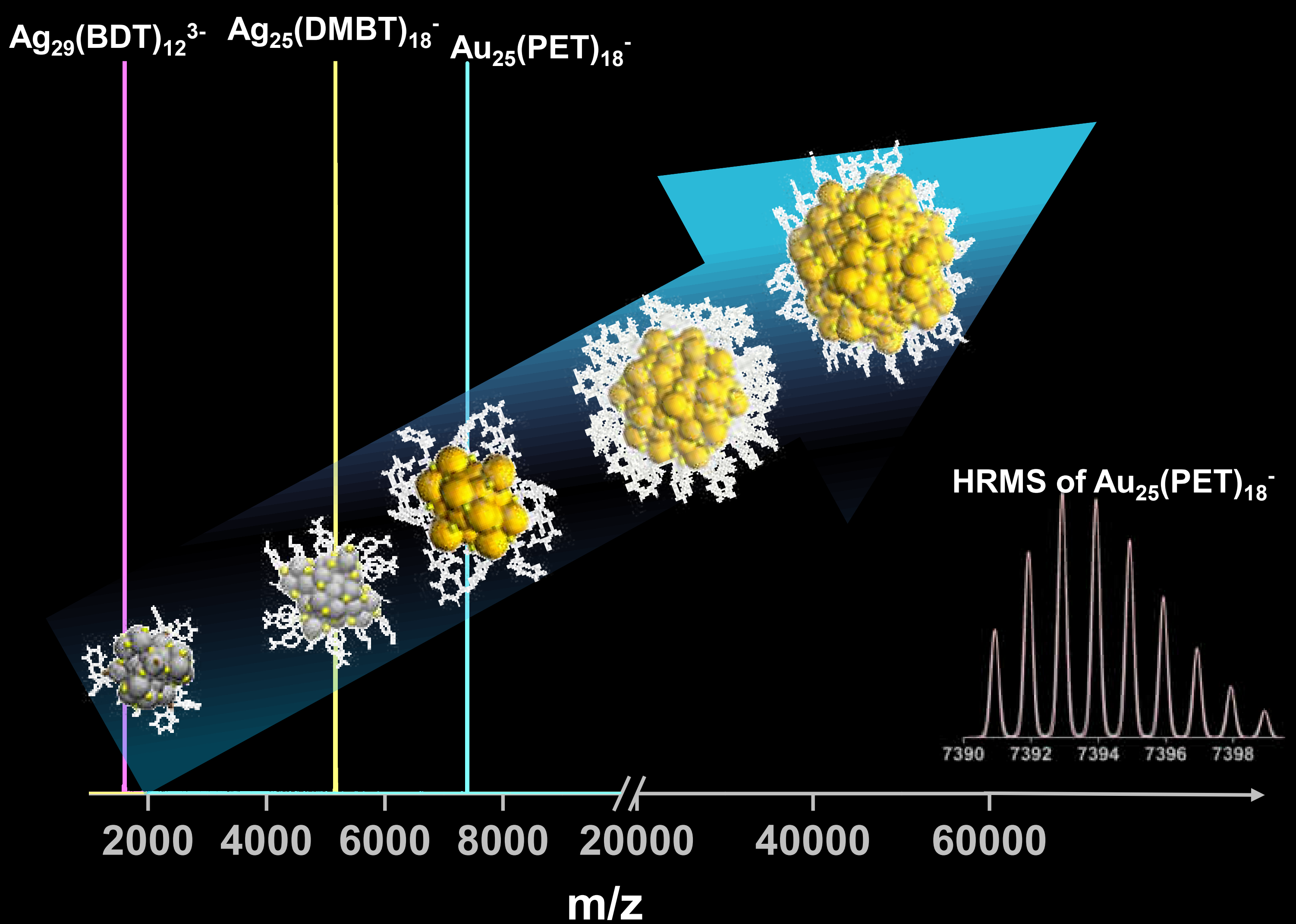

Ag29(BDT)12 3-
Ag25(DMBT)18 -
Au25(PET)18 -
HRMS of Au25(PET)18 -
7390
7392
7394
7396
7398
2000
4000
6000
8000
20000
40000
60000
m/z

Molecular materials

ACCOUNTS
of chemical research

Approaching Materials with Ato Cluster Assemblies

Papri Chakraborty, Abhijit Nag, Amrita Chakral
DST Unit of Nanoscience (DST UNS) and Thematic Unit Technology Madras, Chennai 600 036, India

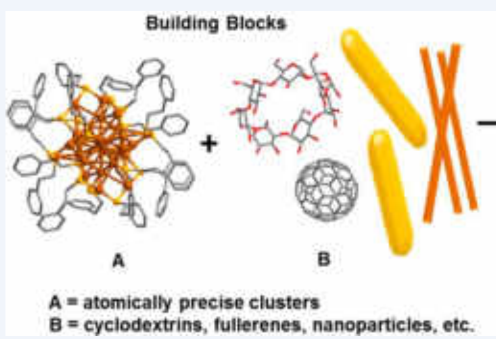

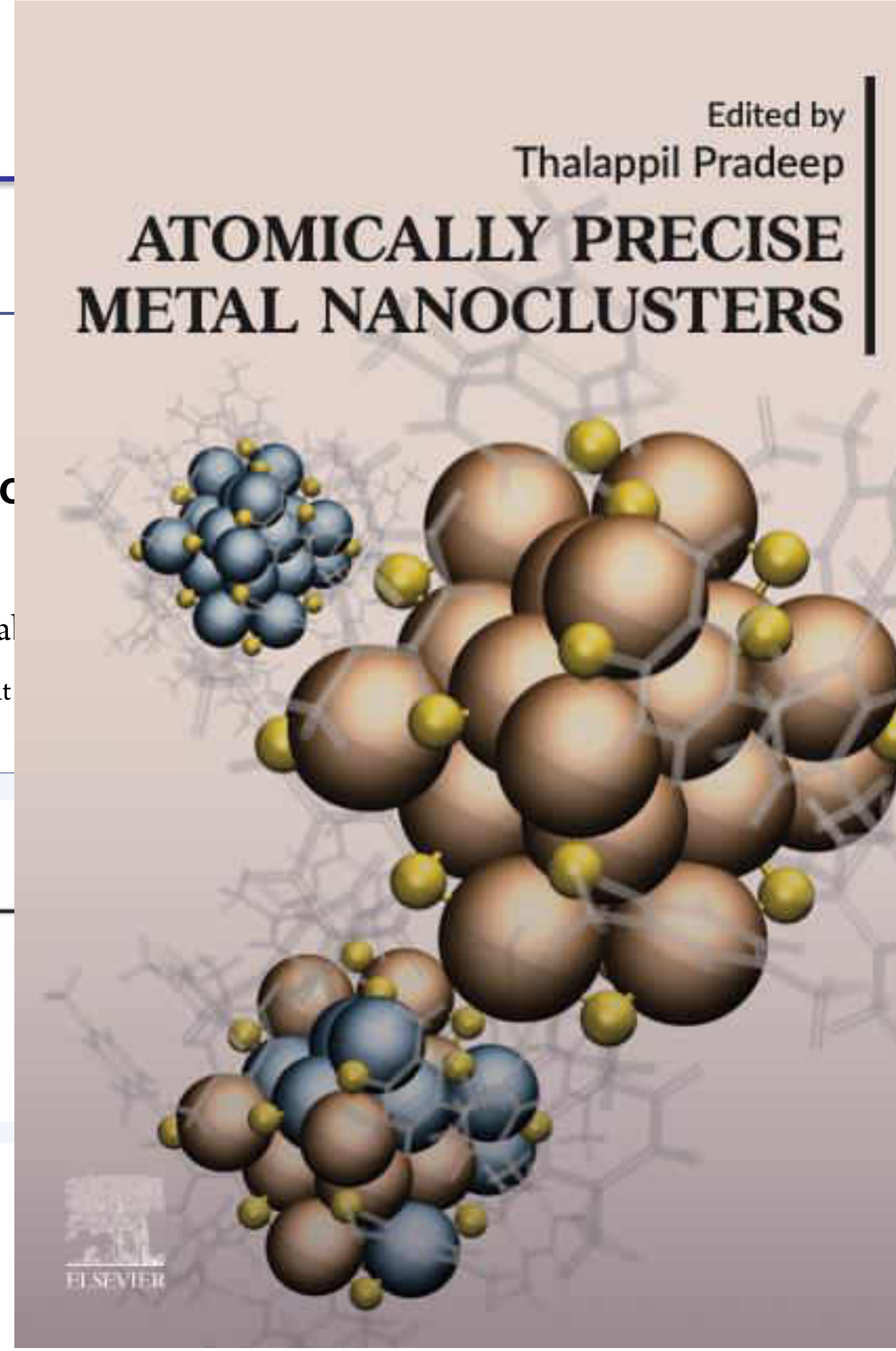

Molecules and their properties

Chemical formula	H_2O
Molecular weight	18.0148
Critical temperature	373.91°C
Critical pressure	22.05 MPa
Critical density	315.0 kg/m^3
Triple point temperature	0.01°C
Triple point pressure	615.066 Pa
Normal boiling point	100.0°C
Normal freezing point	0.0°C
Density of ice at normal melting point	918.0 kg/m^3
Maximum density, 3.98°C	999.973 kg/m^3
Viscosity, 25°C	0.889 mN s/m^2
Surface tension, 25°C	72 mN/m
Heat Capacity, 25°C	4.1796 kJ/kg.K
Enthalpy of vaporisation, 100°C	2,257.7 kJ/kg
Enthalpy of fusion, 0°C	333.8 kJ/kg
Velocity of sound, 0°C	1.403 km/s
Dielectric constant, 25°C	78.40
Electrical conductivity, 25°C	8 µS/m
Refractive index, 25°C	1.333
Liquid compressibility, 10°C	$480. \times 10^{-12}$ m^2/N
Coefficient of thermal expansion, 25°C	256.32×10^{-6} K^{-1}
Thermal Conductivity, 25°C	0.608 W/m.K

Molecular formula
Molecular weight
Molecular structure
Molecular absorption and emission
Molecular reactions
Molecular assembly
Molecular co-crystals
Ionization potential
Electron affinity

Phases - phase transitions
Physical properties
Electrical, magnetic
Mechanical properties
Electrochemical properties

Future?

Molecular reactions

Reactions on clusters

Reactions <u>between</u> clusters

Inter-cluster reactions

JACS
JOURNAL OF THE AMERICAN CHEMICAL SOCIETY
Article
pubs.acs.org/JACS

Intercluster Reactions between $Au_{25}(SR)_{18}$ and $Ag_{44}(SR)_{30}$

K. R. Krishnadas, Atanu Ghosh, Ananya Baksi, Indranath Chakraborty,[†] Ganapati Natarajan, and Thalappil Pradeep*

DST Unit of Nanoscience (DST UNS) and Thematic Unit of Excellence, Department of Chemistry, Indian Institute of Technology Madras, Chennai, 600 036, India

Supporting Information

$$A + B \rightarrow C + D$$

$Au_{25}(FTP)_{18} + Ag_{44}(FTP)_{30} \longrightarrow Au_{25-x}Ag_x(FTP)_{18}$

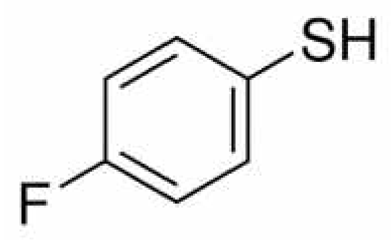

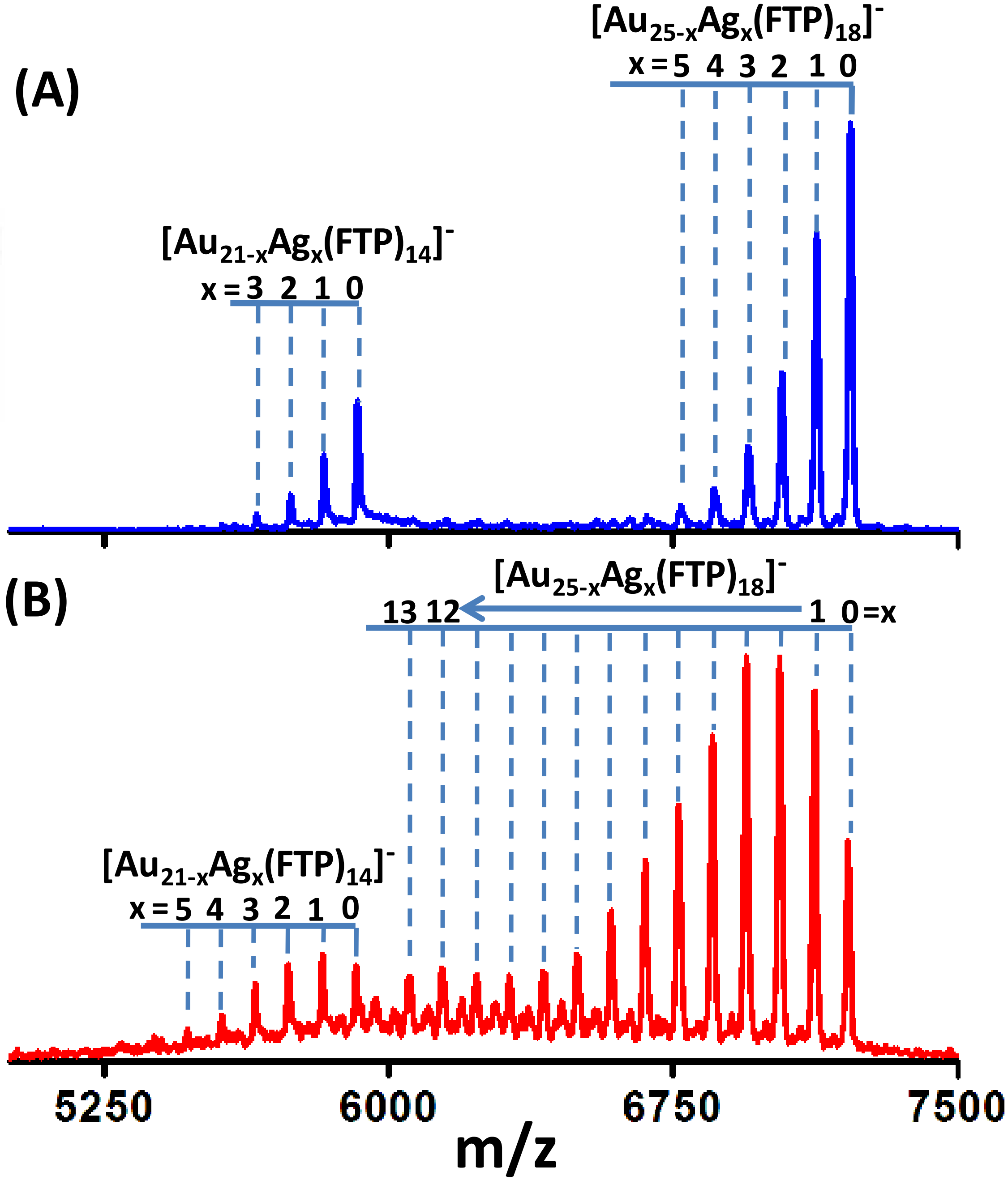

Ag_{25}-Au_{25} experiments

K. R. Krishnadas et al. *Nature Commun.* 2016

Reaction between $Au_{25}(PET)_{18}$ and $Ag_{25}(DMBT)_{18}$

DMBT

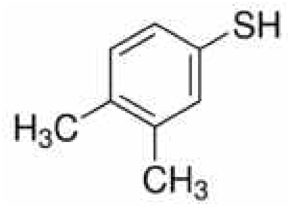

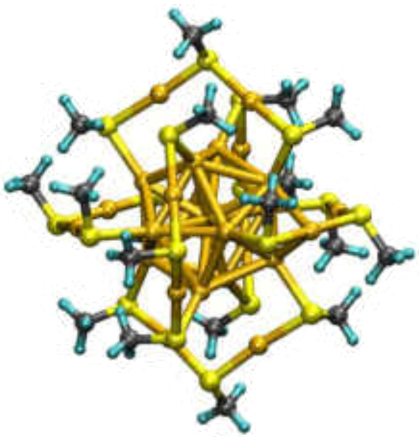

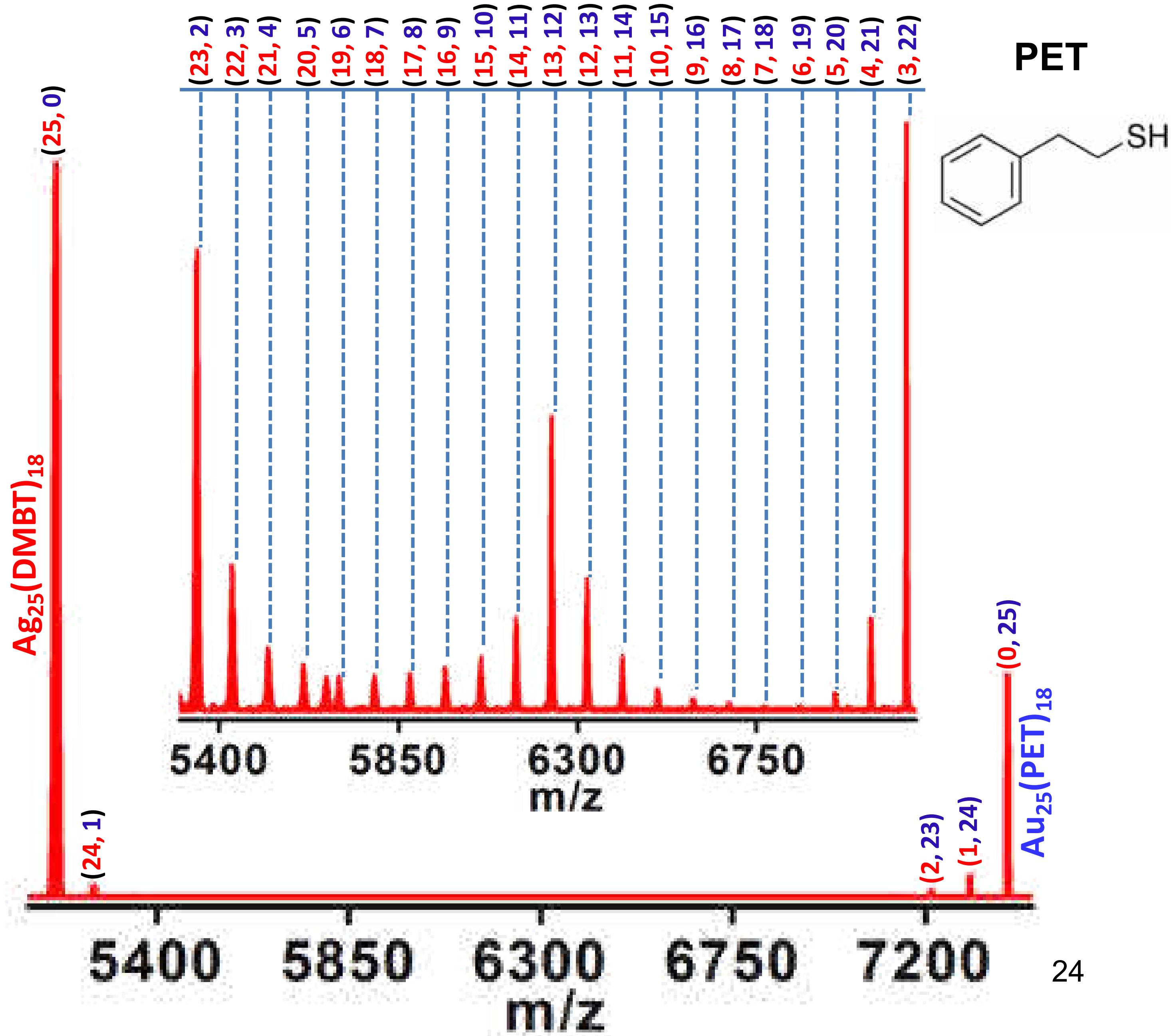

$[Ag_{25}(DMBT)_{18}+Au_{25}(PET)_{18}]^{2-}$

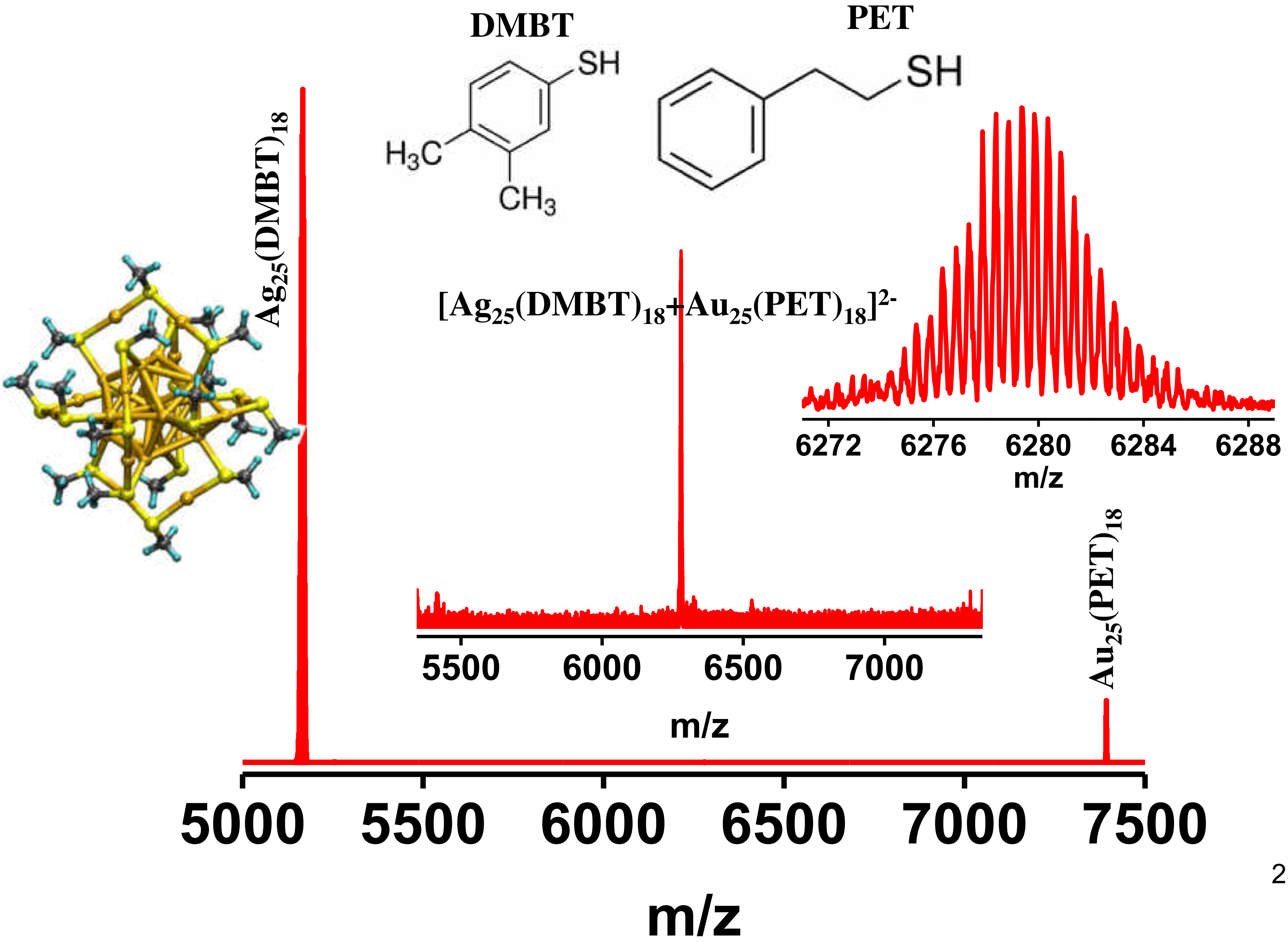

Evolution of alloy clusters from the dianionic adduct, $[Ag_{25}Au_{25}(DMBT)_{18}(PET)_{18}]^{2-}$

$Ag_{25}(DMBT)_{18}$:$Au_{25}(PET)_{18}$
0.3:1.0

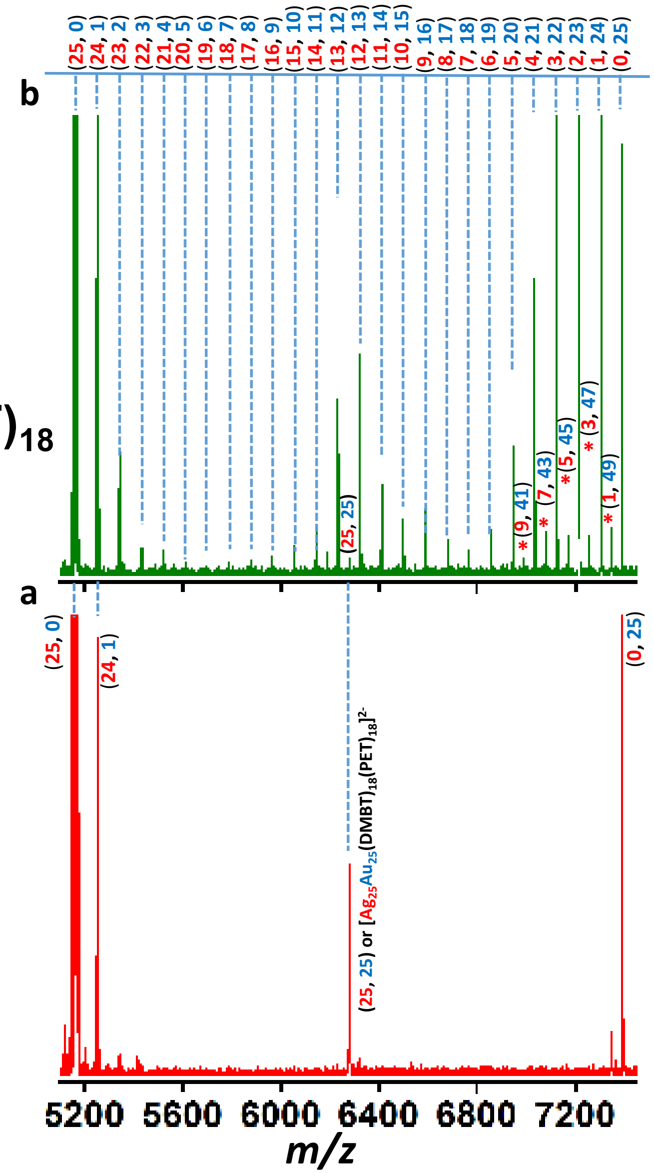

within 5 min

within 2 min

Optimized structure of $[Ag_{25}Au_{25}(DMBT)_{18}(PET)_{18}]^{2-}$

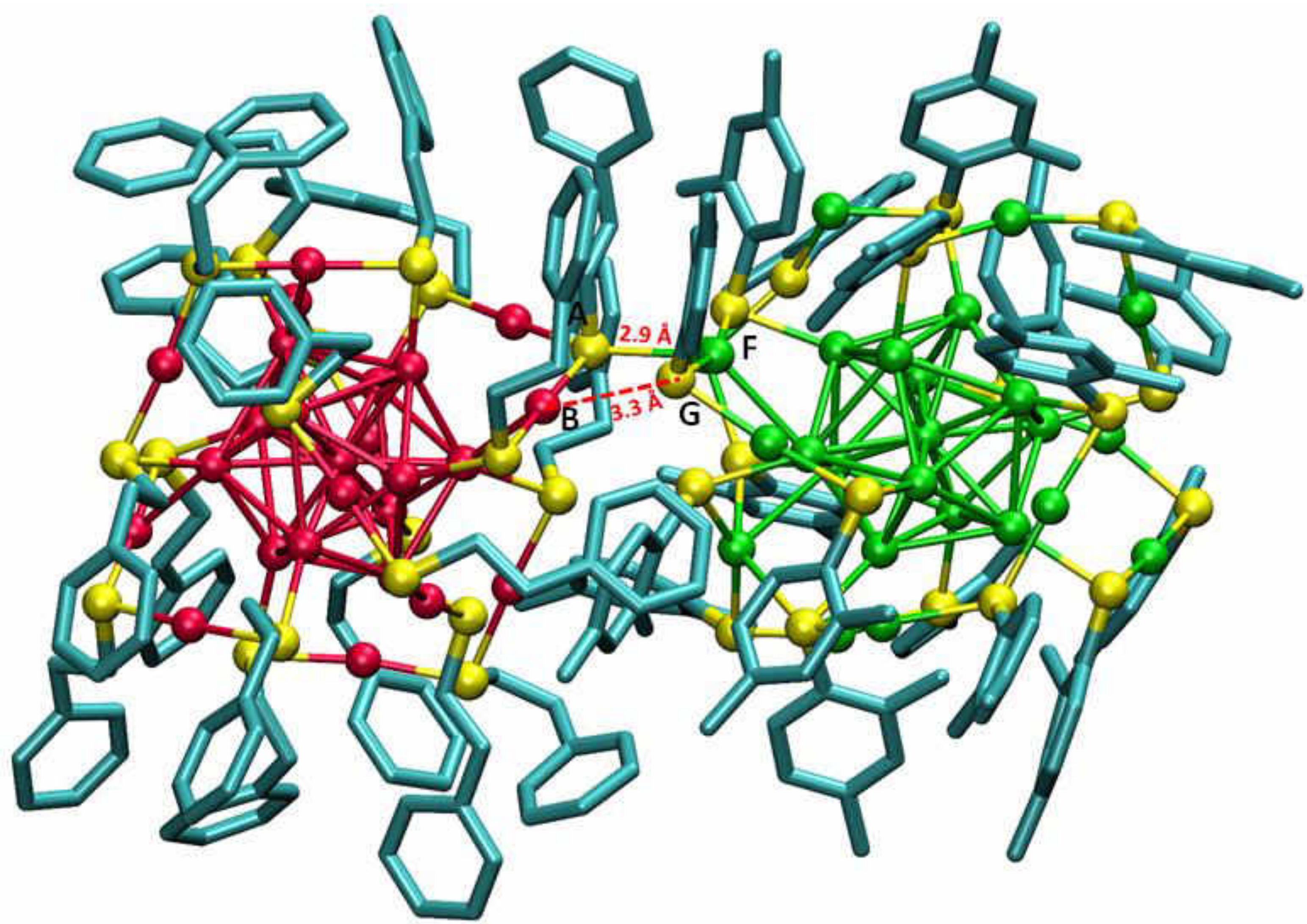

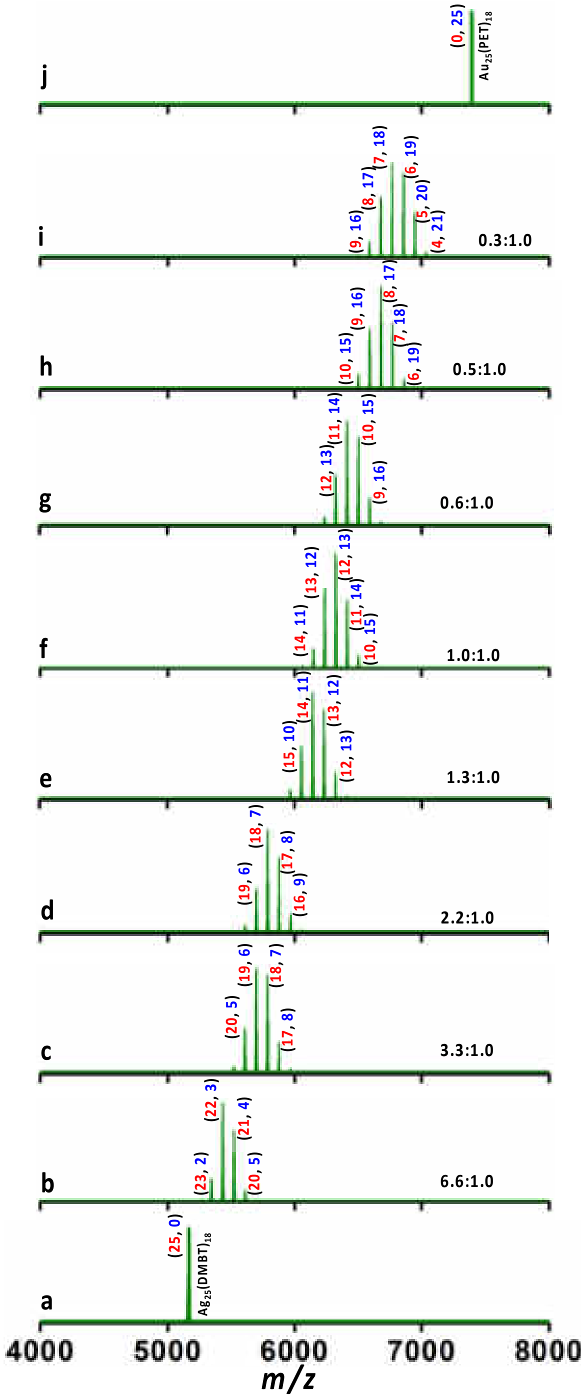

j
(0, 25)
Au25(PET)18
i
(9, 16)
(8, 17)
(7, 18)
(6, 19)
(5, 20)
(4, 21)
0.3:1.0
h
(10, 15)
(9, 16)
(8, 17)
(7, 18)
(6, 19)
0.5:1.0
g
(12, 13)
(11, 14)
(10, 15)
(9, 16)
0.6:1.0
f
(14, 11)
(13, 12)
(12, 13)
(11, 14)
(10, 15)
1.0:1.0
e
(15, 10)
(14, 11)
(13, 12)
(12, 13)
1.3:1.0
d
(19, 6)
(18, 7)
(17, 8)
(16, 9)
2.2:1.0
c
(20, 5)
(19, 6)
(18, 7)
(17, 8)
3.3:1.0
b
(23, 2)
(22, 3)
(21, 4)
(20, 5)
6.6:1.0
a
(25, 0)
Ag25(DMBT)18
4000
5000
6000
7000
8000
m/z

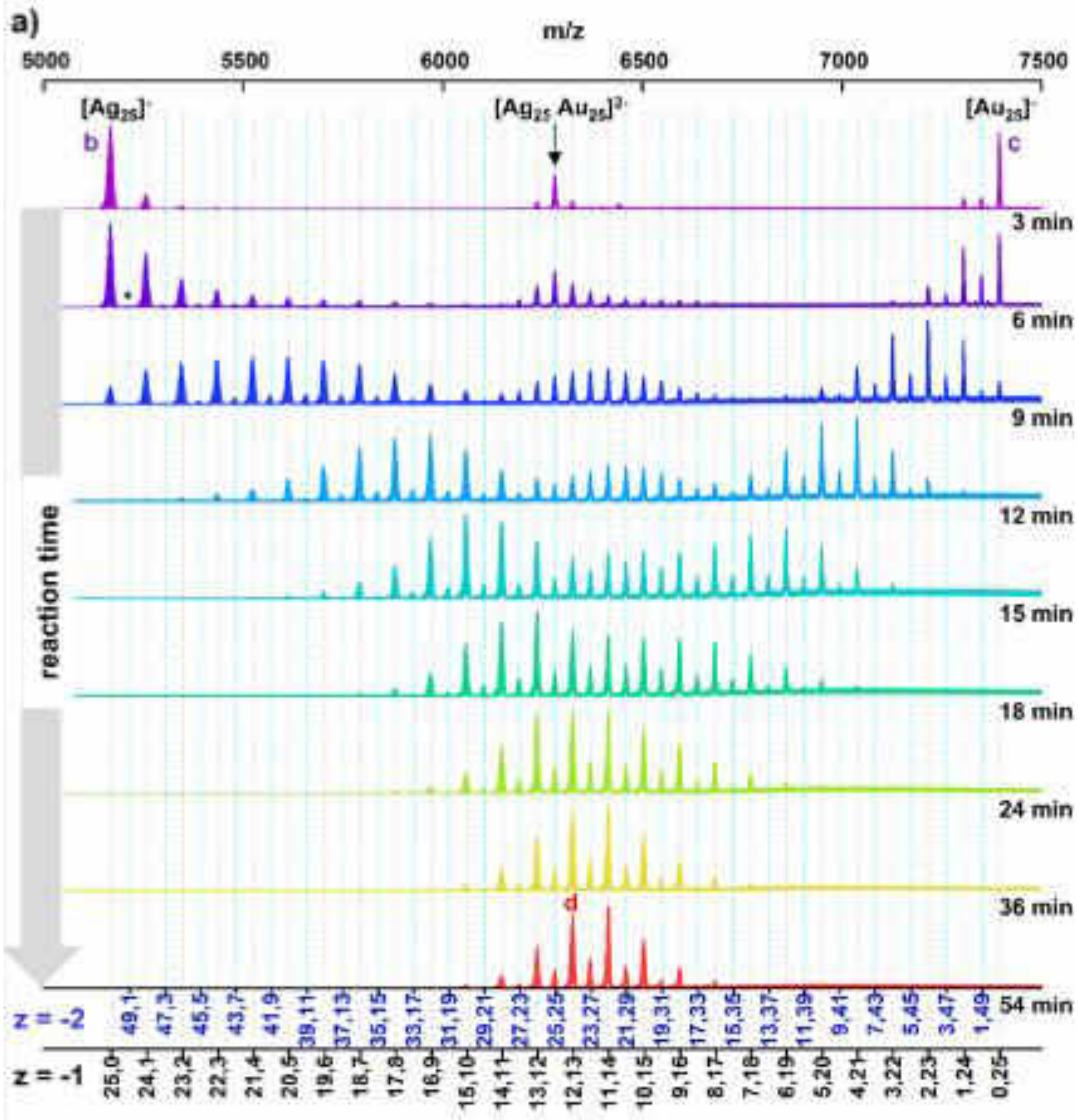

Manfred Kappes, KIT

M. Neumaier, A. Baksi, et. al., *JACS* 2021

Kinetics of the exchange (monitored on the Ag_{25} side)

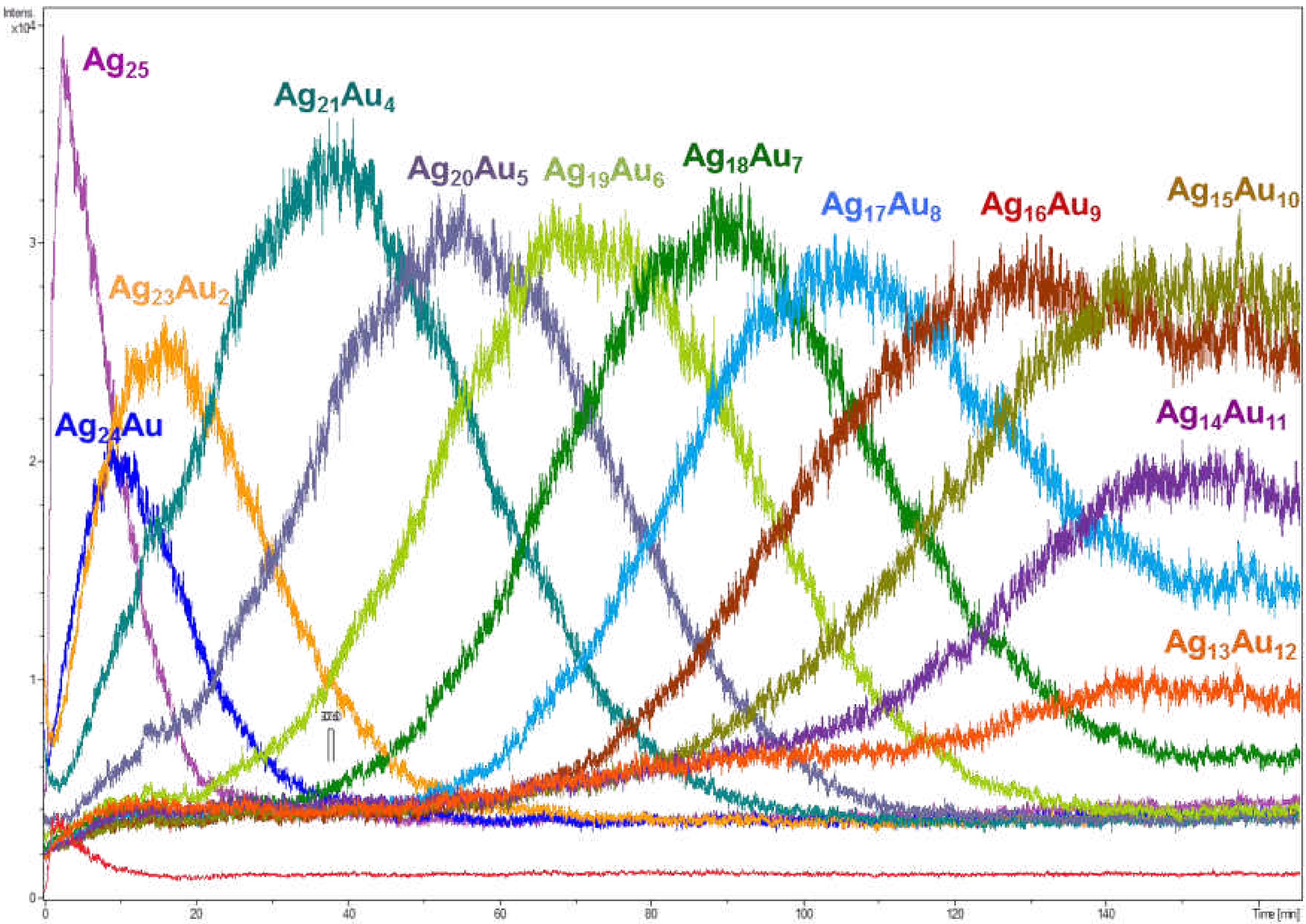

Isotopic exchange

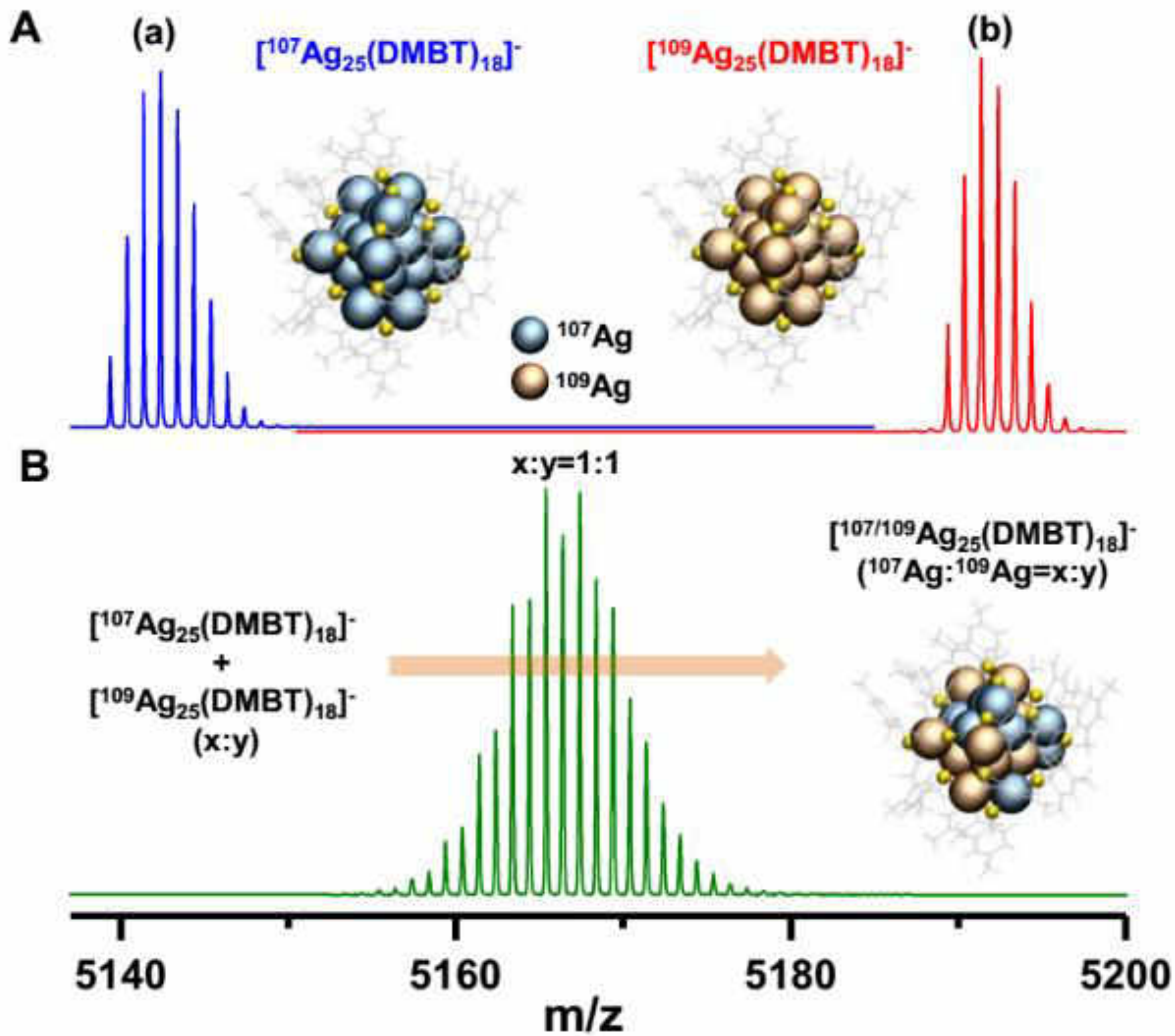

Papri Chakraborti, et. al. *Science Advances*, 2019.

New Clusters and new Ligands

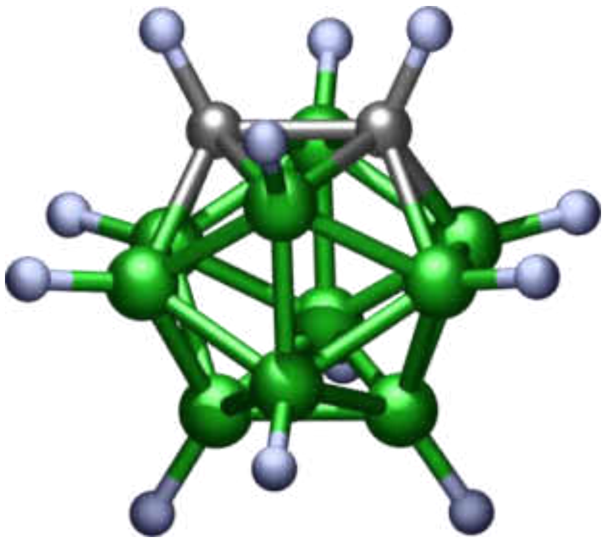

$1,2\text{-}C_2B_{10}H_{12}$

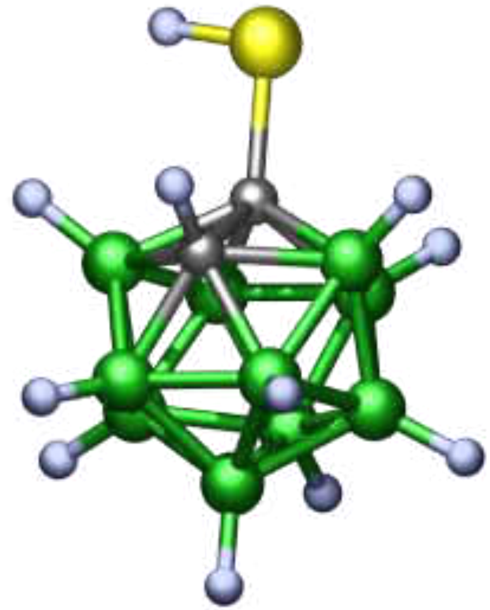

$1\text{-}HS\text{-}1,2\text{-}C_2B_{10}H_{11}$

Vivek Yadav, et. al., *Nature Communications*, 2024

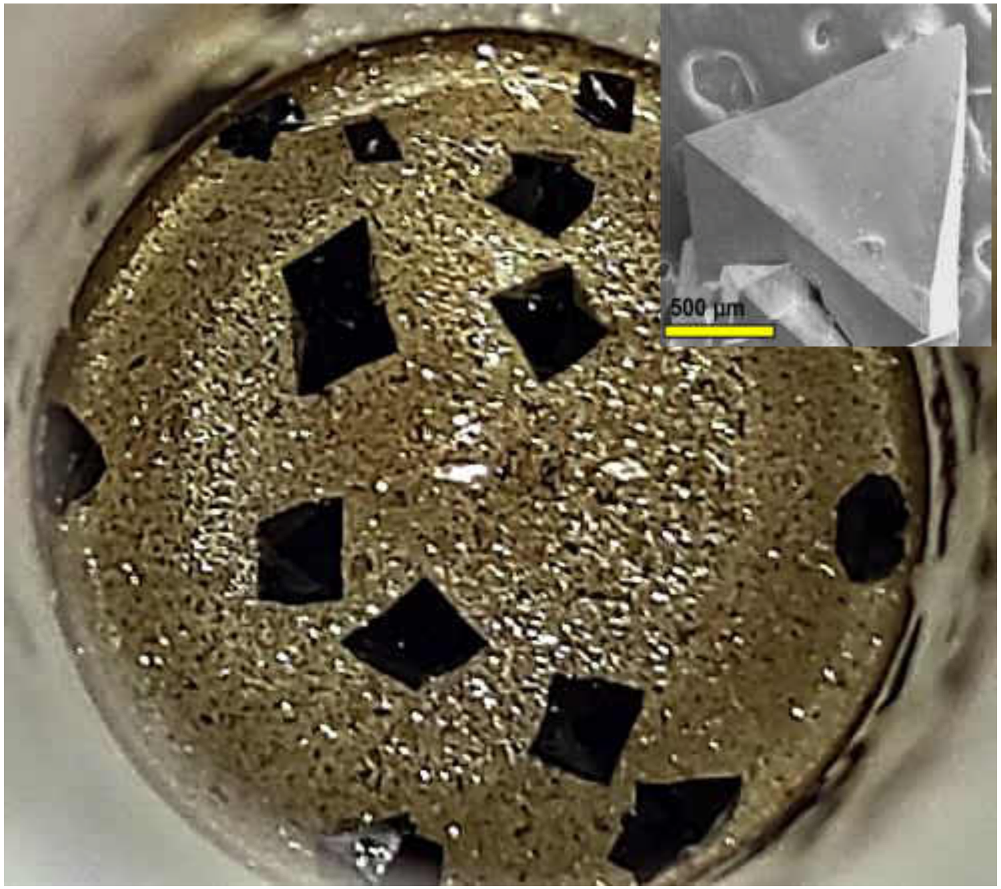
500 µm

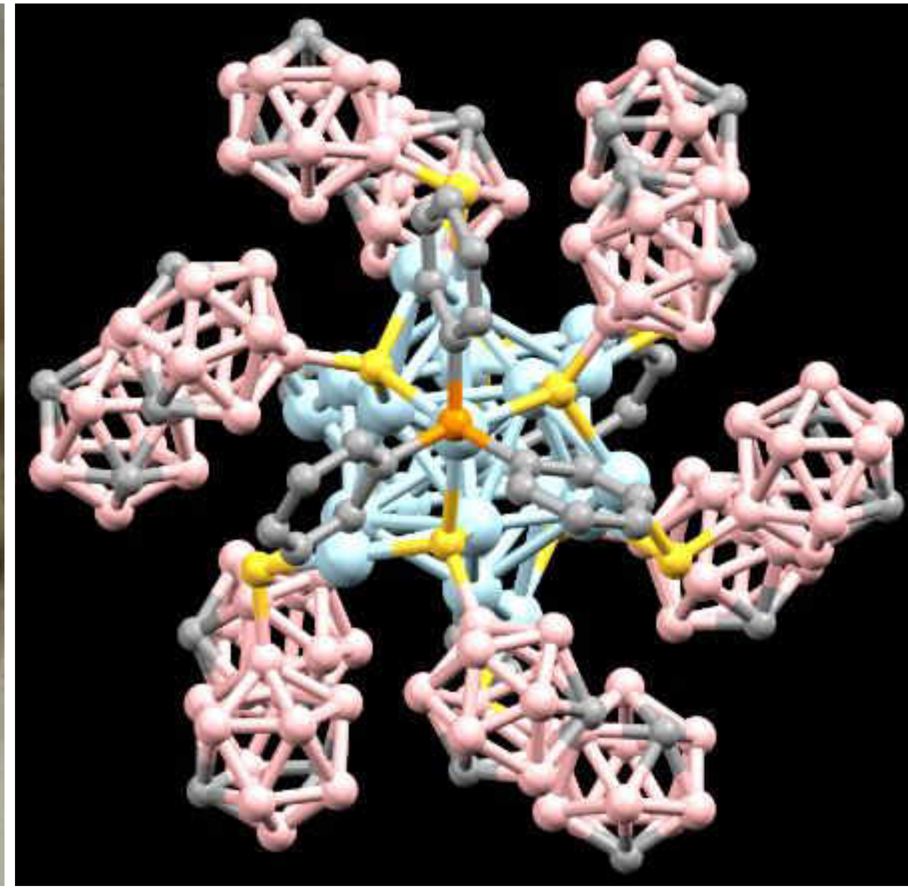

Structure of $[Ag_{17}(o_1\text{-}CBT)_{12}]^{3-}$

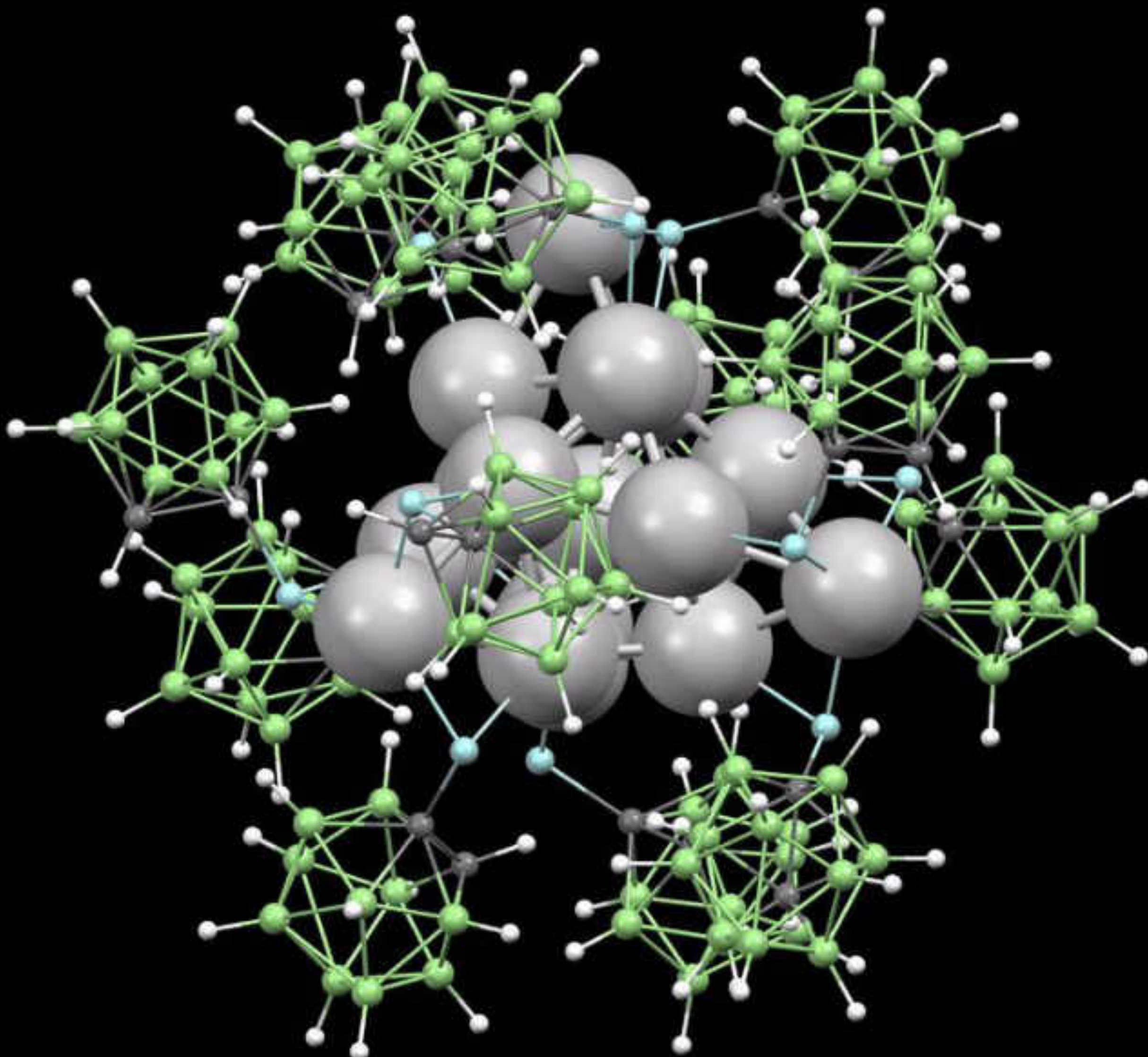

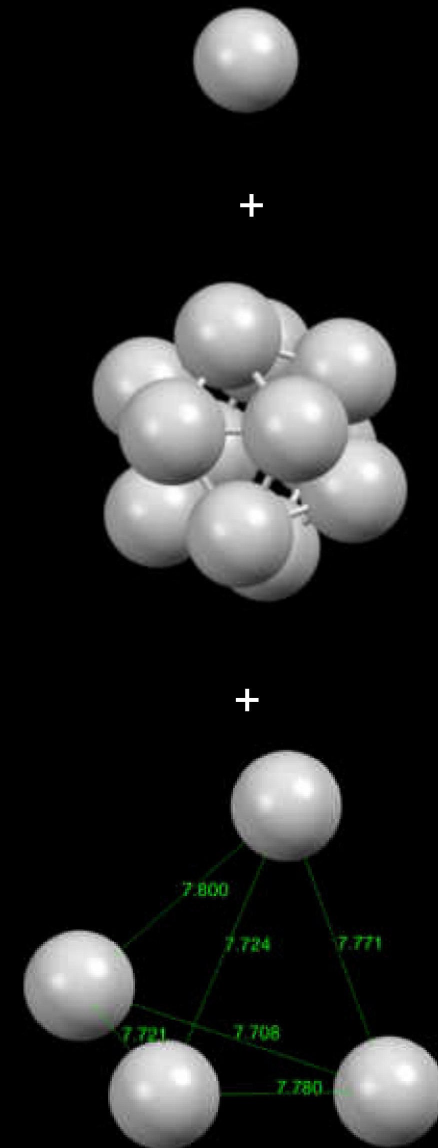

Vivek Yadav, et. al. *Nature Comunications* 2024

Structures of M_{17} Nanoclusters

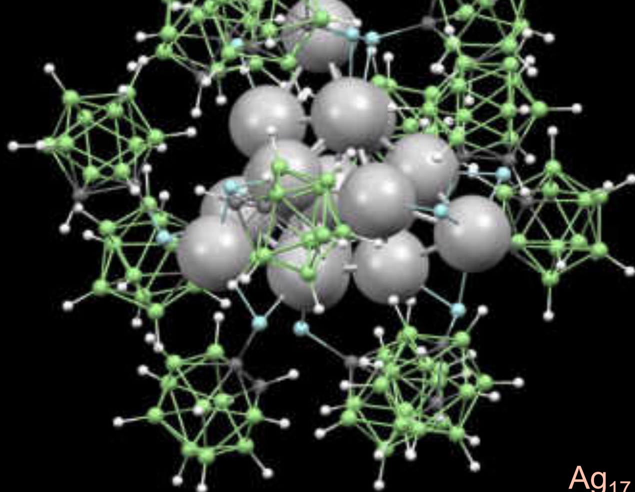

Ag_{17}

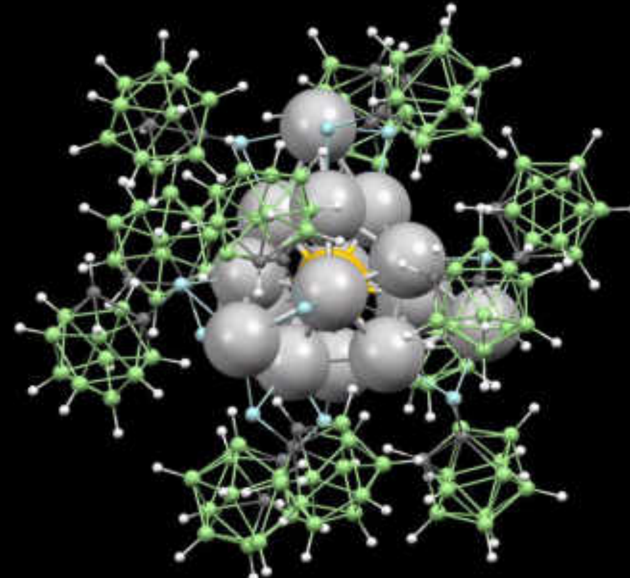

$Au@Ag_{16}$

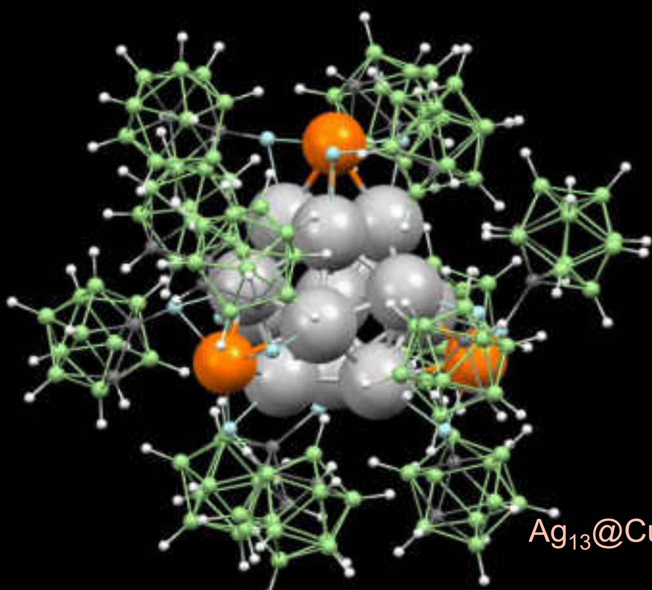

$Ag_{13}@Cu_4$

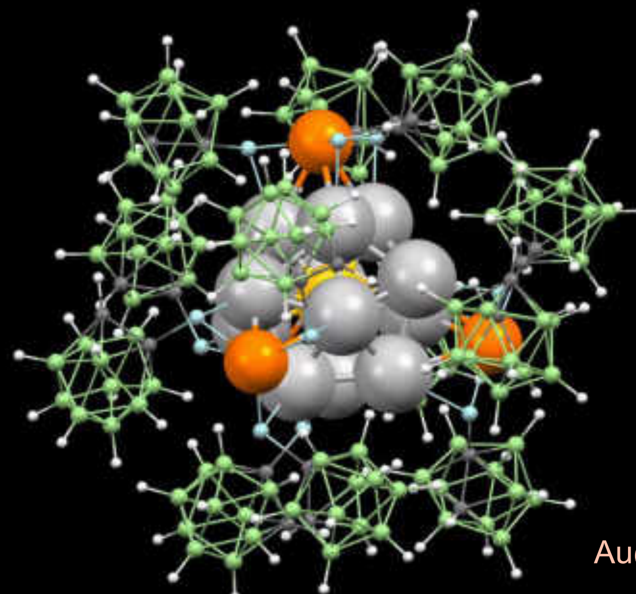

$Au@Ag_{12}@Cu_4$

Atomically precise nanocluster assemblies encapsulating plasmonic gold nanorods

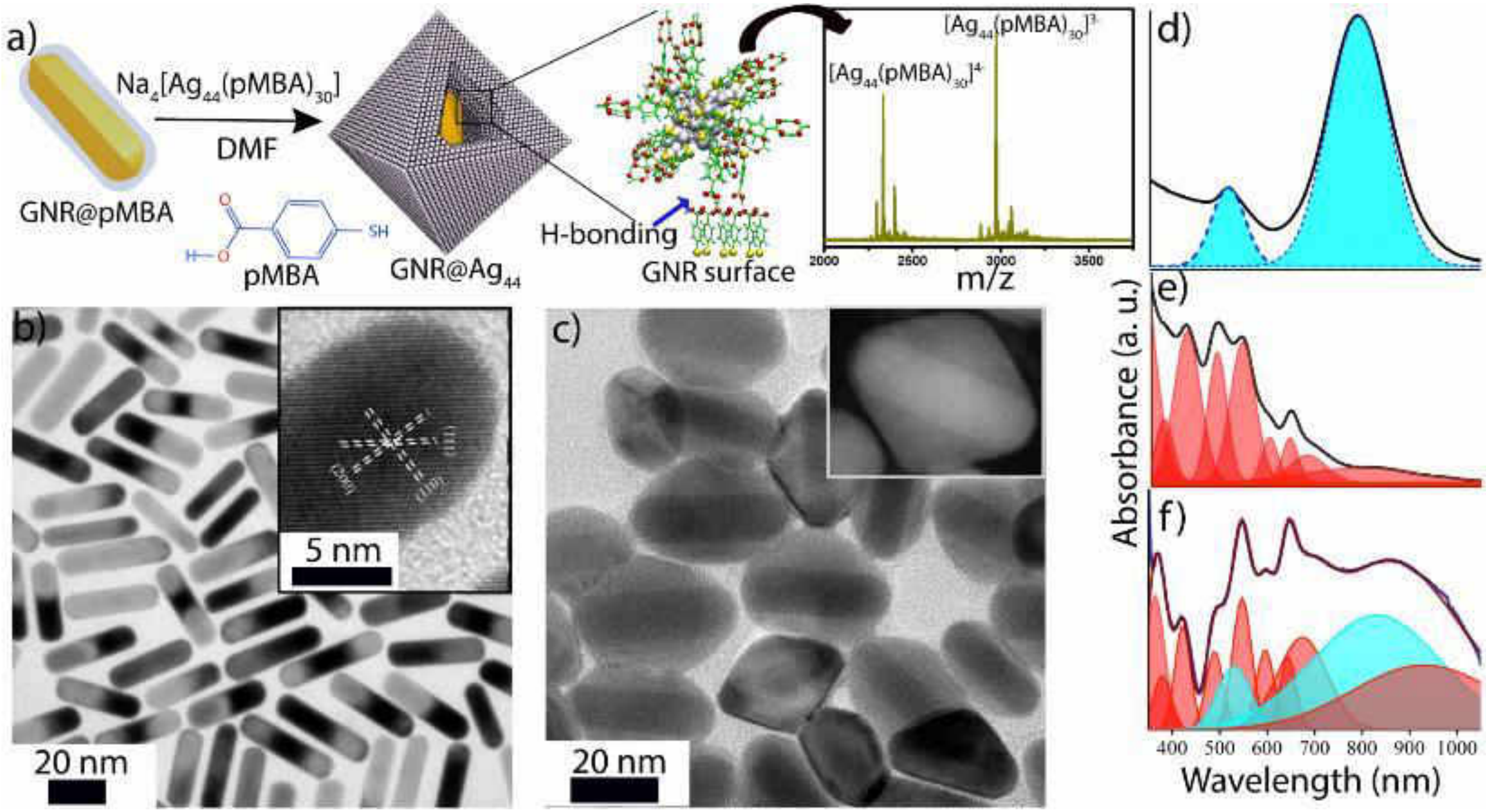

Chakraborty, A. et al., Angew. Chem. Int. Ed. **2018,** 57, 6522–6526.

Biopolymer-re nanocomposit water purifica

Mohan Udhaya Sankar[1], Saha
Kamalesh Chaudhari, and Tha

Unit of Nanoscience and Thematic Uni

Edited by Eric Hoek, University of Calif

Creation of affordable materials fo
water is one of the most promising
drinking water for all. Combinin
composites to scavenge toxic sp
other contaminants along with tl
affordable, all-inclusive drinking
without electricity. The critical p
synthesis of stable materials tha
uously in the presence of comp
drinking water that deposit and
surfaces. Here we show that suc
be synthesized in a simple and effe
out the use of electrical power. T
sand-like properties, such as highe
forms. These materials have beer
water purifier to deliver clean drin
ily. The ability to prepare nanos
ambient temperature has wide
water purification.

hybrid | green | appropriate technolog

Work was featured in several journals

Nature Nanotechnology, July 2014 issue

We developed environmentally friendly water positive nanoscale materials for affordable, sustainable and rapid removal of arsenic from drinking water.

There are over 1700 community installations across the country, serving 1.3 million people with arsenic and iron-free water every day.

Quantum cluster based metal ion sensing paper
Large area uniform illumination using quantum cluster

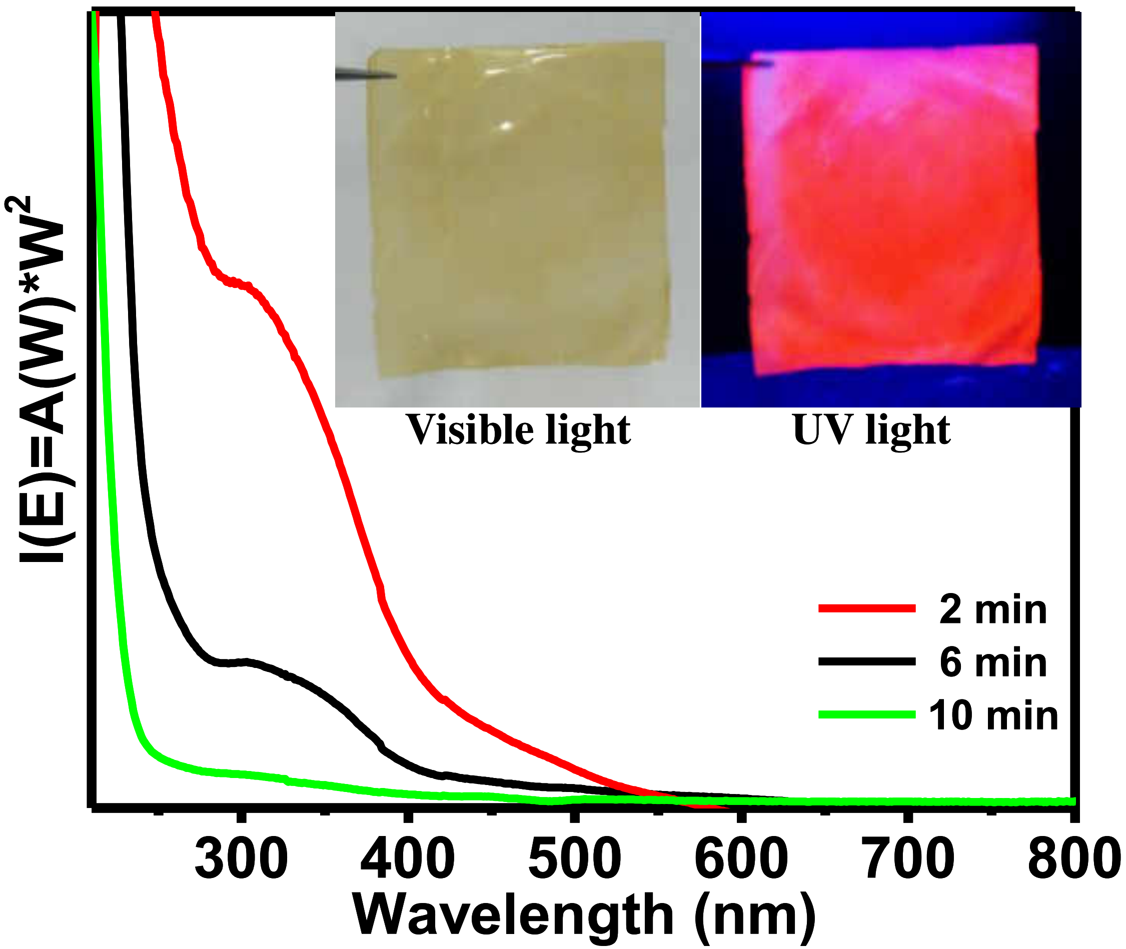

Decrease in the absorption of Au_{15} as a biofilm is dipped into the cluster solution. Inset: Free standing quantum cluster loaded film in visible light and UV light.

Approaching detection limits of tens of Hg^{2+}

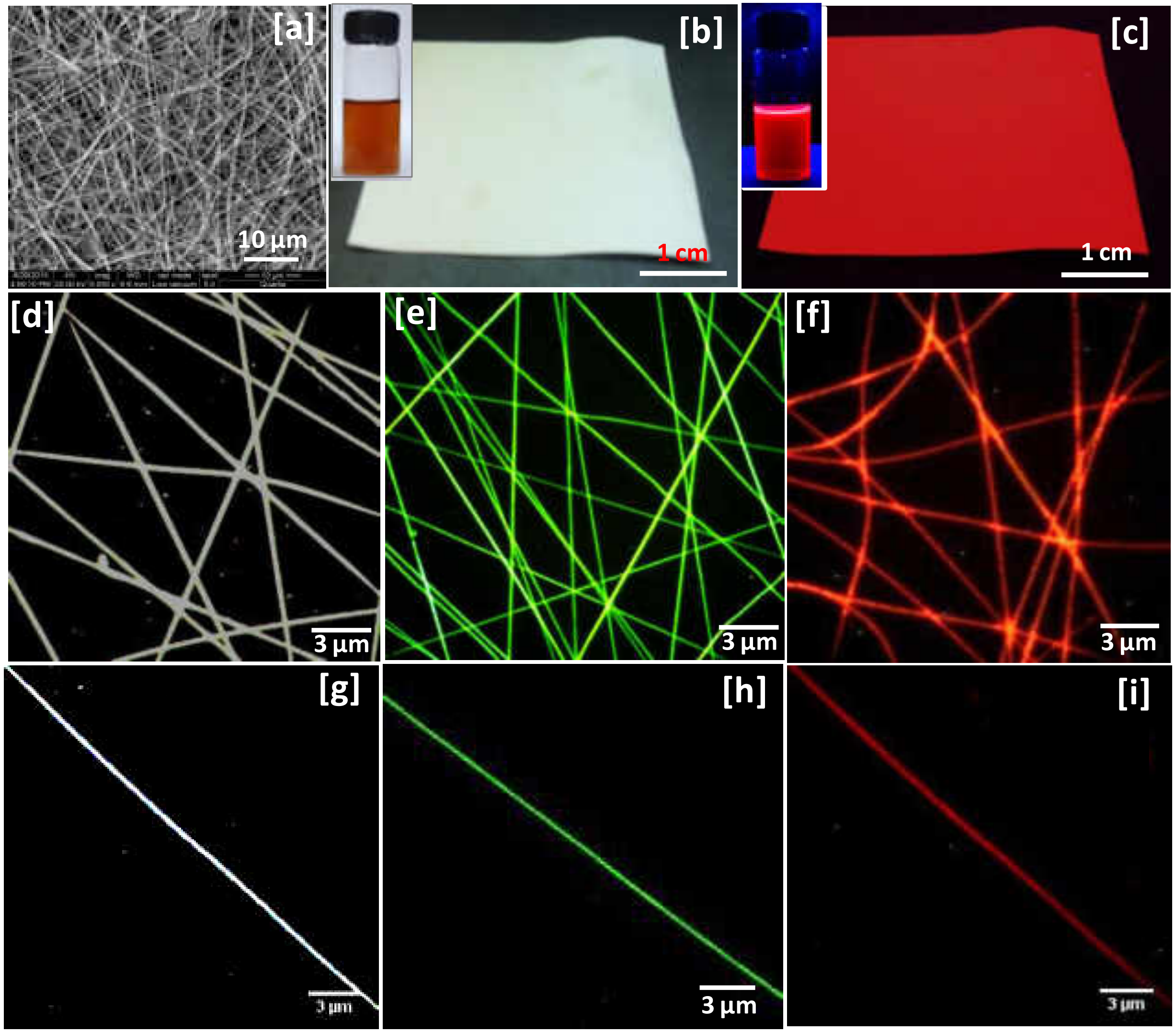

Atanu Ghosh et al. Anal. Chem.2014.

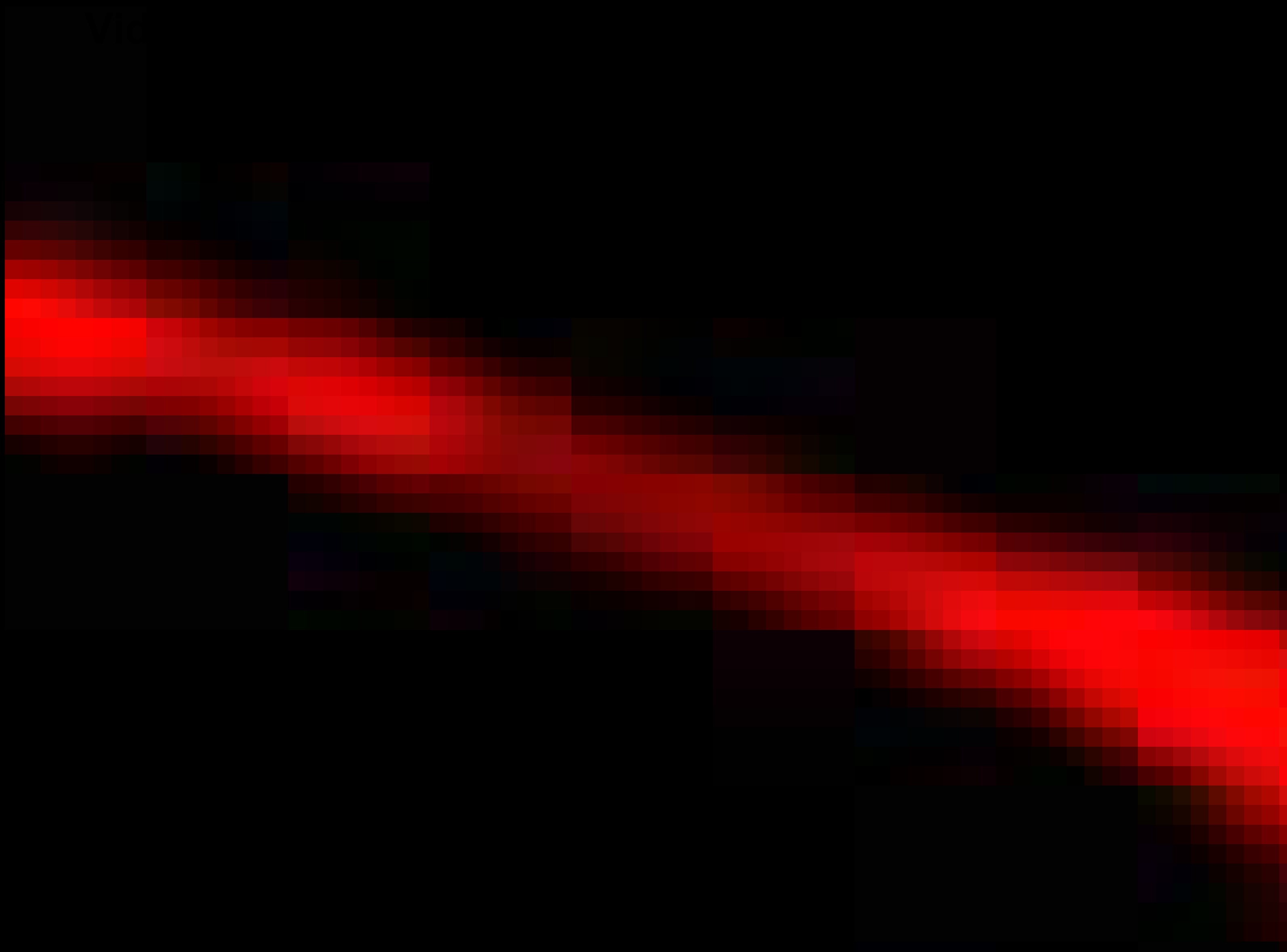

Sensors and new opportunities

Analog/Grating Equipment
$ 5~6 Billion (2017)
a few **100k units (2017)**

Ultra compact Low Cost Spectral Sensor Module
~ Billions units (? 2027)

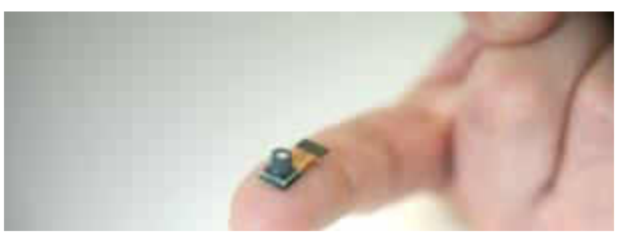

Water quality measurement – In the pipeline

nanoλ

New electrodes - Aligned nanoplates of Co_6S_8

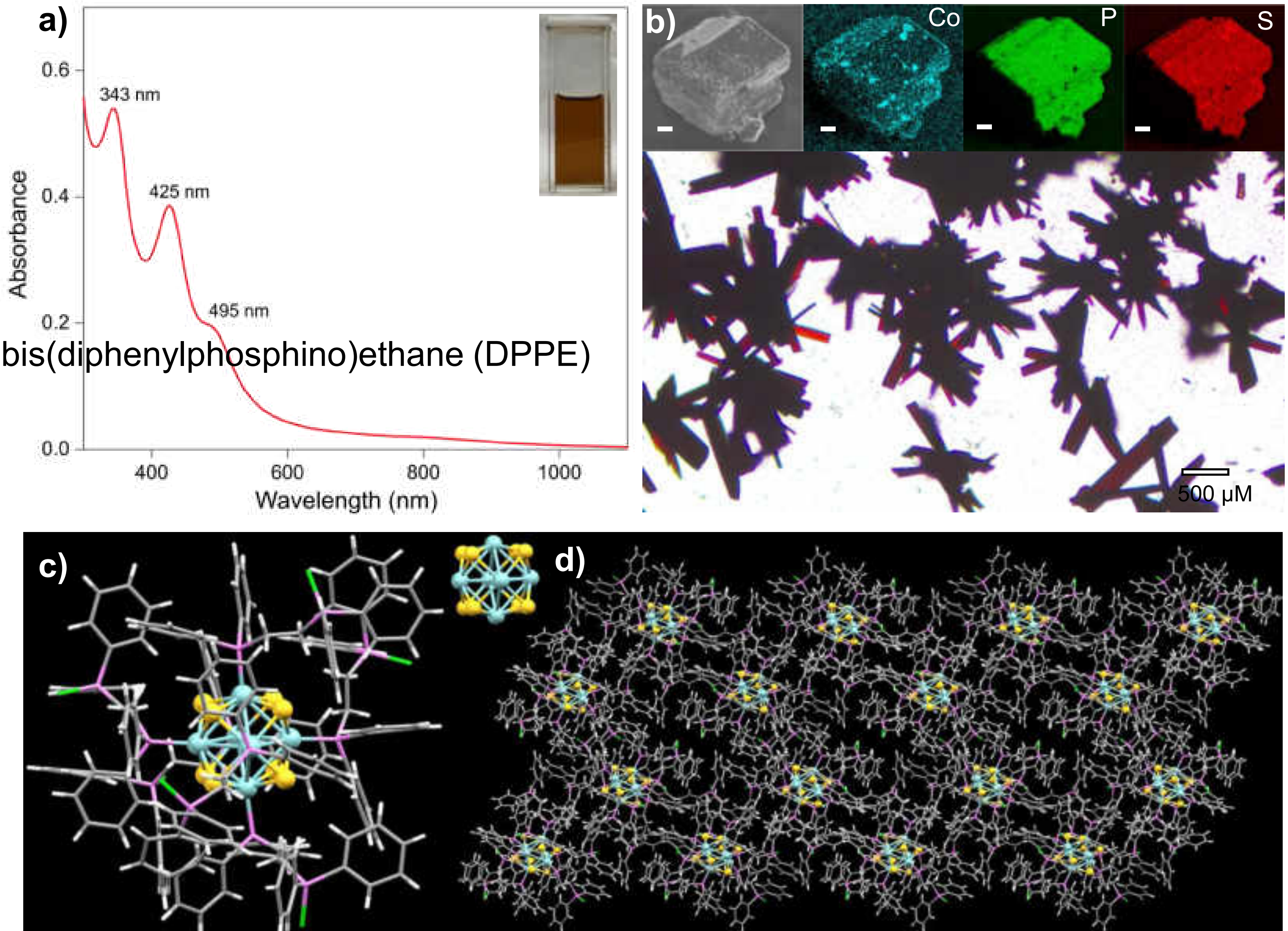

1,2-bis(diphenylphosphino)ethane (DPPE)

Electrospray deposition

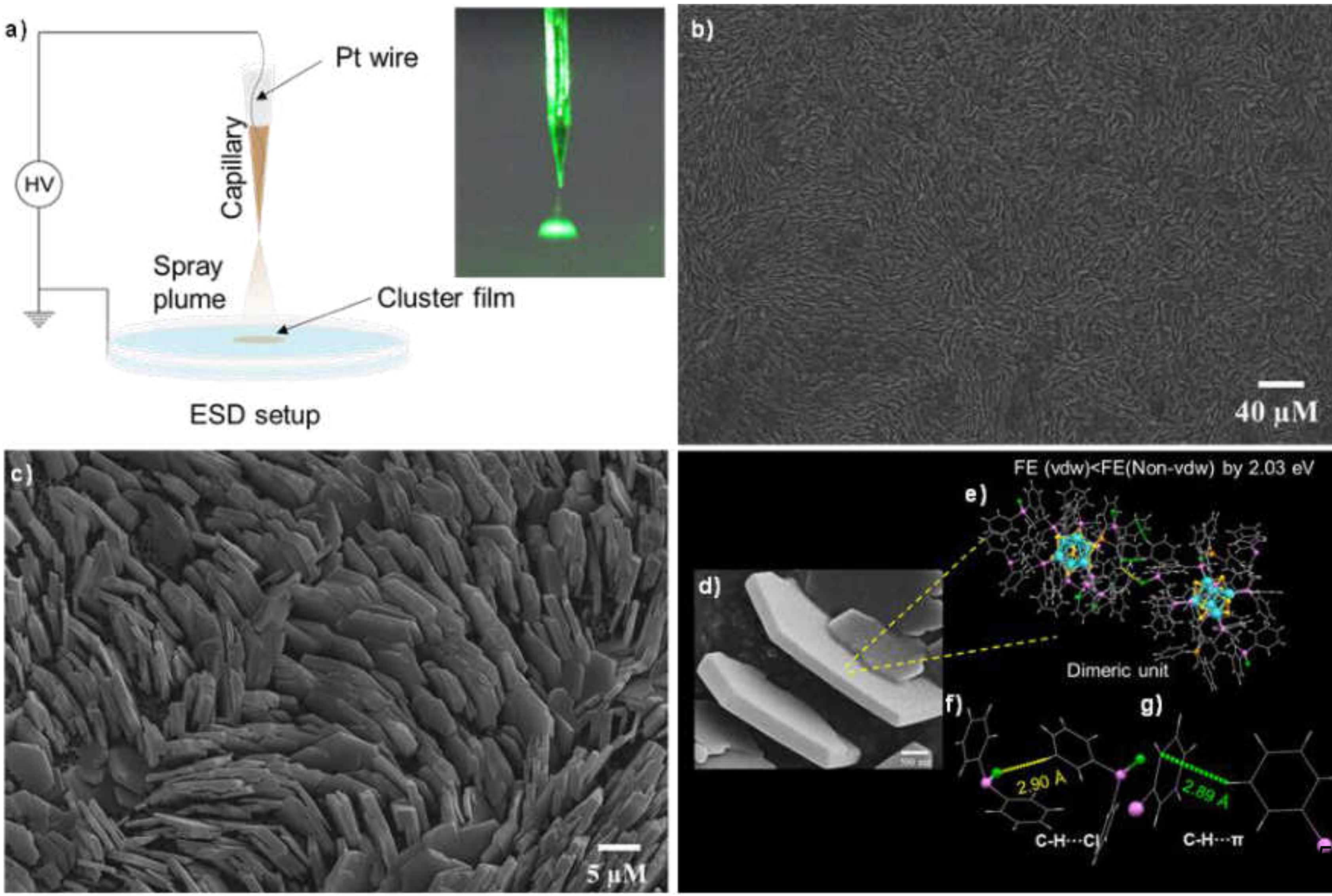

Sensing

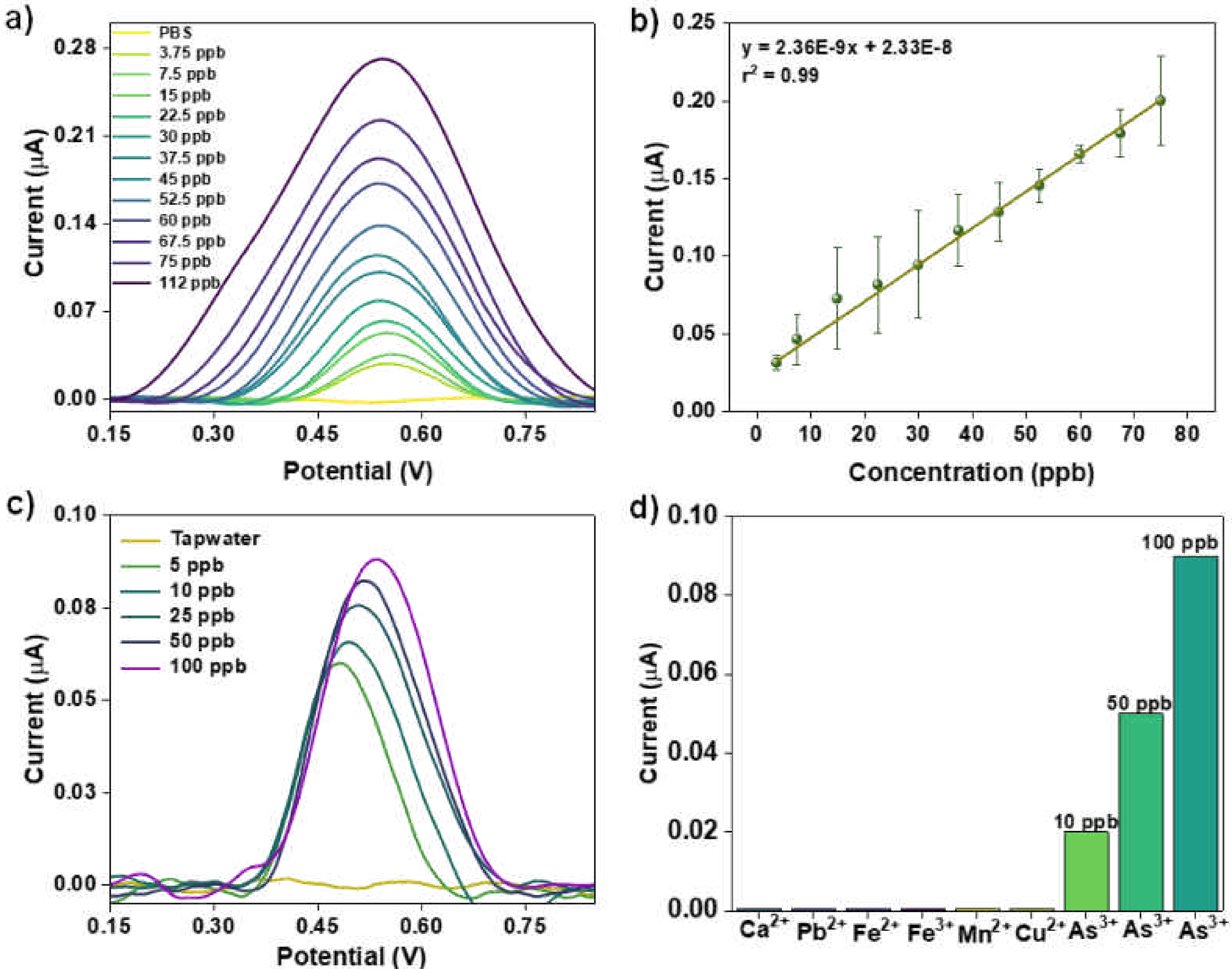

a)
PBS
3.75 ppb
7.5 ppb
15 ppb
22.5 ppb
30 ppb
37.5 ppb
45 ppb
52.5 ppb
60 ppb
67.5 ppb
75 ppb
112 ppb
Current (μA)
Potential (V)
b)
y = 2.36E-9x + 2.33E-8
r² = 0.99
Current (μA)
Concentration (ppb)
c)
Tapwater
5 ppb
10 ppb
25 ppb
50 ppb
100 ppb
Current (μA)
Potential (V)
d)
100 ppb
50 ppb
10 ppb
Current (μA)
Ca2+ Pb2+ Fe2+ Fe3+ Mn2+ Cu2+ As3+ As3+ As3+

Working electrode

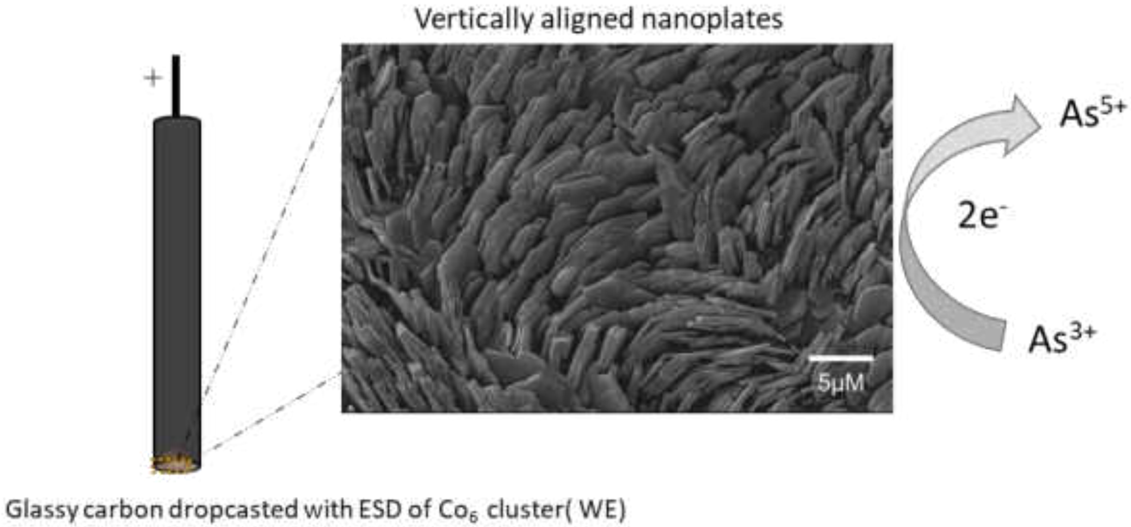

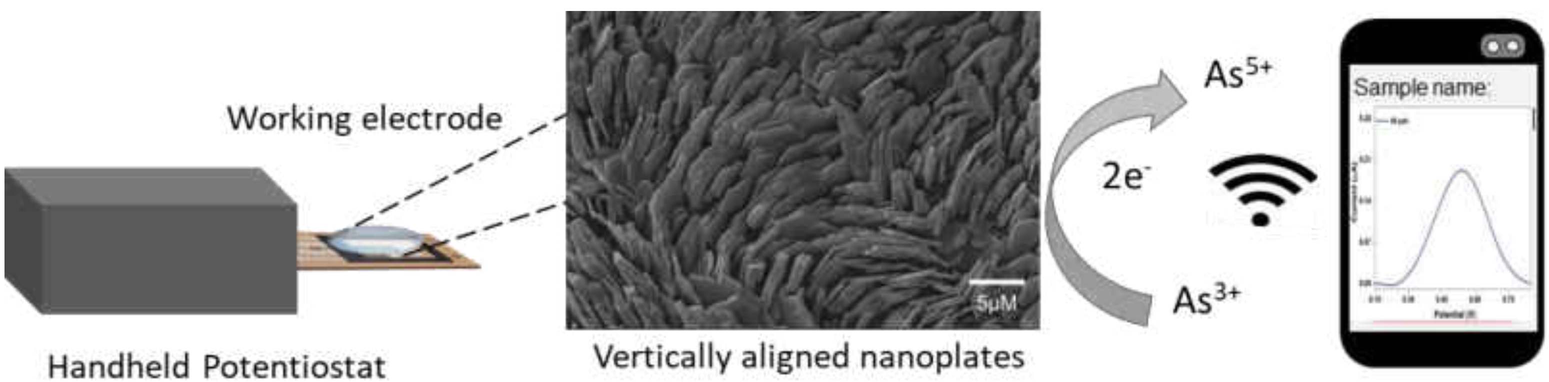

Anagha Jose et al. *ACS Materials Lett.*, 5 (2023) 893–899.

Arsenic poisoning across the world

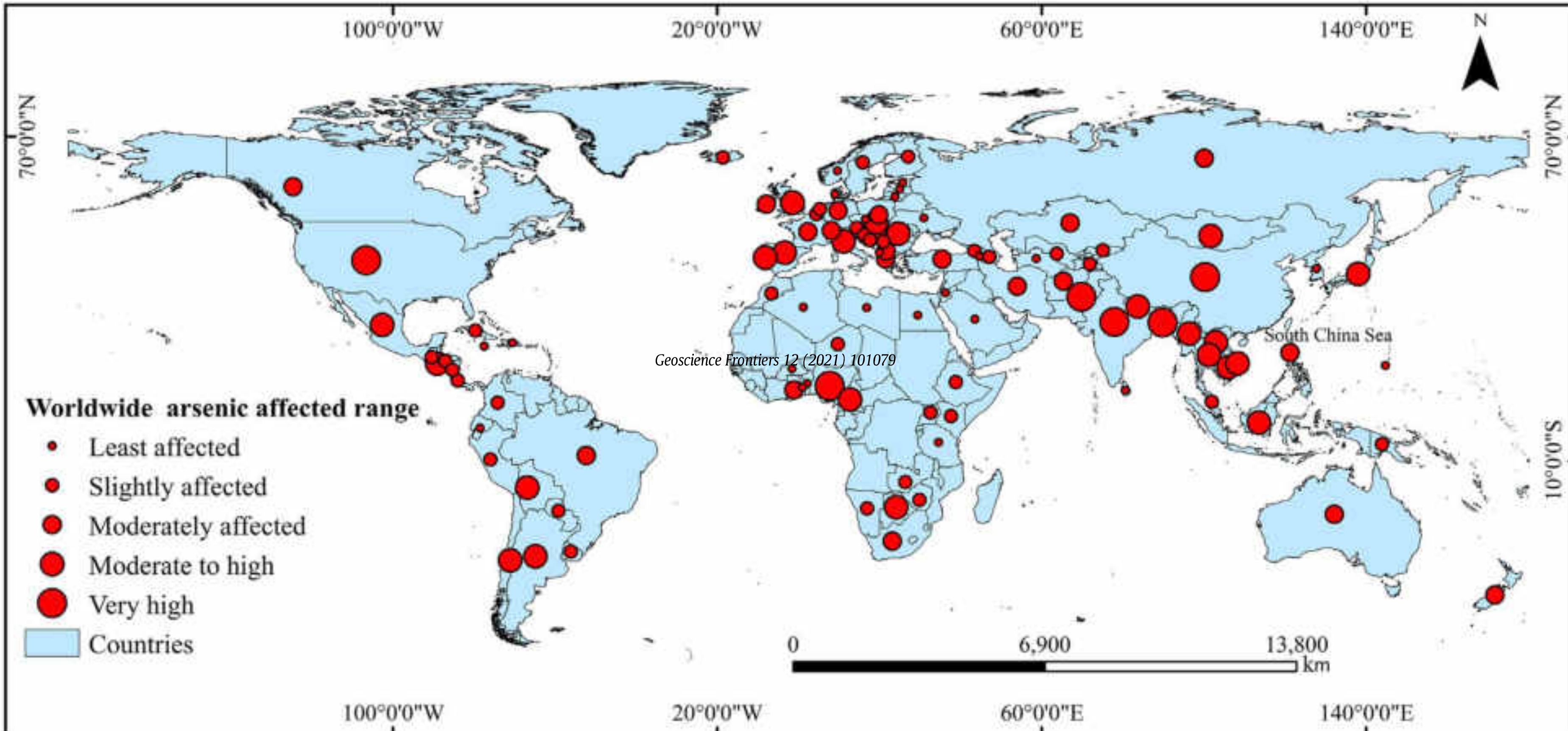

E. Shaji, M. Santosh, K. V. Sarath, Pranav Prakash, V. Deepch and B. V. Divya, *Geoscience Frontiers,* 12 (2021) 101079.

India’s water is being monitored

IITM/IISc

Installations made by four companies

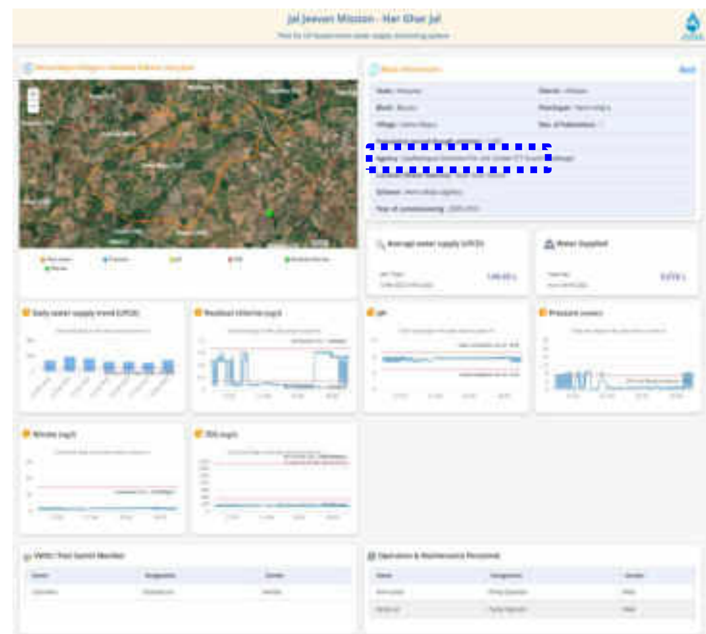

Ice chemistry

Clathrate hydrates in interstellar environme

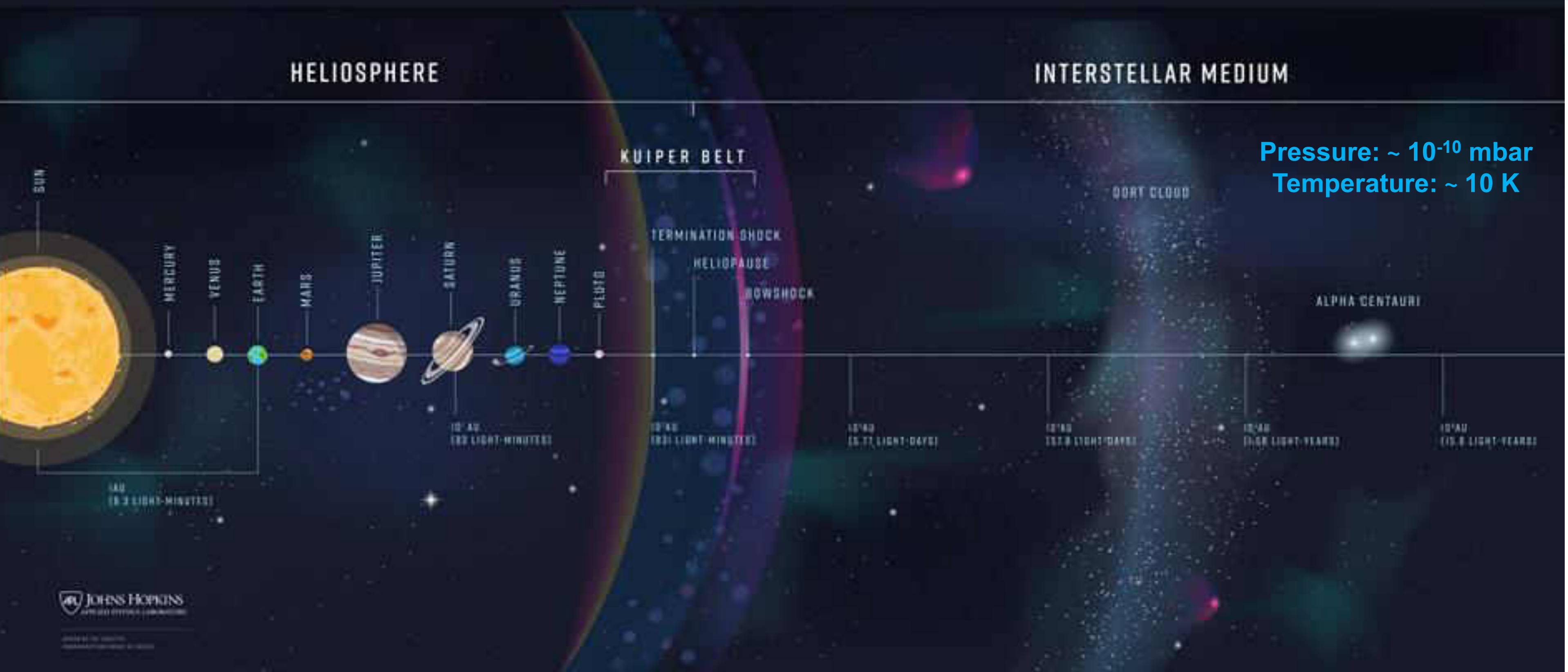

Pressure: ~ 10^{-10} mbar
Temperature: ~ 10 K

Diffuse clouds: T ~ 100 K, n ~ 100 molecules per cm^3
Dense clouds: T ~ 10-100 K, n ~ 10^4-10^8 molecules per cm^3
On Earth sea level: T ~ 300 K, n ~ 3×10^{19} molecules per cm^3

https://spaceref.com/science

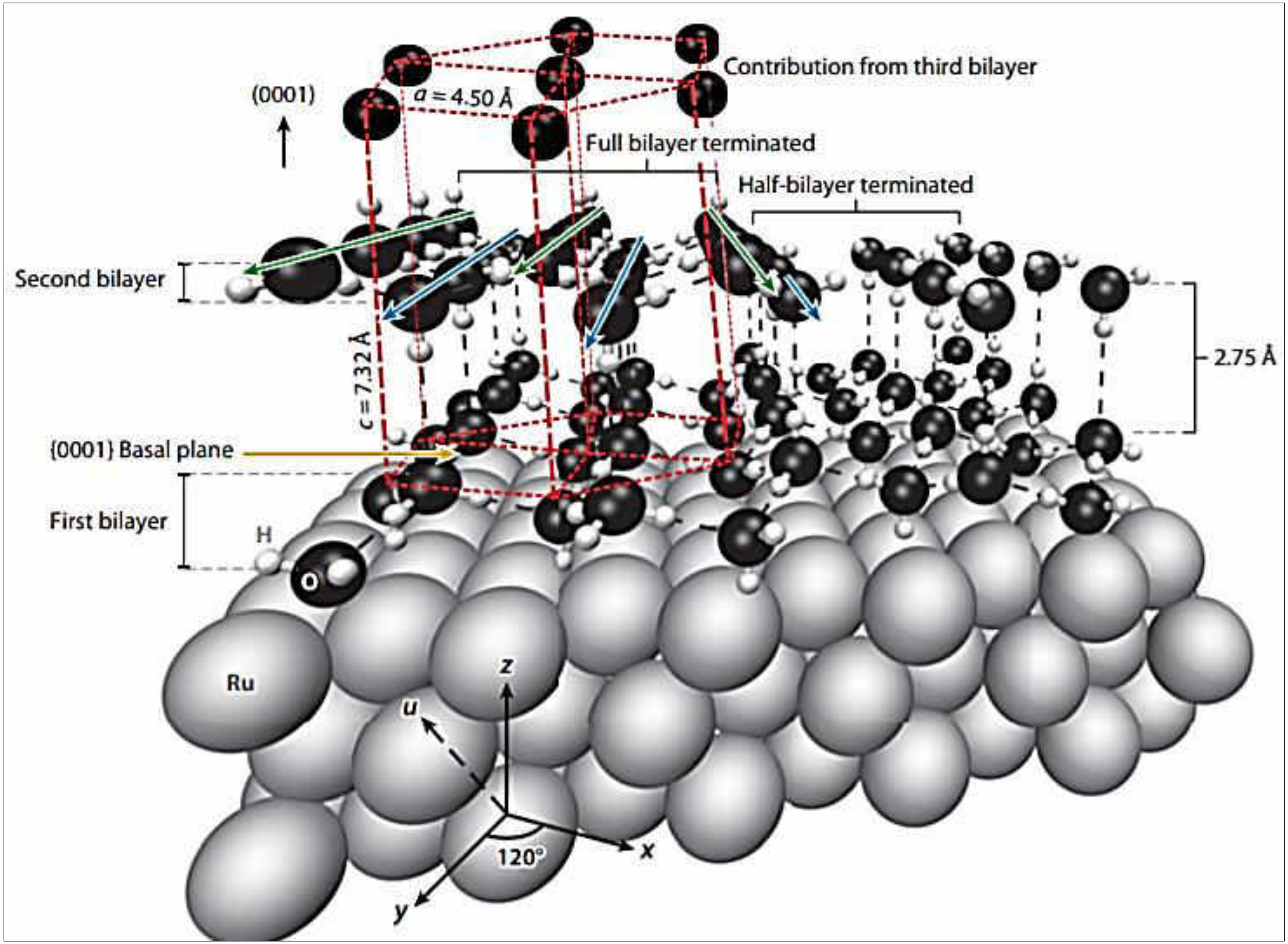

Bag, S. *et al.*, *Annu. Rev. Anal. Chem.* **2013**, *6*, 97–118

Instrumentation

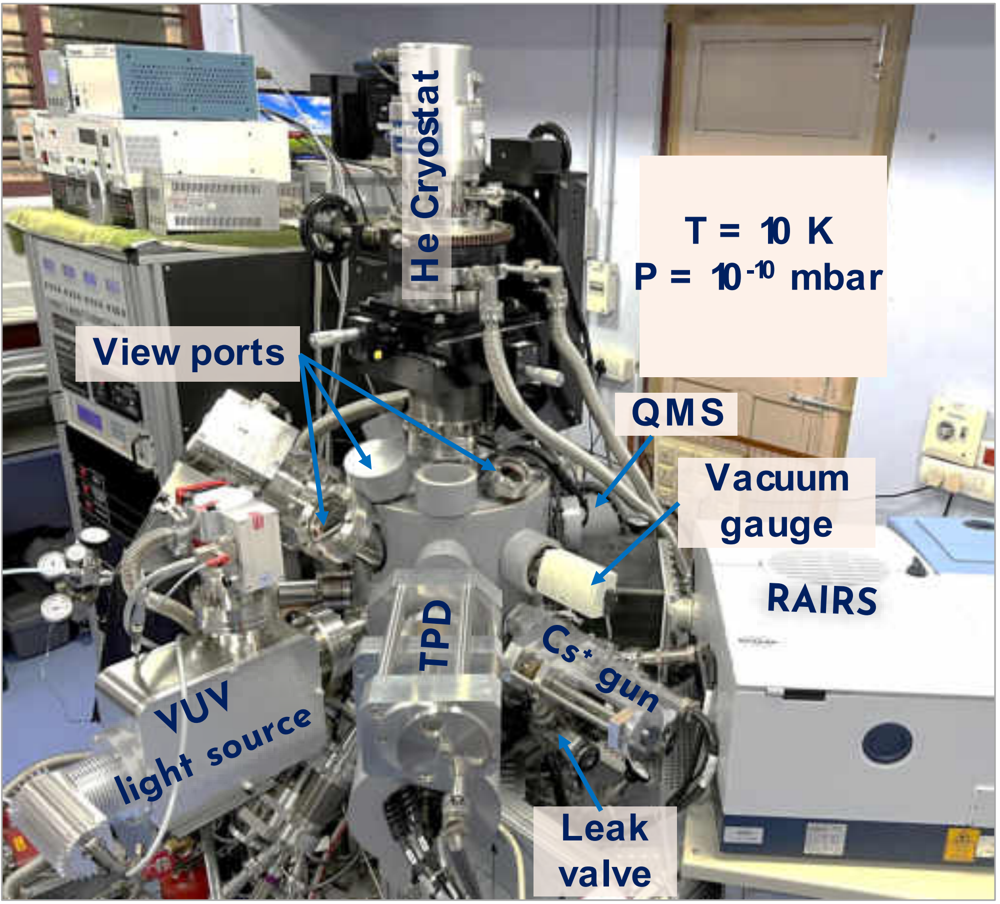

Ice instrument located in HSB-148, IIT Madras

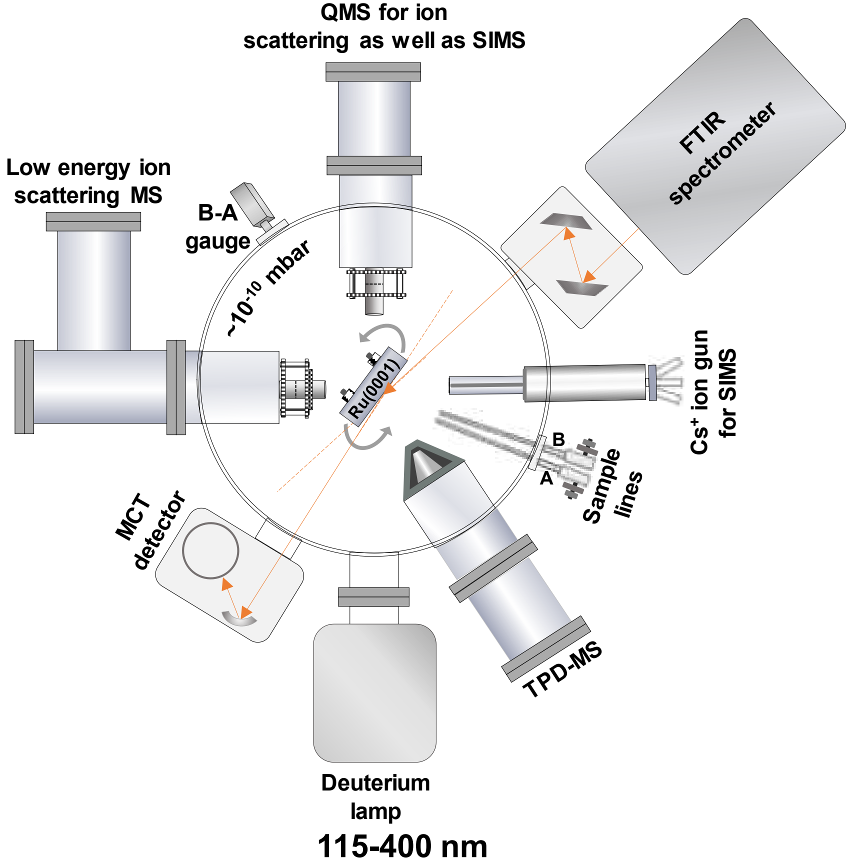

Viswakarma, *G. et al., J. Phys. Chem. Lett.*, **2023**, *14*, 2823–2829

CH in ultrahigh vacuum

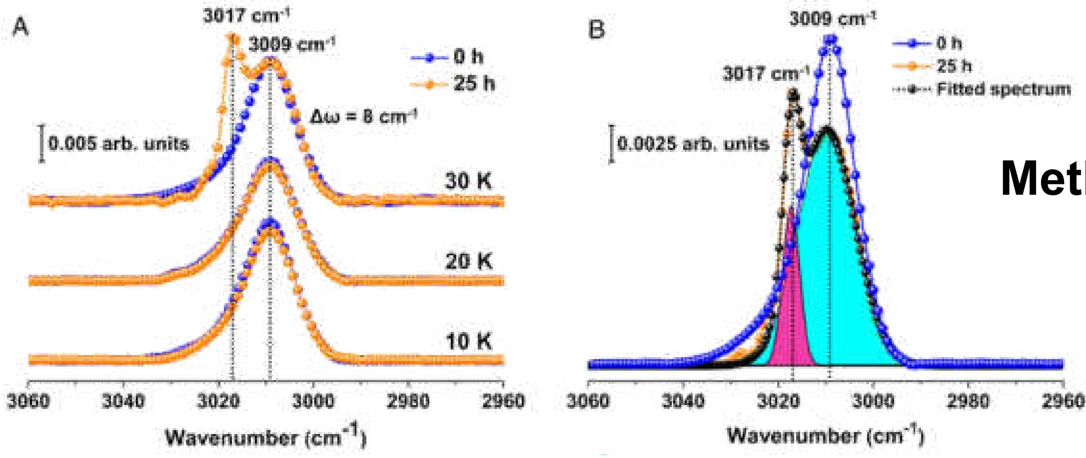

Methane CH

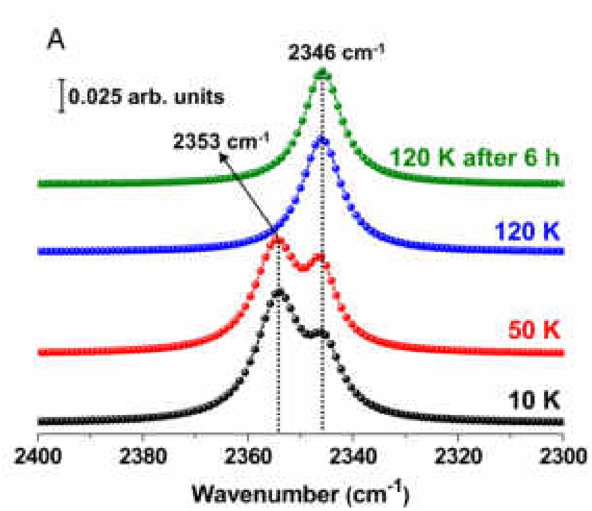

Carbon dioxide CH

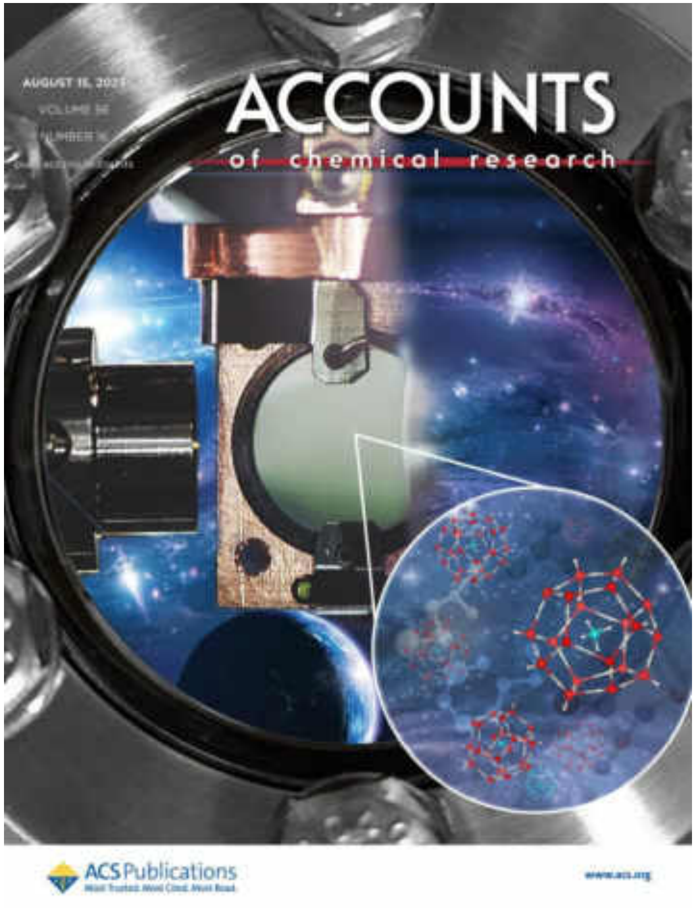

Ghosh, J. *et al.*, *Proc. Natl. Acad. Sci. U.S.A.*, **2018,** *116*, 1526-1531

Microdroplets

Science

NANOPARTICLES

Spontaneous weathering of natural minerals in charged water microdroplets forms nanomaterials

B. K. Spoorthi[1], Koyendrila Debnath[2], Pallab Basuri[1], Ankit Nagar[1], Umesh V. Waghmare[2], Thalappil Pradeep[1,3]*

In this work, we show that particles of common minerals break down spontaneously to form nanoparticles in charged water microdroplets within milliseconds. We transformed micron-sized natural minerals like quartz and ruby into 5- to 10-nanometer particles when integrated into aqueous microdroplets generated via electrospray. We deposited the droplets on a substrate, which allowed nanoparticle characterization. We determined through simulations that quartz undergoes proton-induced slip, especially when reduced in size and exposed to an electric field. This leads to particle scission and the formation of silicate fragments, which we confirmed with mass spectrometry. This rapid weathering process may be important for soil formation, given the prevalence of charged aerosols in the atmosphere.

Nanoparticles of minerals exist naturally in soil, and some of them are essential for life (1). Microdroplets have been a topic of interest over the past decade, and the confined environment within them is known to cause chemical synthesis at an accelerated rate, as well as other processes such as the formation of nanoparticles (2). We decided to explore whether natural minerals could disintegrate in microdroplets, through a process opposite to chemical synthesis.

For our experiments, we prepared micron-scale particles of natural quartz (SiO_2) and ruby (Cr-substituted Al_2O_3) for use in an electrospray setup (Fig. 1, A and B). We ground commercial millimeter-sized quartz particles well using a mortar and pestle and used centrifugation to separate the differently sized particles that formed. We carefully excluded all the particles smaller than 1 nm in size and used particles of 5 to 10 nm that were suspended in water for the experiment (Fig. 1C). Even after ultrasonication to detach any adhered particles, we found some smaller particles attached to a few larger ones (Fig. 1C). These adhering particles had dimensions greater than 100 nm (fig. S1). We took an optical image of the ground quartz powder and an optical microscopic image of the separated particles that we used for electrospray (fig. S2). We electrosprayed a suspension of about 0.1 mg/ml of the separated quartz particles through a capillary tube that had an inner diameter of 50 mm at a flow rate of 0.5 ml/hour and observed the resulting plume (Fig. 1A). We collected the product of electrospray 1.5 cm away from the spray tip, which resulted in a flight time on the order of 10 ms, consistent with similar experiments (3, 4). The product that was deposited on a transmission electron microscopy (TEM) grid had only 5- to 10-nm-diameter particles (Fig. 1D) throughout the grid. Under higher magnification, particles of different morphologies were observed. The particles showed the (110) plane of quartz (inset of Fig. 1D). Sonication had no effect on the breaking of silica particles. Experimental methods are presented in the supplementary materials, including a video of the electrospray process (movie S1).

To ensure that our initial observations were truly representative of the process, we performed measurements on larger quantities of samples. We built a multinozzle electrospray unit composed of six nozzles. We electrosprayed 1 liter of the suspension that contained 100 mg of the crushed micron-sized particles discontinuously over a month at the optimized conditions (spray voltage and distance) and a 3 ml/hour flow rate, and a deposit

[1]Department of Chemistry, Indian Institute of Technology Madras, Chennai 600036, India. [2]Theoretical Sciences Unit, Jawaharlal Nehru Centre for Advanced Scientific Research, Bangalore 560064, India. [3]International Centre for Clean Water, IIT Madras Research Park, Chennai 600113, India.
*Corresponding author. Email: pradeep@iitm.ac.in

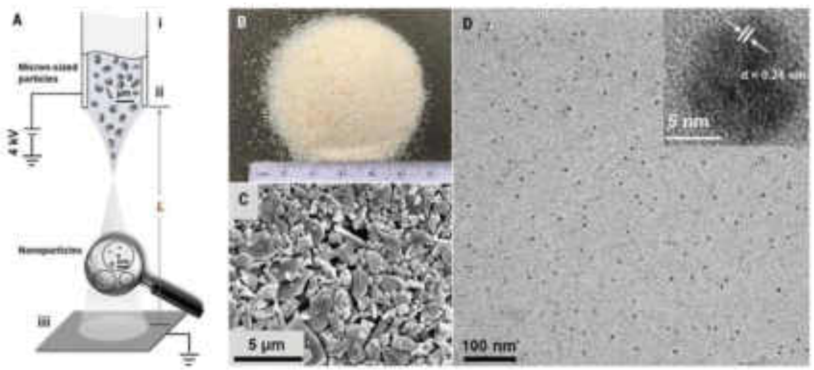

Spoorthi et al., Science 384, 1012–1017 (2024) 31 May 2024

A scale of 1000

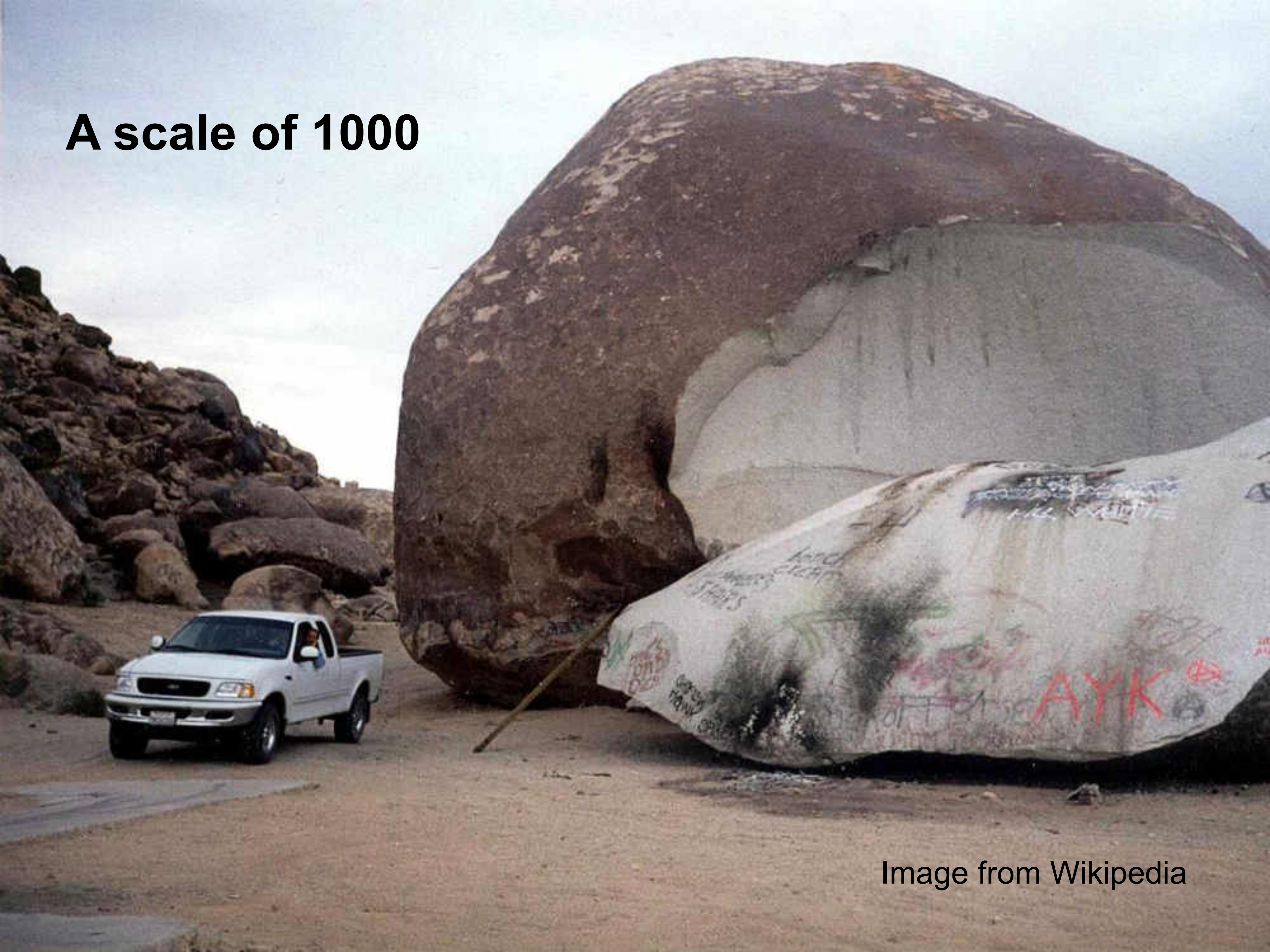

Image from Wikipedia

Functional Nanomaterials

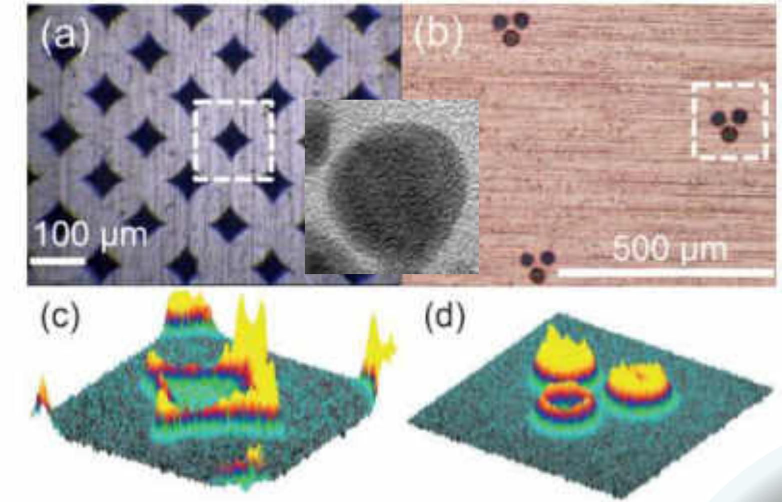

Anyin Li, et. al., Angew. Chem. Int. Ed. 2014, 53, 12528 –12531.

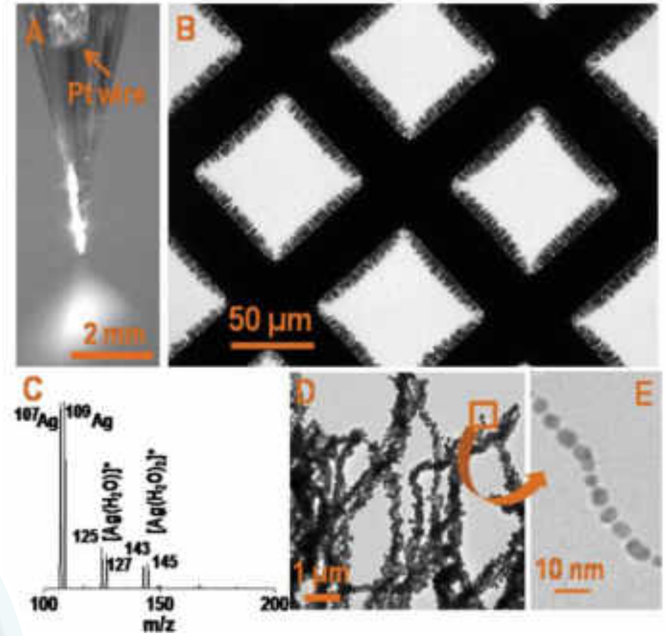

Depanjan Sarkar et. al., *Adv. Mater.* 2016, 28, 2223–2228.

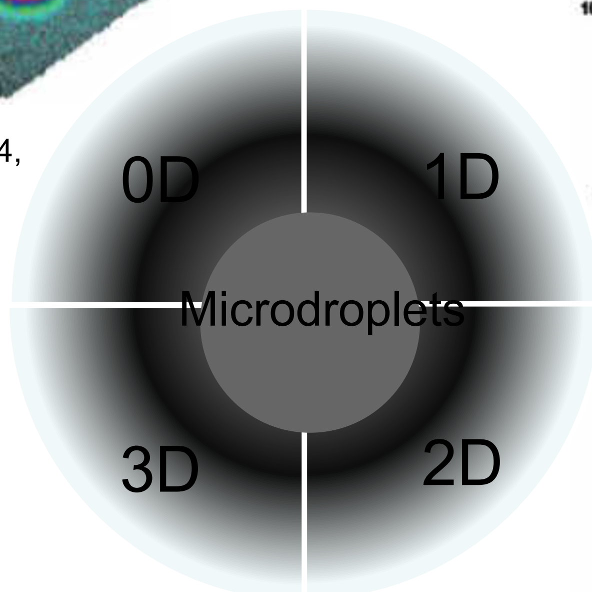

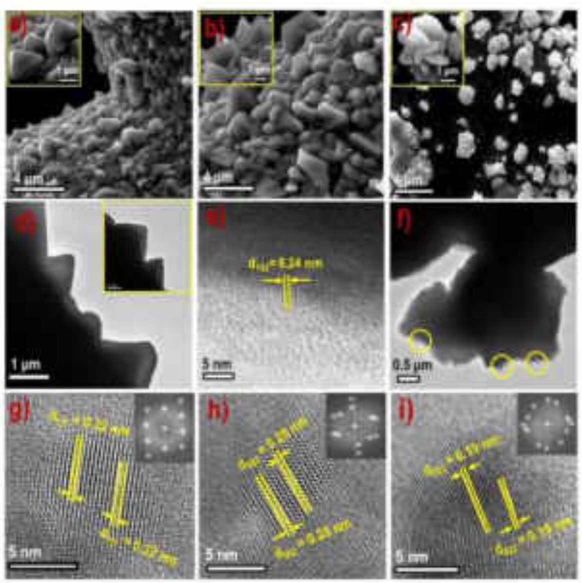

Arijit Jana et. al., *J. Mater. Chem. A,* 2019, 7, 6387–6394.

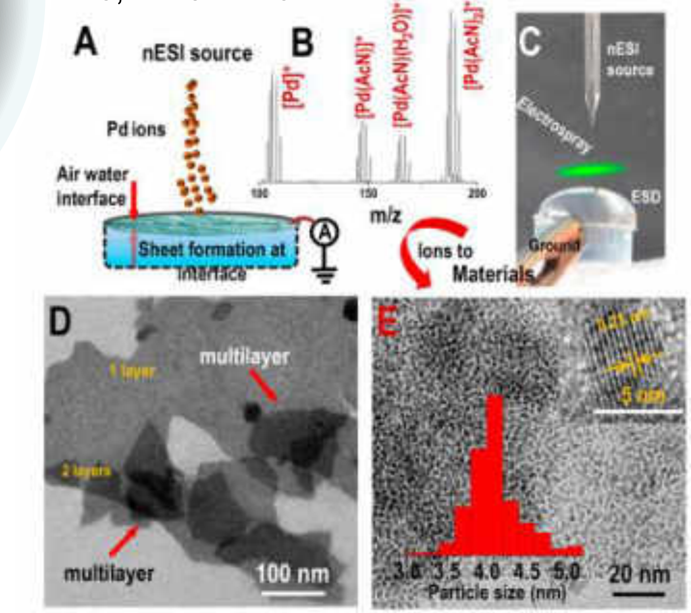

Depanjan Sarkar, et. al., *J. Phys. Chem. C* 2018, 122, 17777−17783.

Bimetallic Nanobrushes

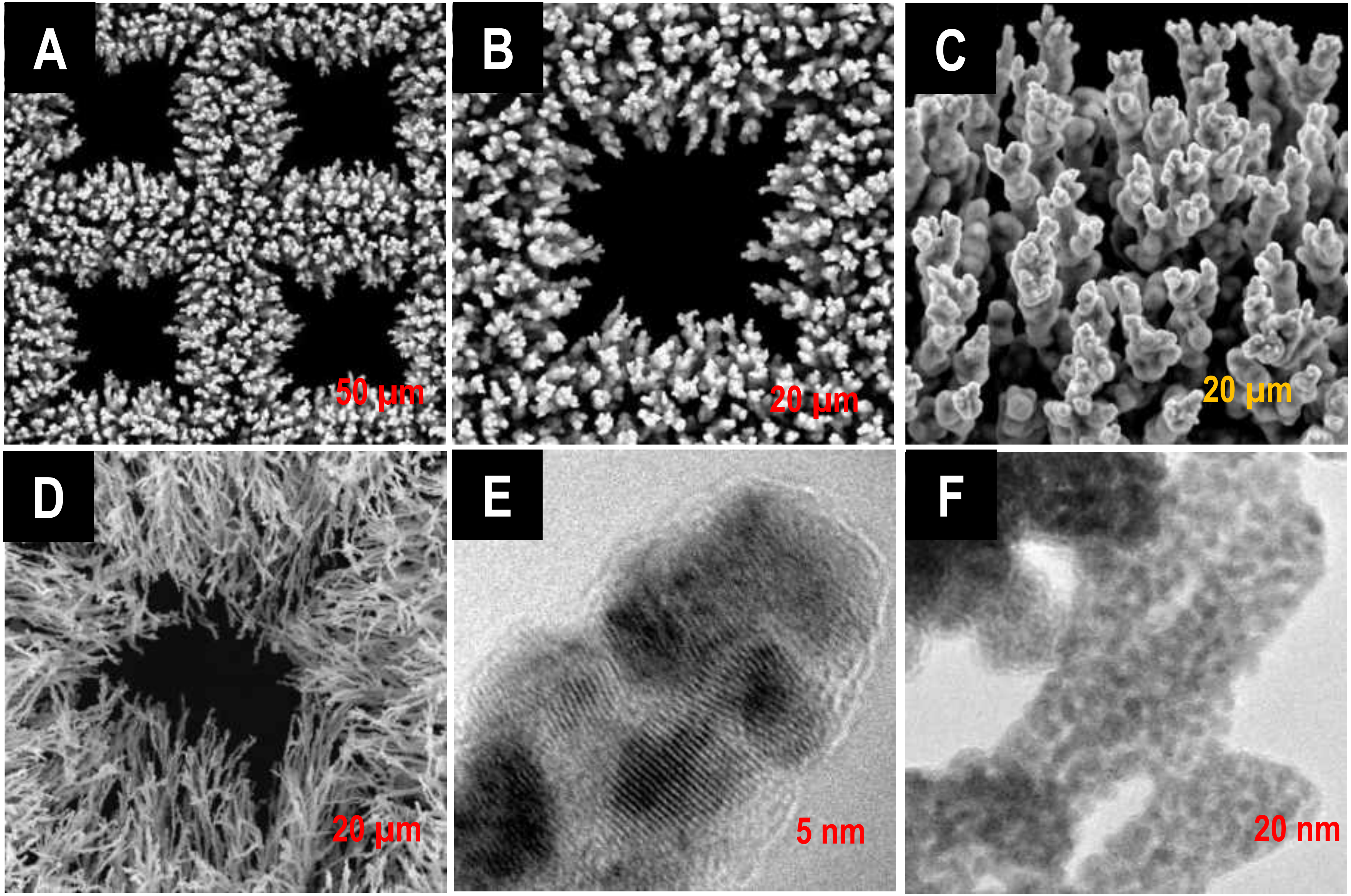

Formation of Ag-Pd bimetallic brushes


Nature is a best teacher, a great source of wisdom

Patterned Surfaces Using Microdroplets

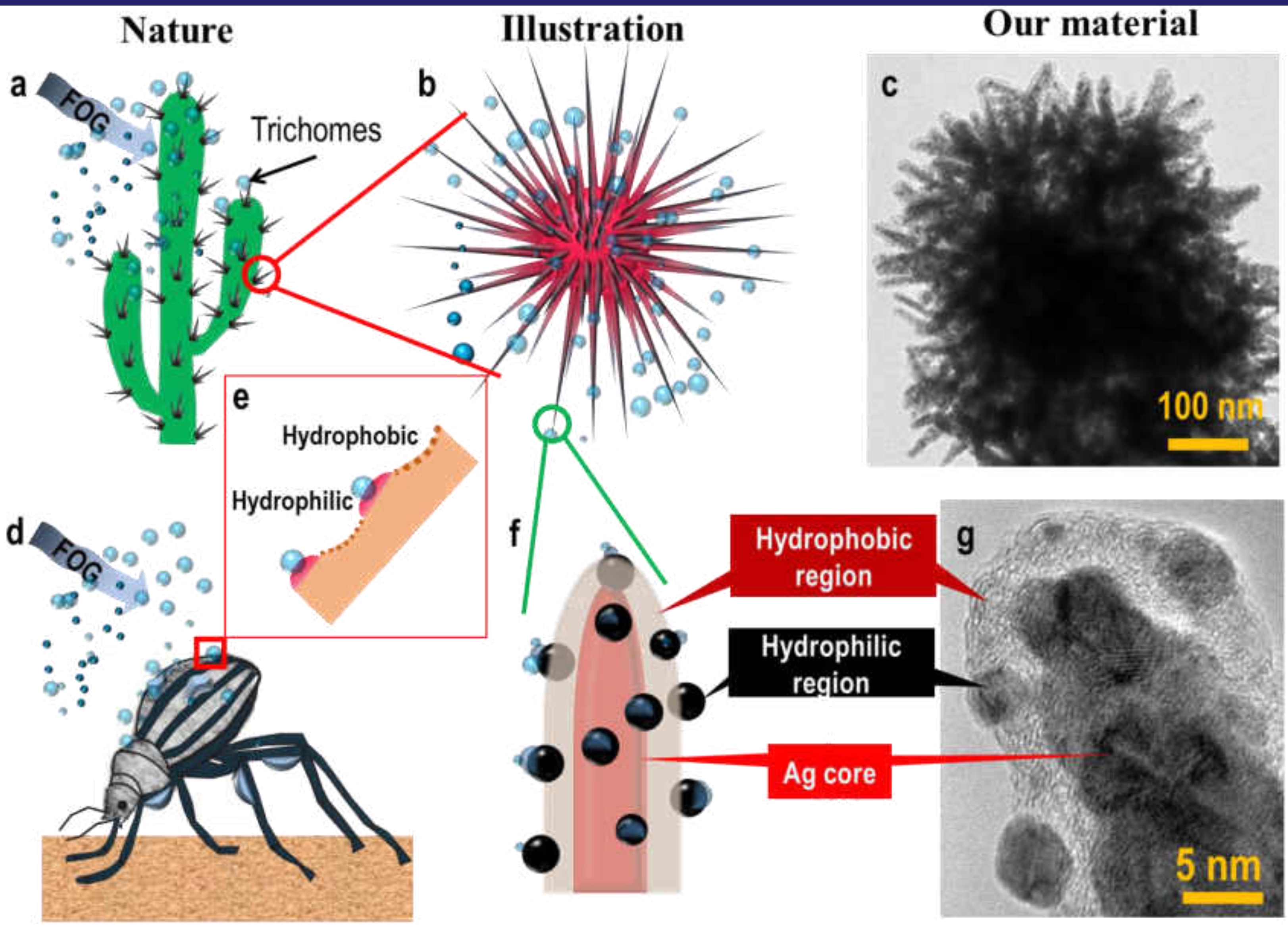

Depanjan Sarkar et. al., Adv. Mater. Interfaces, 2018, 1800667.

Atmospheric Water Capture

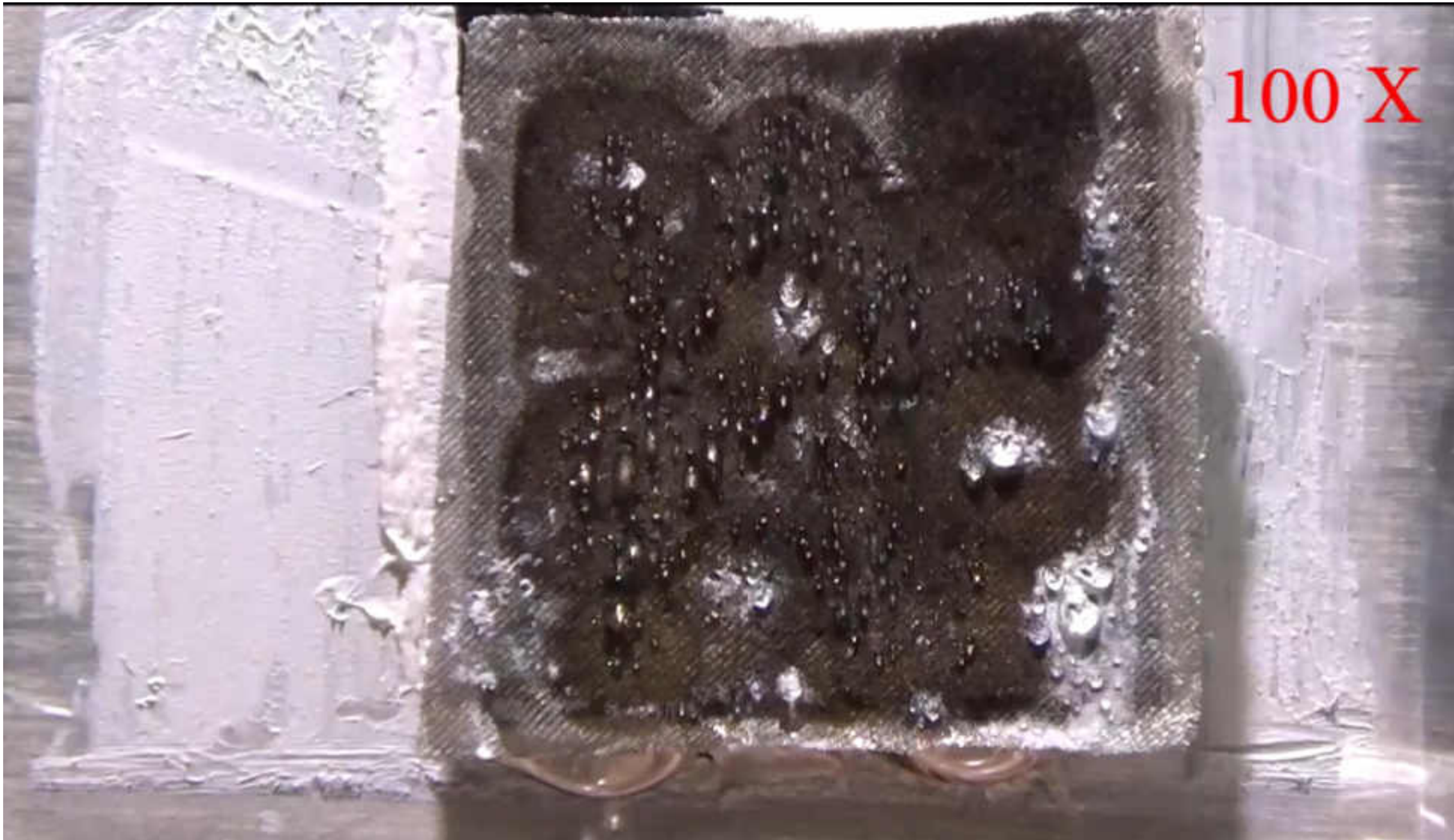

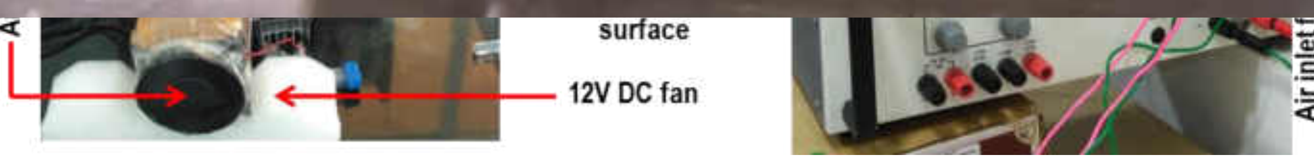

Efficiency of
56.6 L m^{-2} d^{-1}

Volume 13
Number 45
7 December 2022
Pages 13251–13634

Chemical Science

rsc.li/chemical-science

ISSN 2041-6539

ROYAL SOCIETY OF CHEMISTRY

EDGE ARTICLE
Thalappil Pradeep *et al.*
Spatial reorganization of analytes in charged aqueous microdroplets

Understanding Microdroplets

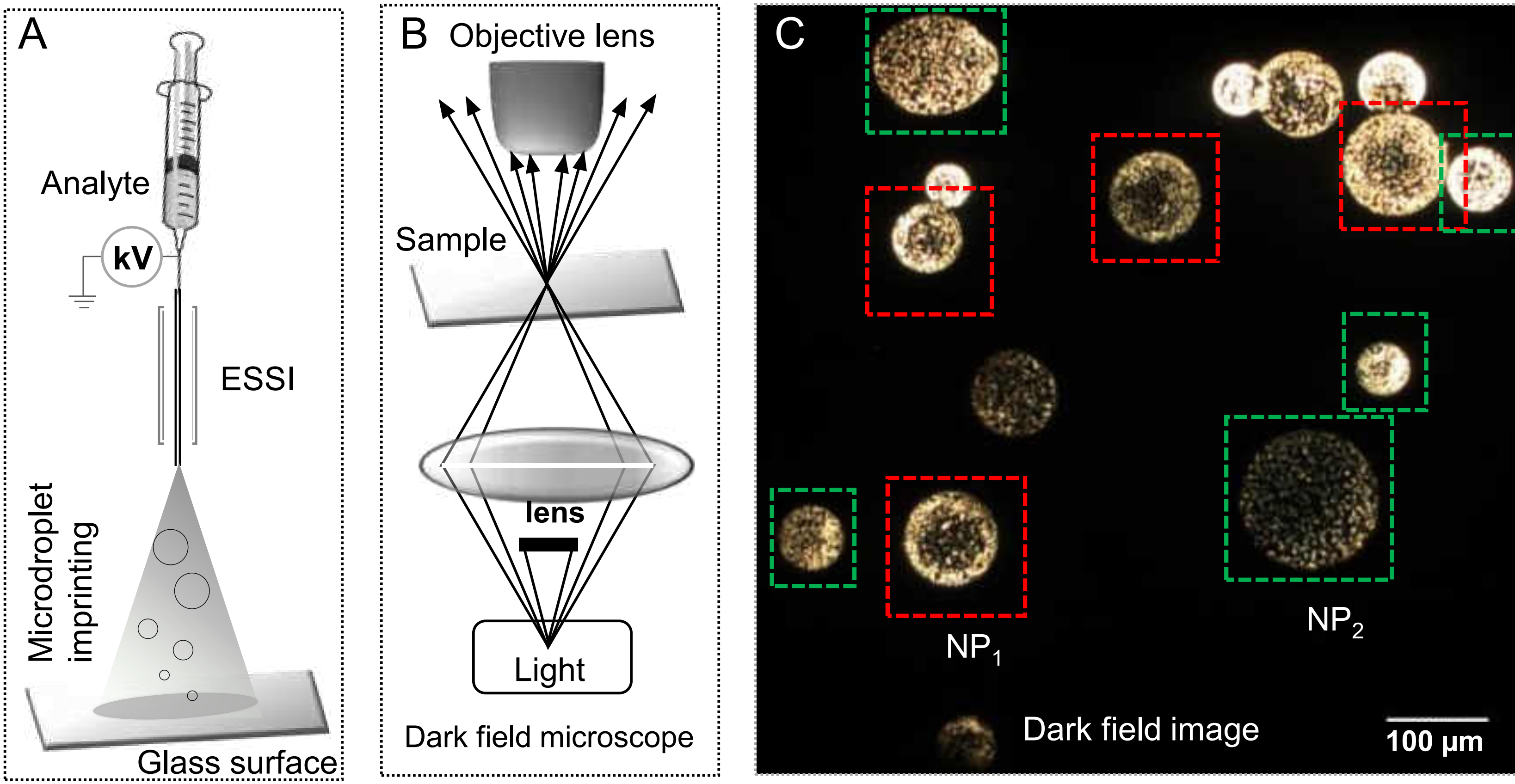

Pallab Basuri et. al. *Chem. Sci.*, 2022, 13, 13321–13329.

Transformation of Materials in Microdroplets

Ambient Microdroplet Annealing of Nanoparticles

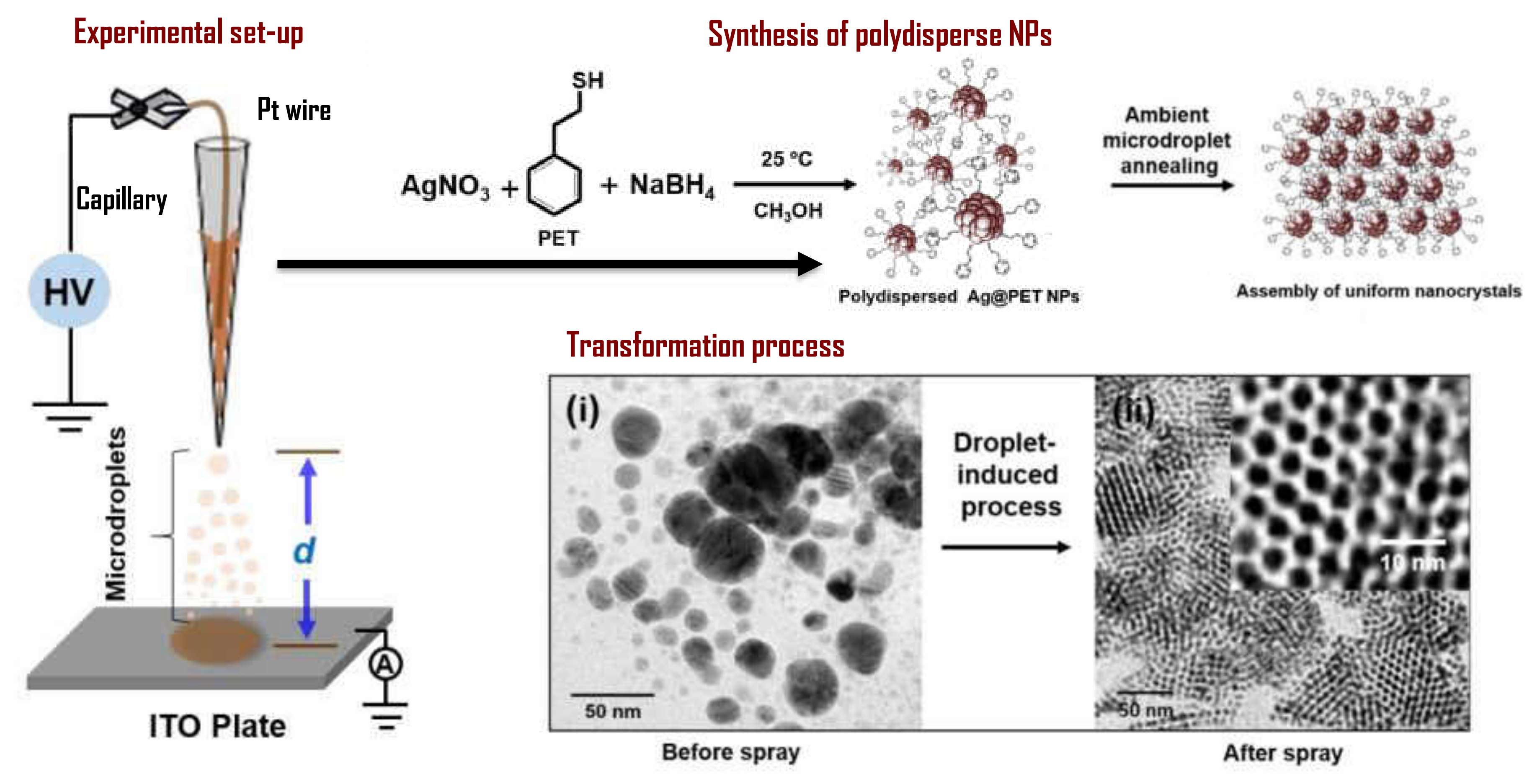

Angshuman Ray Chowdhuri et. al., *Chem. Sci.*, 2021, 12, 6370–6377.

Thanks to ChatGPT

Weathering in Nature

Sand, the Ubiquitous Material

Images from Wikipedia

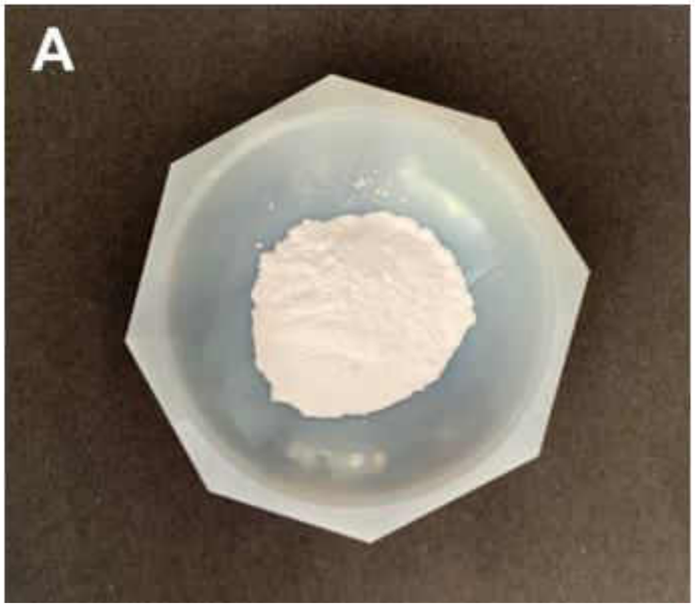

Ground silica

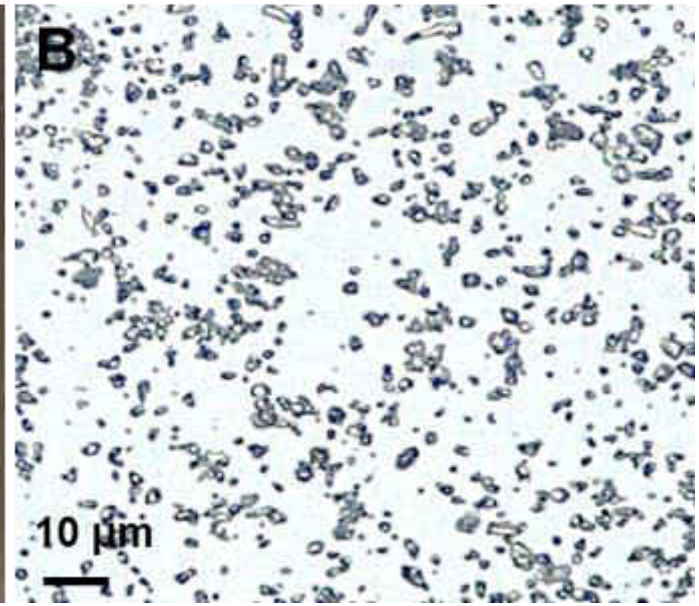

Optical image of silica

Weathering of Minerals in Microdroplets

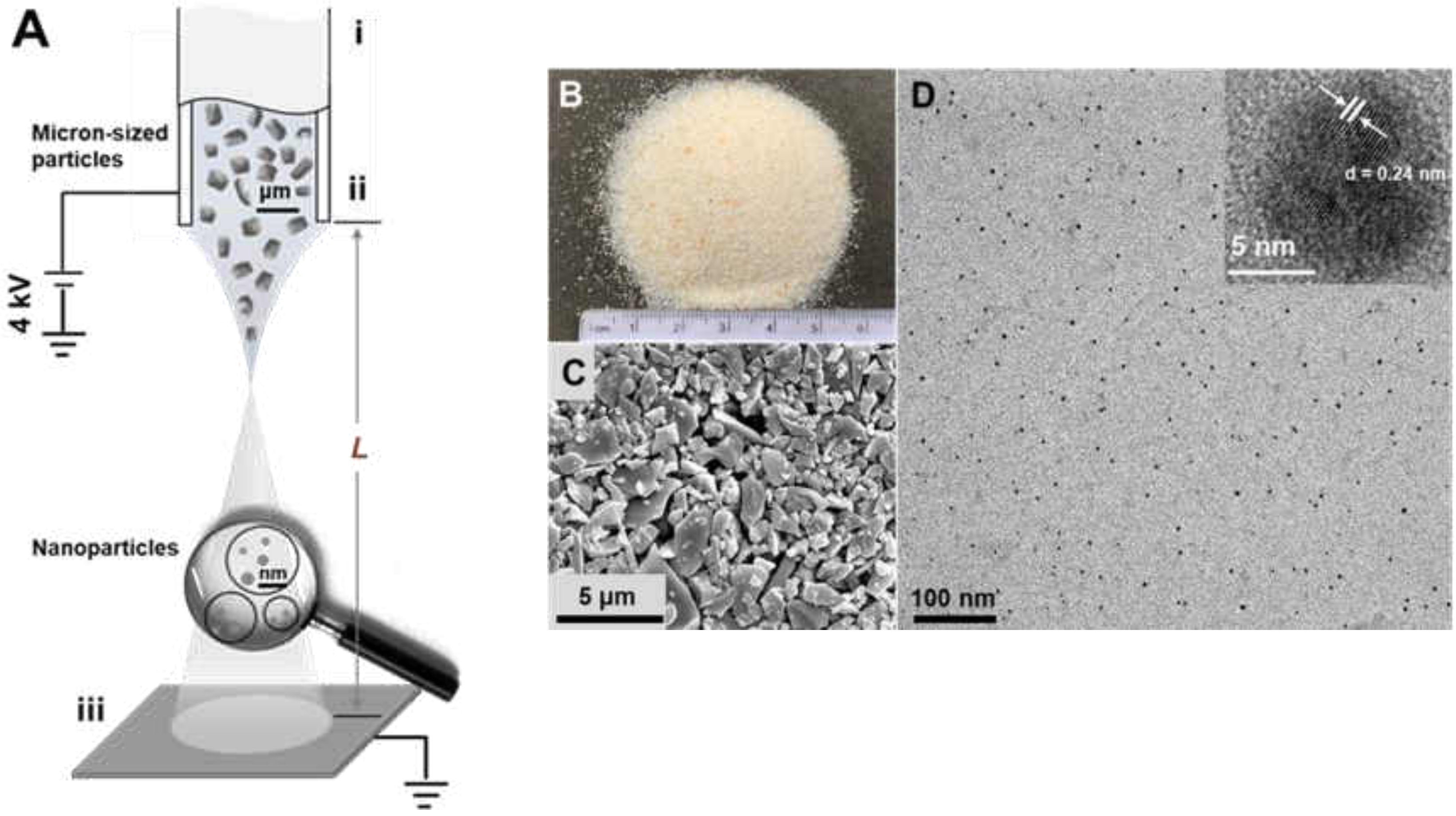

Spoorthi, et. al., *Science*, 2024

Ruby, Fused Alumina

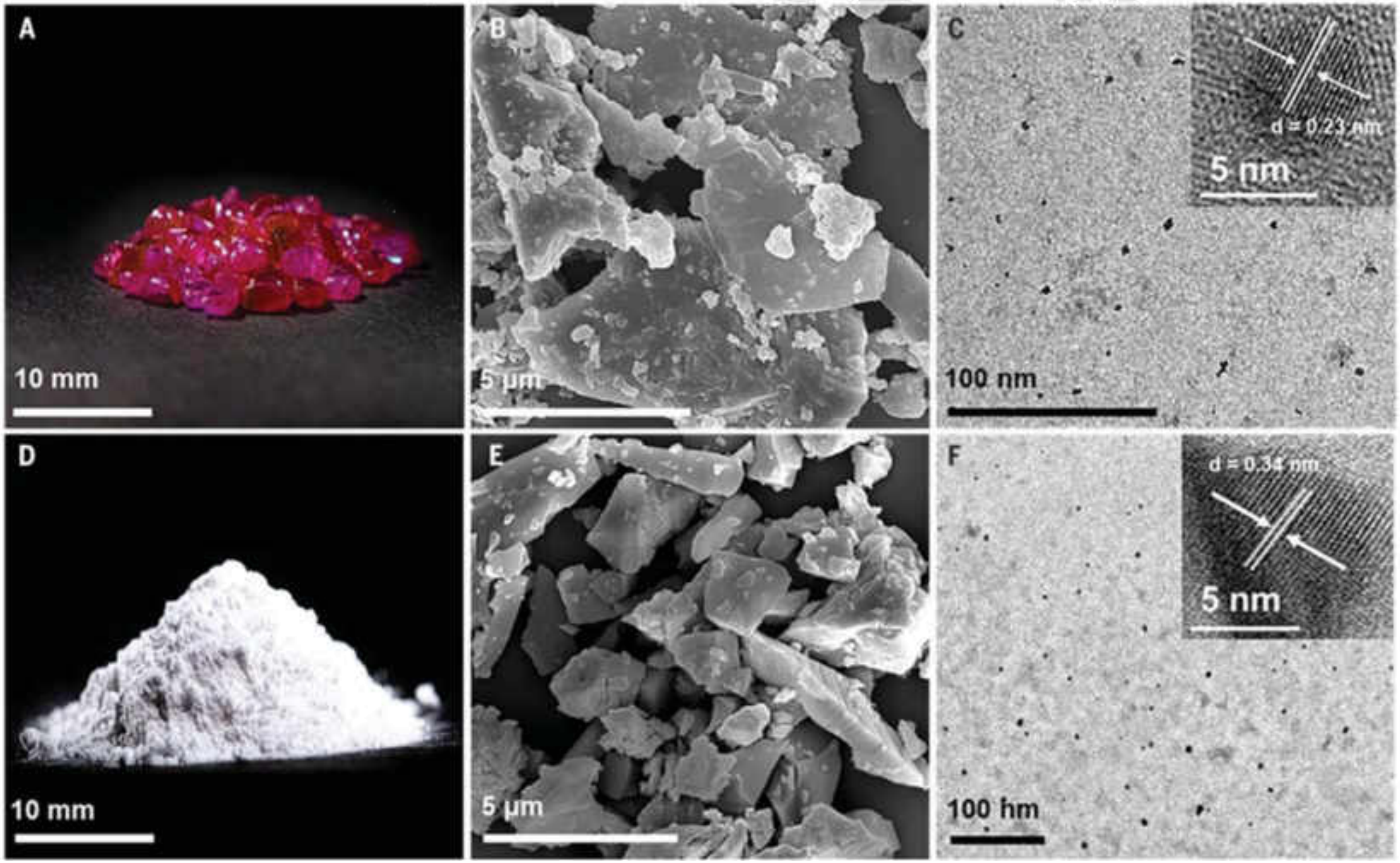

Fragmentation of Silica – Varying Conditions

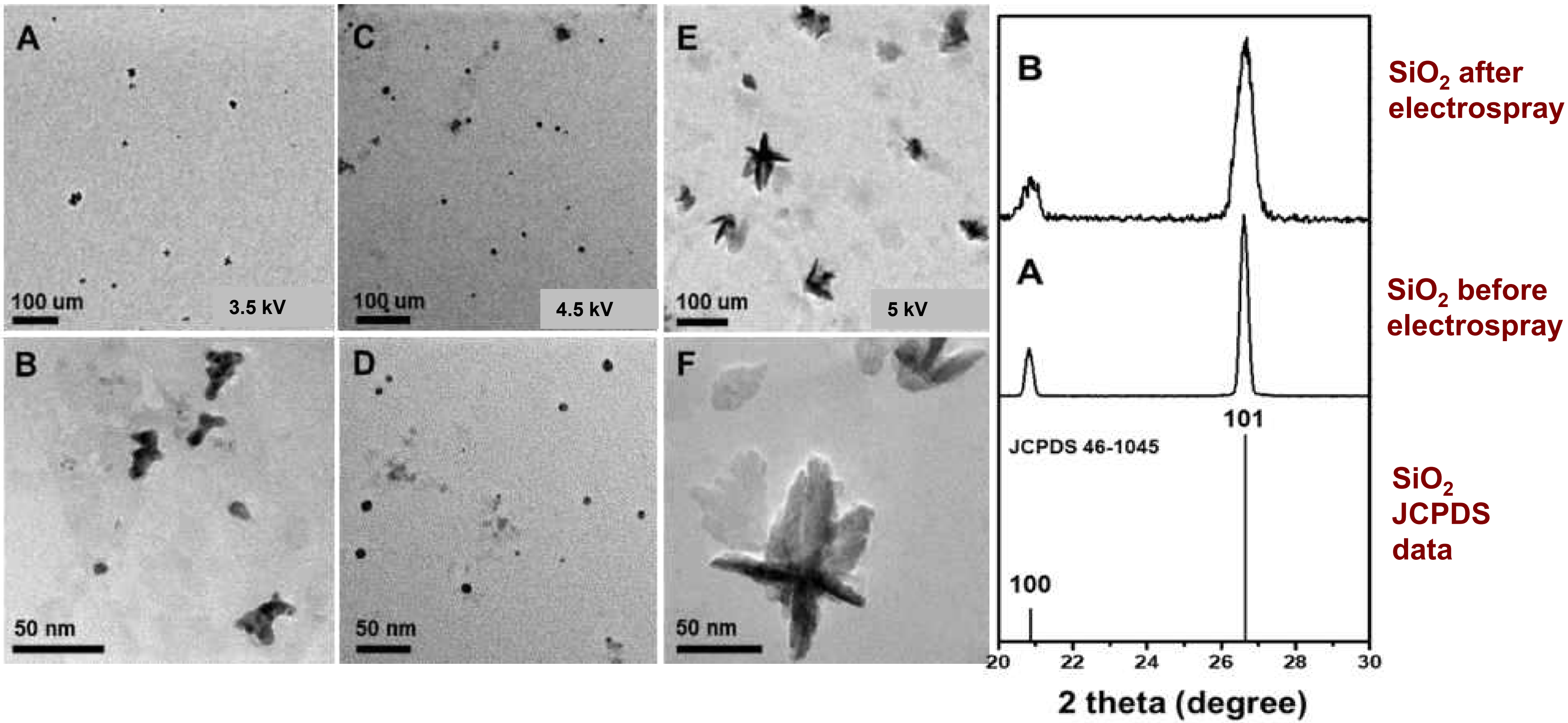

Mechanism: Cleavage

The process of cleavage and surface reconstruction visualized with first-principles simulations

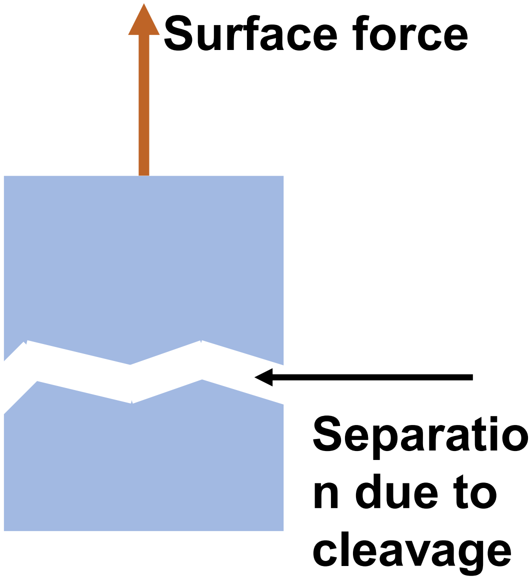

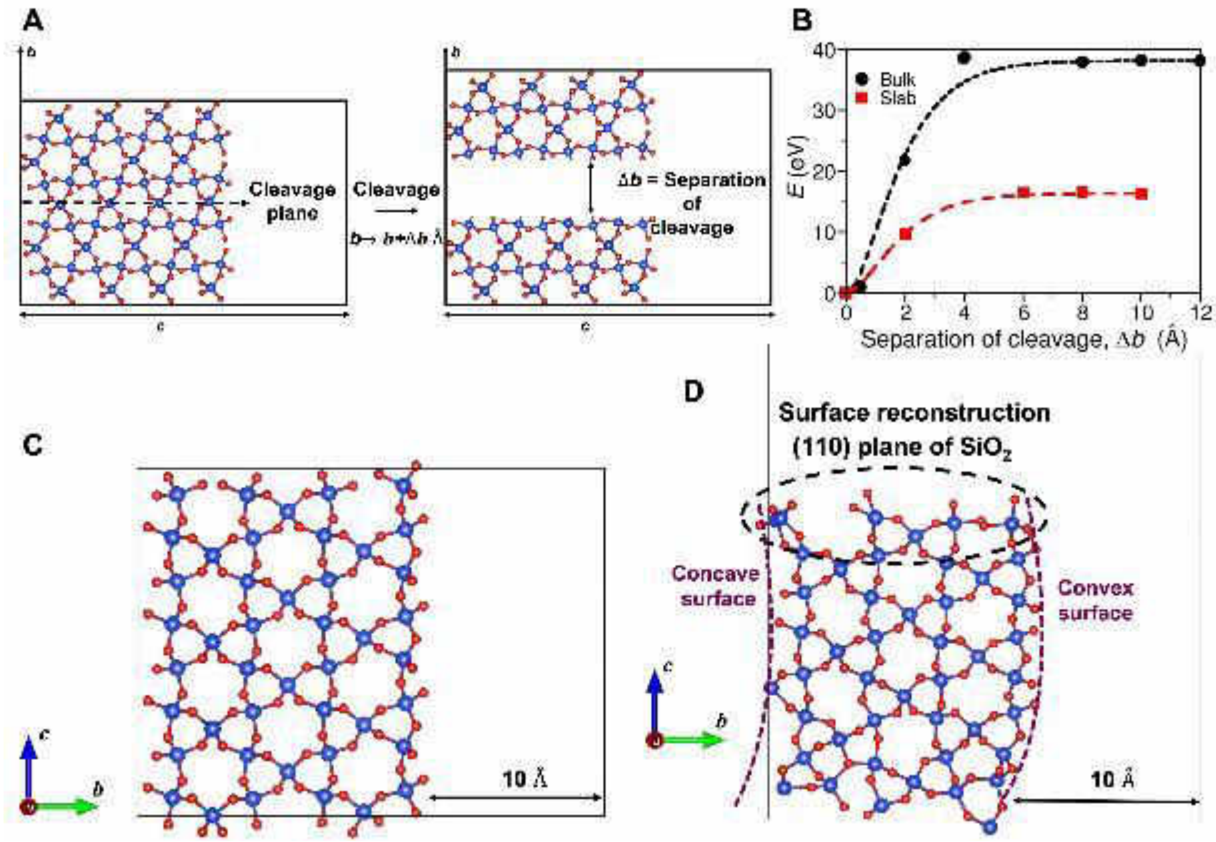

Mechanism: Slip

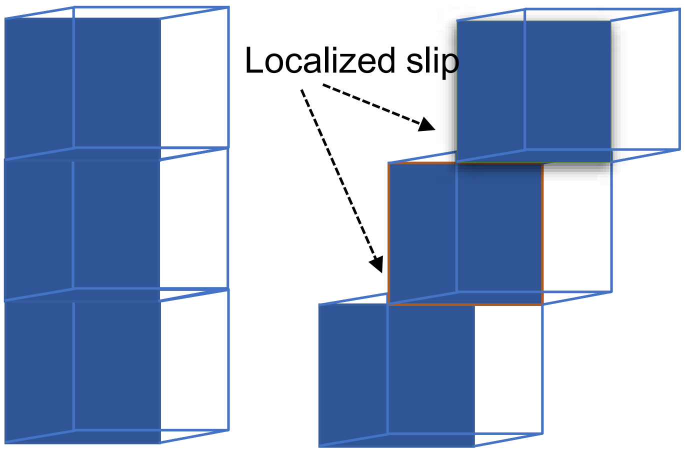

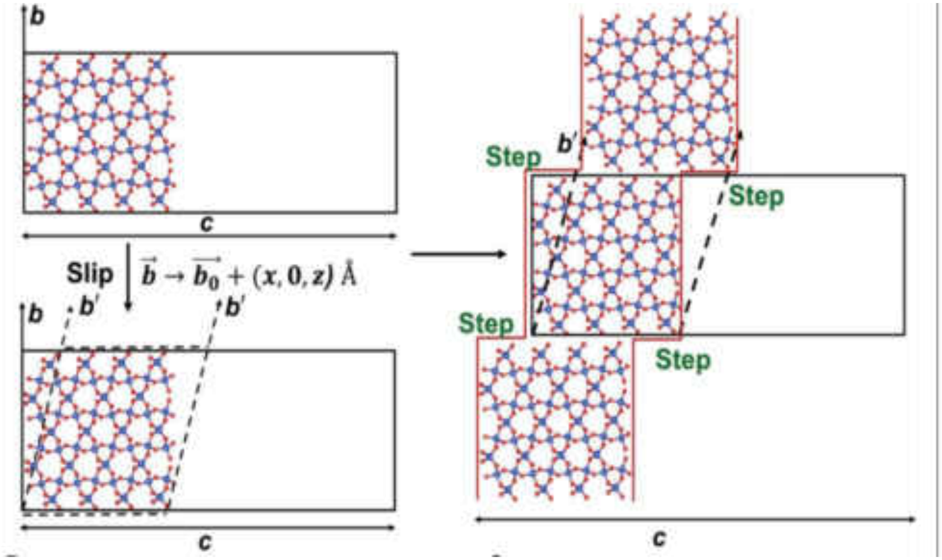

This instability leads to the formation of a stacking fault on the (010) plane, achieved with slip localized at (010) plane

Stacking fault

$\vec{b} \rightarrow \overrightarrow{b_0} + (x, 0, z)$.

(x, z ∈ [0,1]) - fractional coordinates

SFEs of (010) direction with (0, 0), (0, 0.5), (0.5, 0) and (0.5, 0.5) slip configurations on the (110) plane of SiO_2

SFE (J/m^2)	Slab					
	x	z	w/o H-atom	1 H-atom	2 H-atoms	E
	0.0	0.0	0	0	0	0
	0.5	**0.5**	**-1.21**	**-0.93**	**-0.88**	**-1.20**
	0.5	0.0	1.20	1.18	0.90	1.12
	0.0	**0.5**	**-0.07**	**0.89**	**-0.83**	**-0.09**

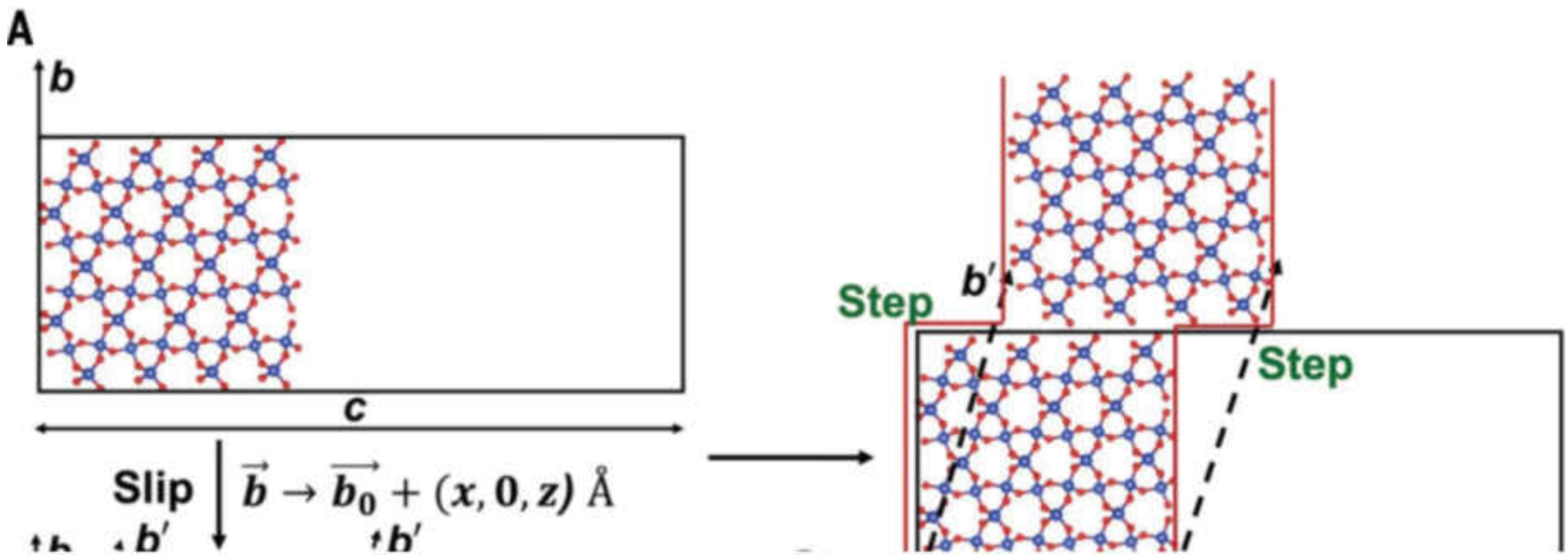

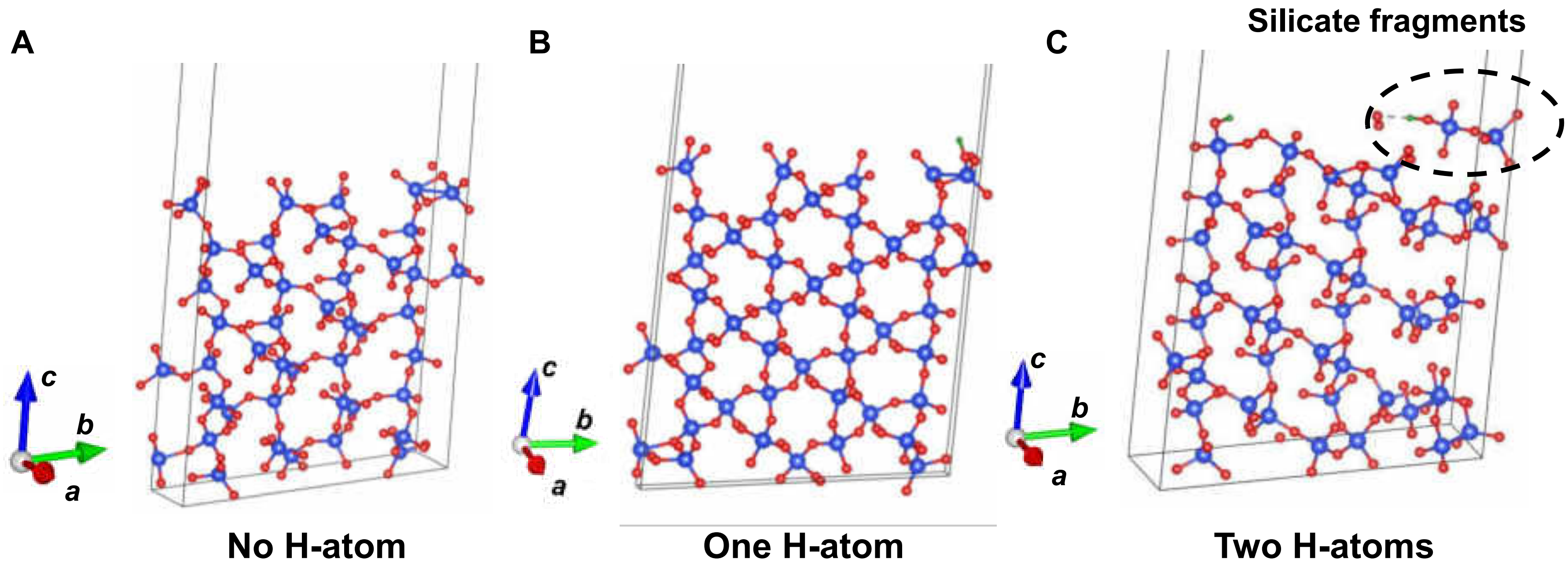
A
B
C
Silicate fragments
c
b
a
No H-atom
One H-atom
Two H-atoms

Mass Spectrometry of the Fragments

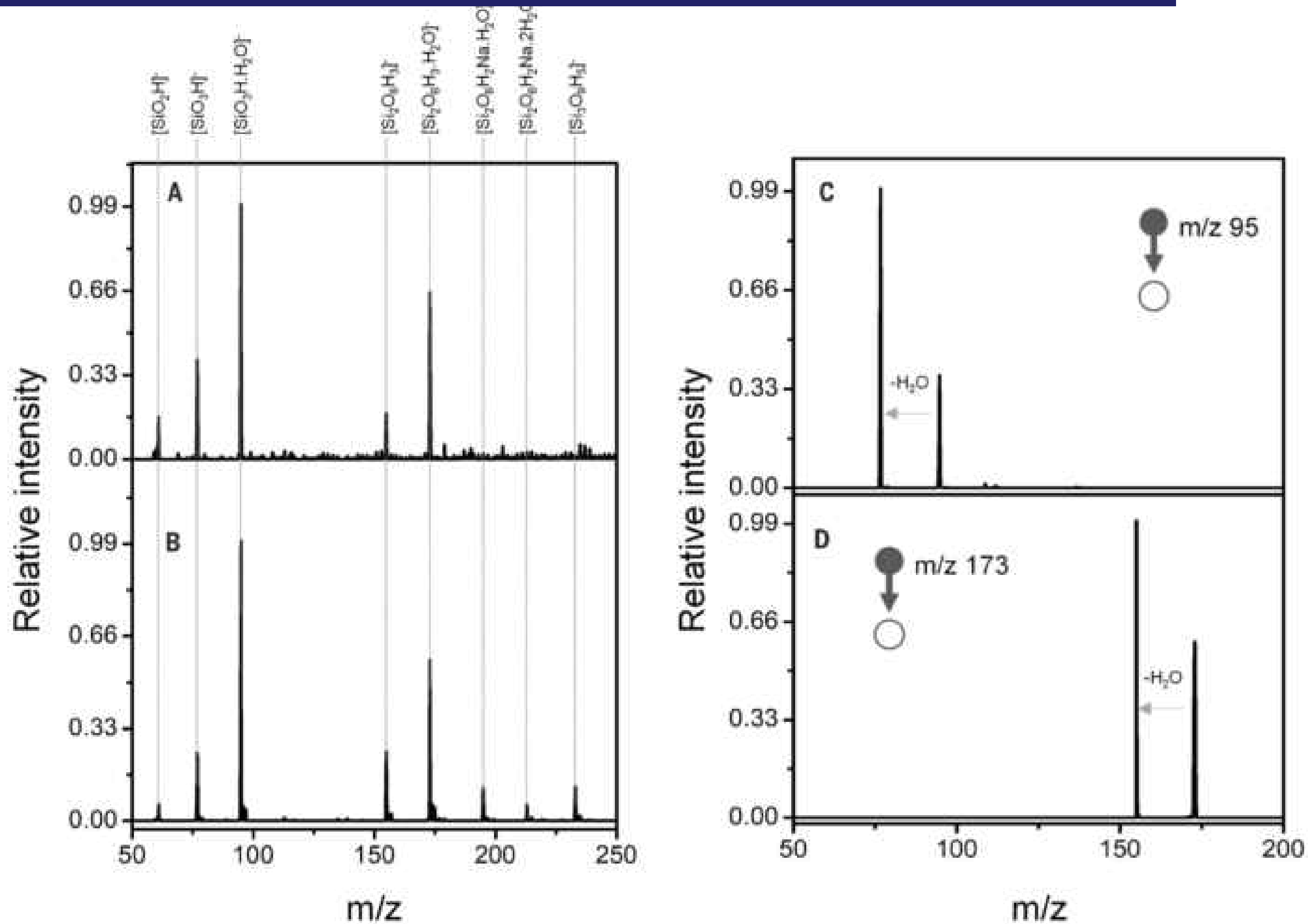

Effect of Charged Microdroplets on Quartz

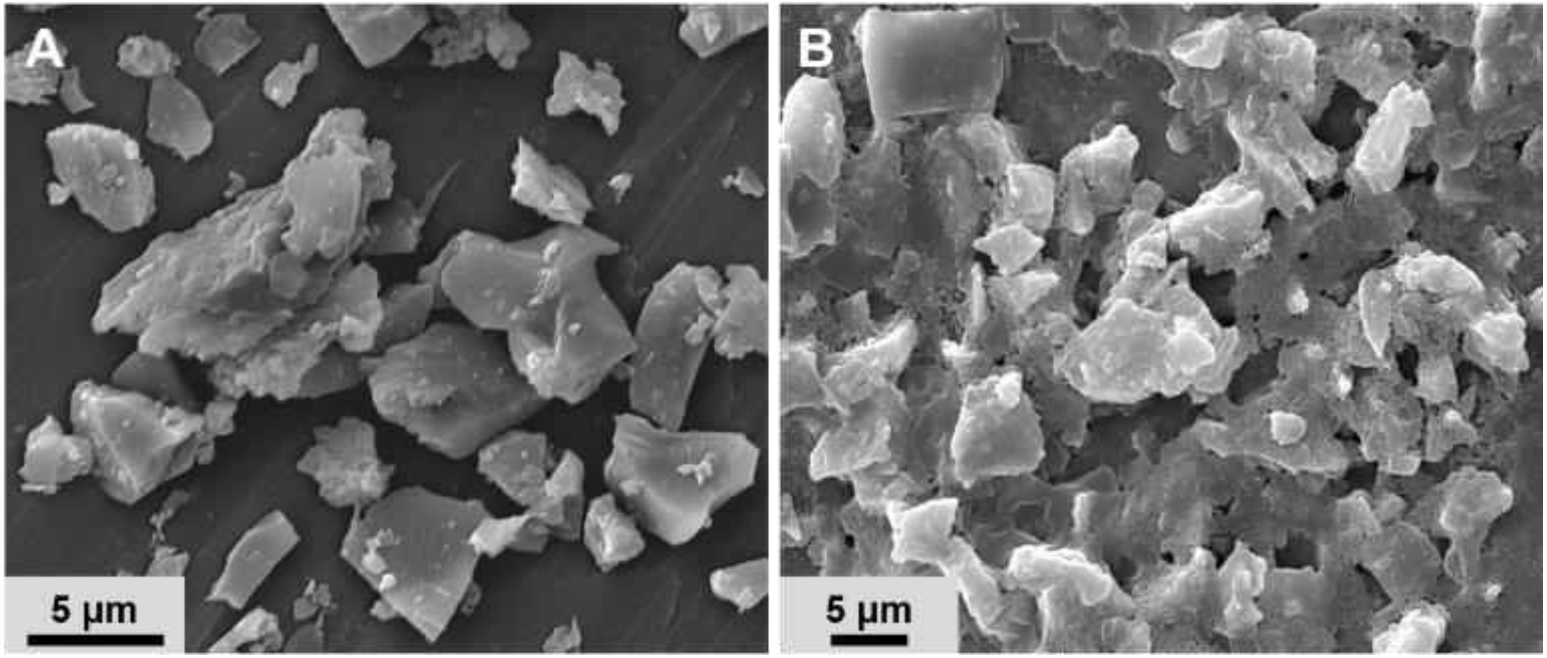

Increased surface roughness after the spray

Mechanism of Nanoparticle Formation

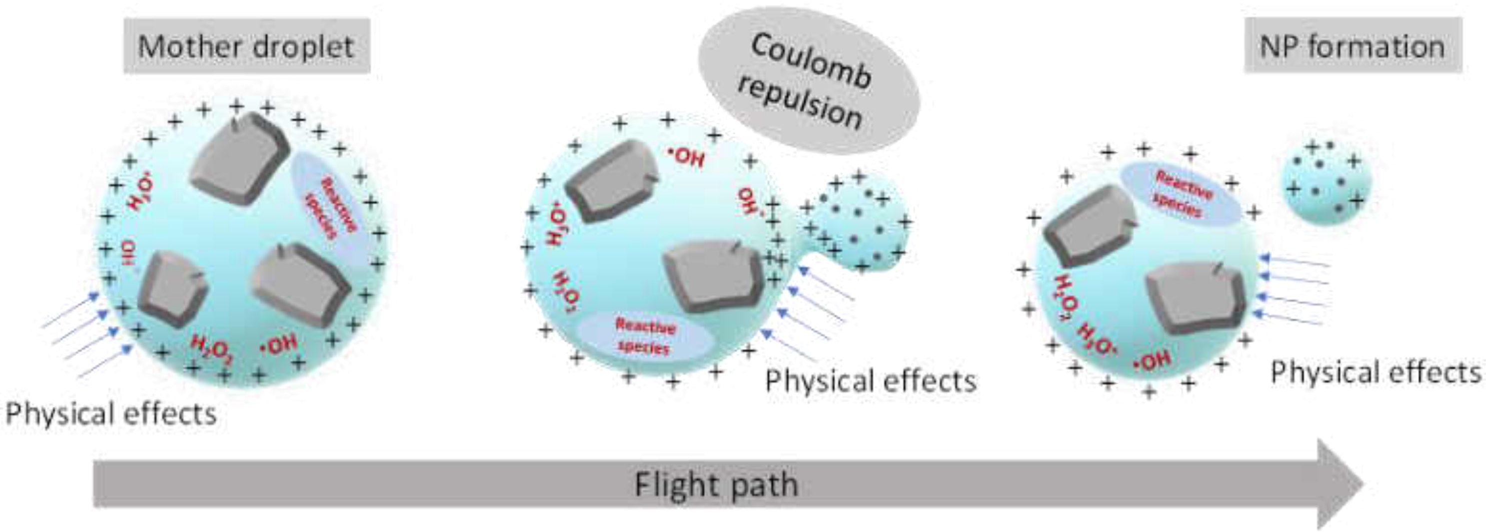

Rayleigh, On the equilibrium of liquid conducting masses charged with electricity, Philosophical Magazine, 1882

$Q = 8\pi\,(\epsilon_0\,\gamma R^3)^{1/2}$

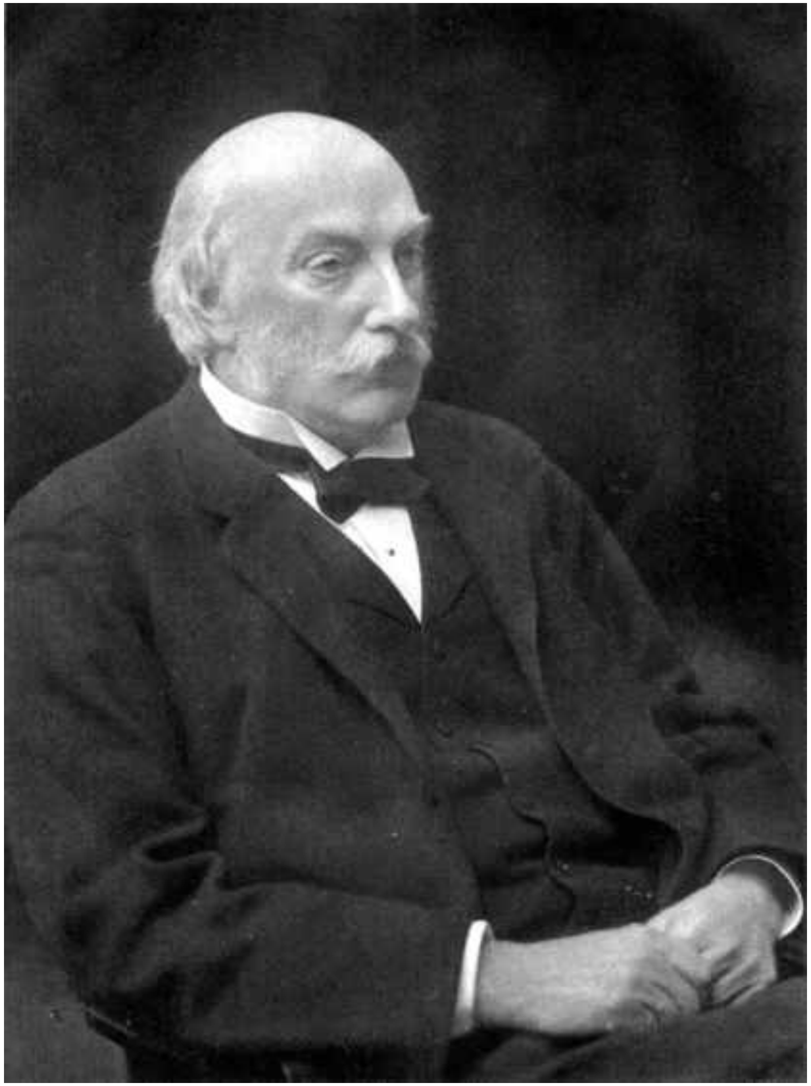

Image from Wikipedia

Understanding Microdroplets

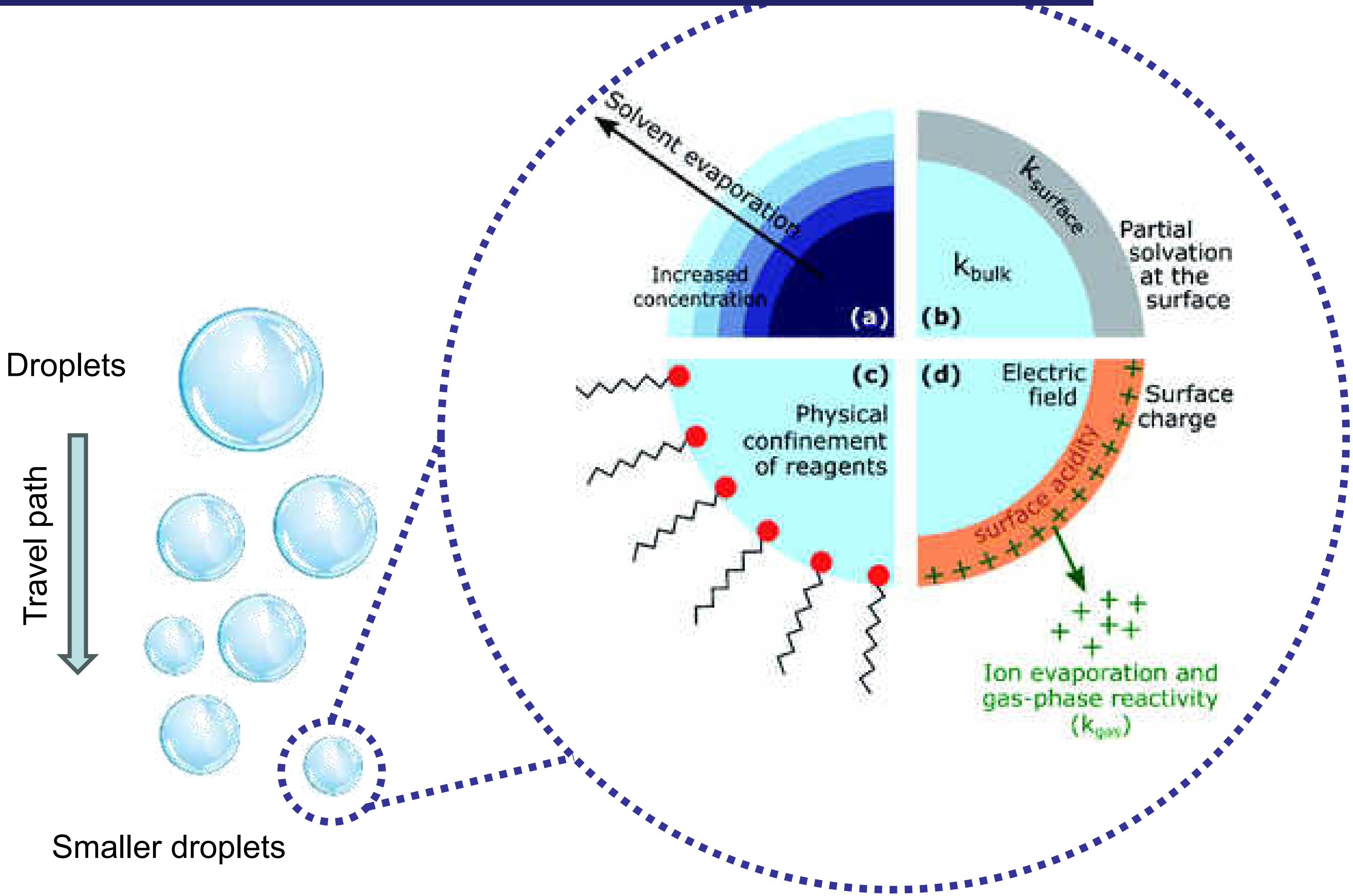

Grazia Rovelli, et. al. *Chem. Sci.*, 2020, 11, 13026–13043.

PERSPECTIVES

CHEMISTRY

Breaking down microdroplet chemistry

Charged microdroplets accelerate mineral disintegration

By **R. Graham Cooks** *and* **Dylan T. Holden**

Charged microdroplets are commonly observed in clouds, sea spray, and other natural aerosols. The chemistry that occurs at the air-water interface of these droplets is often distinct from that observed in bulk solution, which is of considerable interest because chemical reactions can be accelerated at this boundary (*1*, *2*). This may have implications for environmental processes such as the weathering of rocks, which contributes to soil formation. On page 1012 of this issue, Spoorthi *et al*. (*3*) report that micrometer-scale mineral particles can rapidly break down into nanoparticles when in charged aqueous microdroplets (see the figure). This points to a potential role for atmospheric water droplets in the natural disintegration of minerals.

To examine material degradation, Spoorthi *et al*. borrowed methodology used to accelerate bond-forming chemical reactions. By spraying an aqueous suspension of microparticles of natural minerals, the authors produced nanoparticles of minerals in high yield. Specifically, Spoorthi *et al*. used an electrospray device to emit a jet of liquid droplets (by applying high voltage) containing mineral particles of natural quartz, ruby, or synthetic alumina that ranged in size from 1 to 5 μm in diameter. The authors observed the production of nanoparticles that were 5 to 10 nm in diameter. Moreover, the fragmentation occurred in approximately 10 ms.

Such material degradation and chemical synthesis experiments are united by the extremes of chemical reactivity that occur at the air-water interface, where reagents are partially solvated (*4*). Whether formed through nebulization, splashing from a surface, or other means, microdroplet populations will include droplets with nonzero net charges. The small radius of curvature in a microdroplet produces a very strong electric field (*5*) that can support a double layer of electric charge at the air-water interface. The change in geometry (radius of curvature) converts a two-dimensional air-water interface with limited electric field into a sphere with an electric field of a strength approaching the order of chemical bond energies (3 to 4.5 eV/Å). Coulombic fission (the splitting of charged microdroplets due to excess charge overcoming the surface tension) and evaporative processes further increase the surface area, reduce the radius of curvature, and augment the surface electric field of the droplet.

The unusual chemical nature of the air-water interface results in much remarkable chemistry. For example, amino acids in water undergo dehydration to form peptides in this environment (*6*), whereas bulk water simply solvates amino acids. The superacidic interface activates amino acids and removes water to yield peptides. In addition to such acid-base reactions, redox chemistry results from the formation of strong oxidants and reductants from water at the interface. For example, a high hydronium ion (H_3O^+) concentration at the interface derived from fleetingly charged surface water molecules ($H_2O^{\bullet+}/H_2O^{\bullet-}$) coexists with oxidative species such as hydrogen peroxide (H_2O_2) and OH•. These redox species enable a variety of spontaneous chemical transformations, including carbon-oxygen (C–O) bond cleavage in phosphonates, which yields the corresponding phosphonic acid (*7*), and in the Baeyer-Villiger oxidation of aryl ketones to give esters (*8*). These considerations thereby enable simultaneous acid-base and oxidation-reduction chemistry in a single population of droplets (*7*).

Through their study, Spoorthi *et al*. have added natural weathering to a list of processes in which accelerated interfacial microdroplet reactions play an important role. Other processes include those in the atmosphere, both natural and anthropogenic, the latter typified by pollution that involves nitrate photochemistry (*9*). A substantial number of accelerated catalyst-free microdroplet reactions form the basis for chemical syntheses that generate a variety of small molecules (*10*), including the facile and high-throughput functionalization of drugs. This latter approach can be scaled up so that microdroplet reactions produce substantial small-molecule products. Prebiotic chemistry, including peptide and nucleotide formation, is another process that is accelerated at the microdroplet air-water interface (*11*).

The millisecond timescale of quartz degradation reported by Spoorthi *et al*. matches the known microsecond-to-millisecond timescale for accelerated bond-formation and bond-cleavage chemical reactions in microdroplets (*1*). This reinforces the conclusion that the chemical basis for accelerated weathering lies in the powerful acidic and hydrolytic nature of the air-water interface. The authors further suggest a role for the superacid interface in inducing slippage at crystal plane boundaries in quartz and ruby fragmentation. Their simulations show that individual protons inserted into the slip configuration mineral

Micro-to-nano transitions in minerals at the air-water interface

Reactions that promote mineral disintegration are accelerated at the air-water interface of microdoplets. Key reactive species are the result of the effects of a high electric field at the surface of the water droplets.

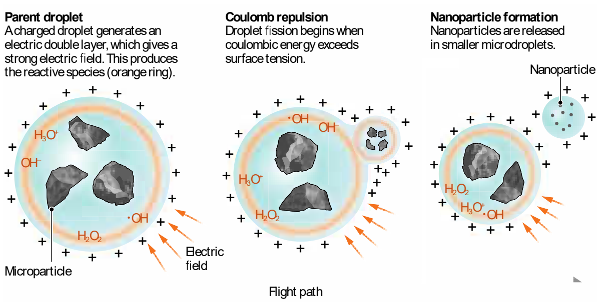

GRAPHIC: K. HOLOSKI/*SCIENCE*

Department of Chemistry, Purdue University, West Lafayette, IN, USA. Email: cooks@purdue.edu

How do They Form?

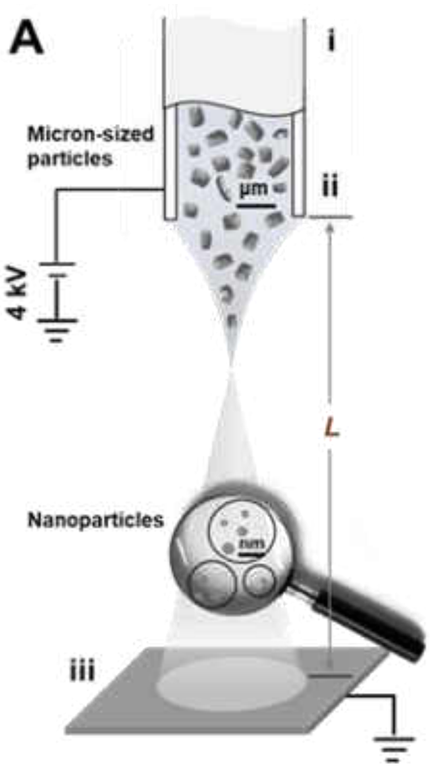

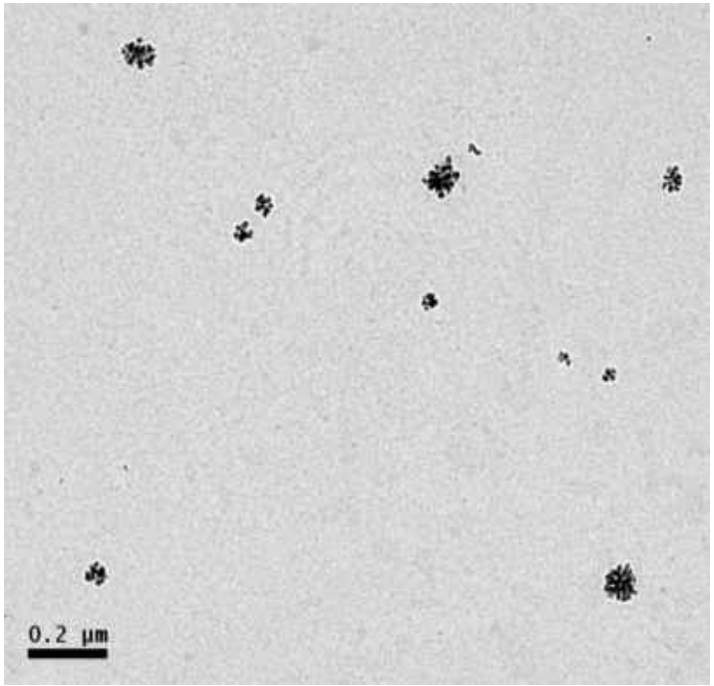

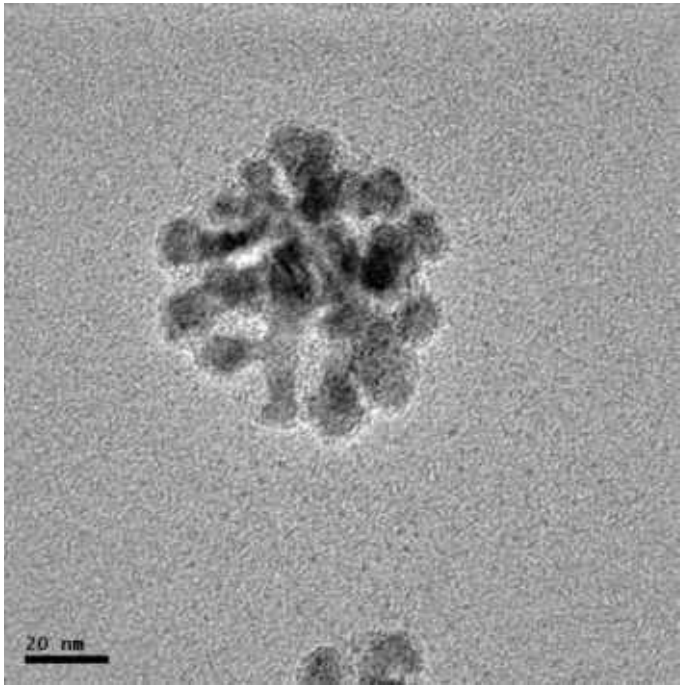

MoS_2 Nanosheets

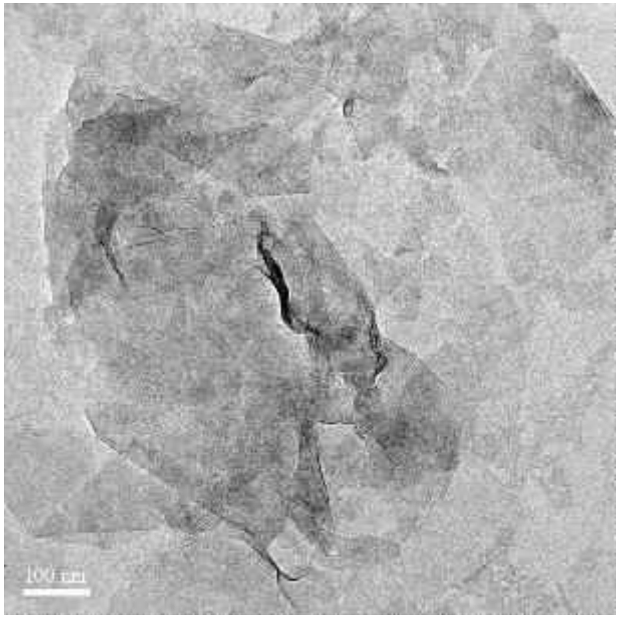

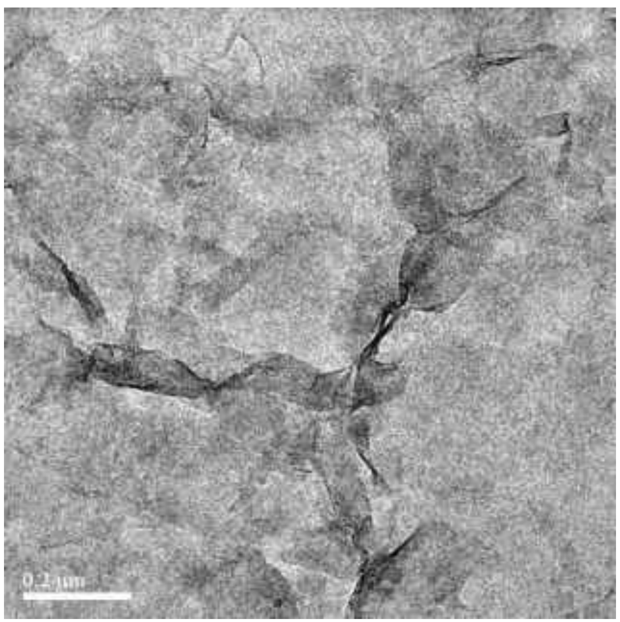

MoS_2 Nanosheet

Ambient electrospray

→

Solvent: Water
Potential: 3.0 kV

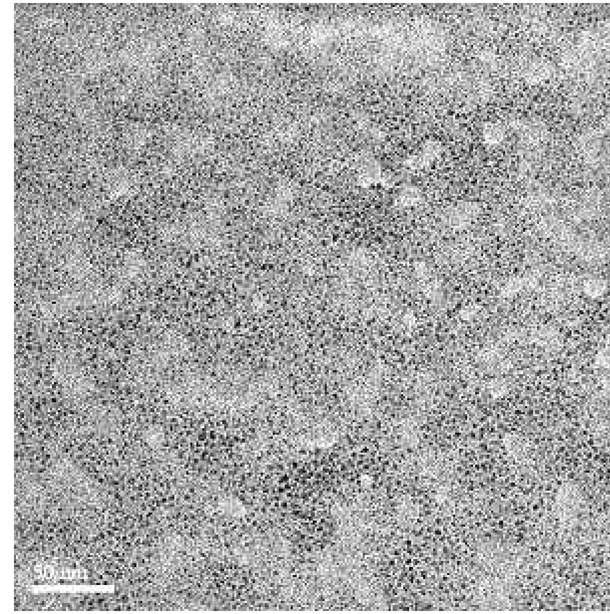

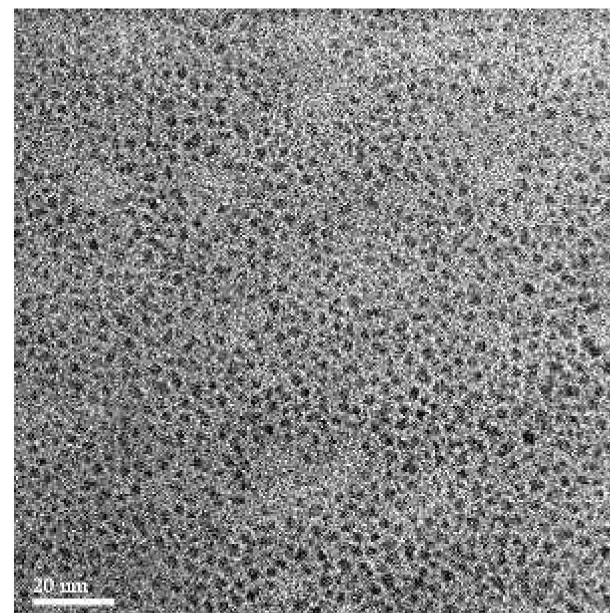

MoS_2 Nanoparticles

Graphene Oxide

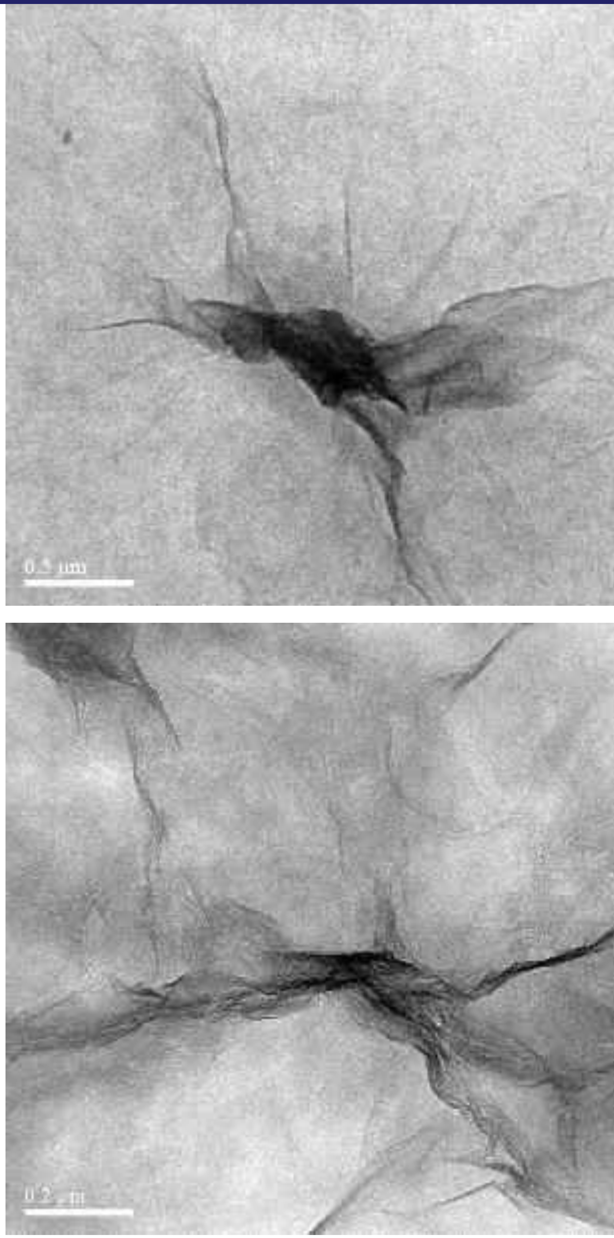

Ambient electrospray

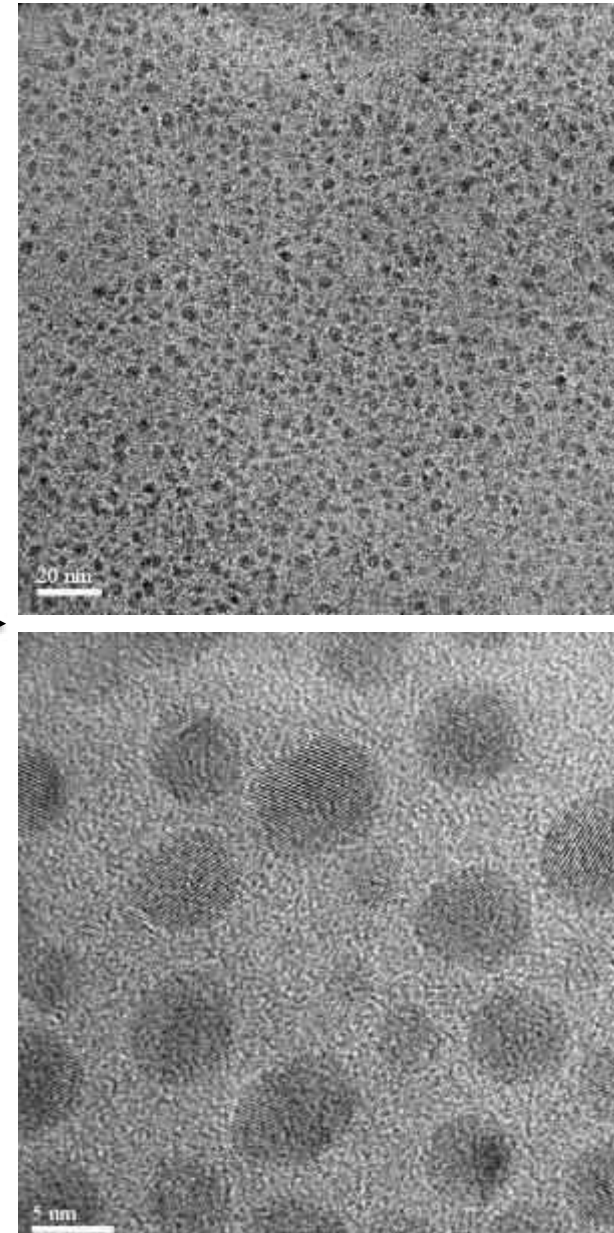

Graphene oxide nanosheet

Graphene oxide nanodiscs

Raman Spectra of MoS_2 and Graphene Oxide Nanosheets

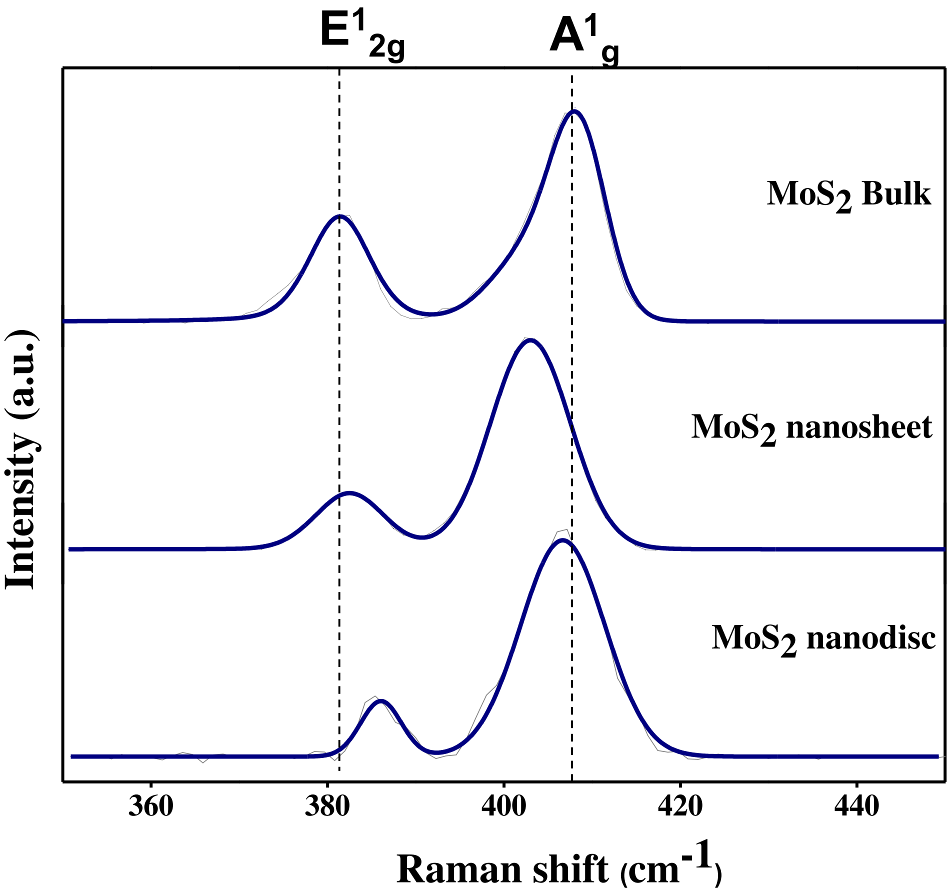

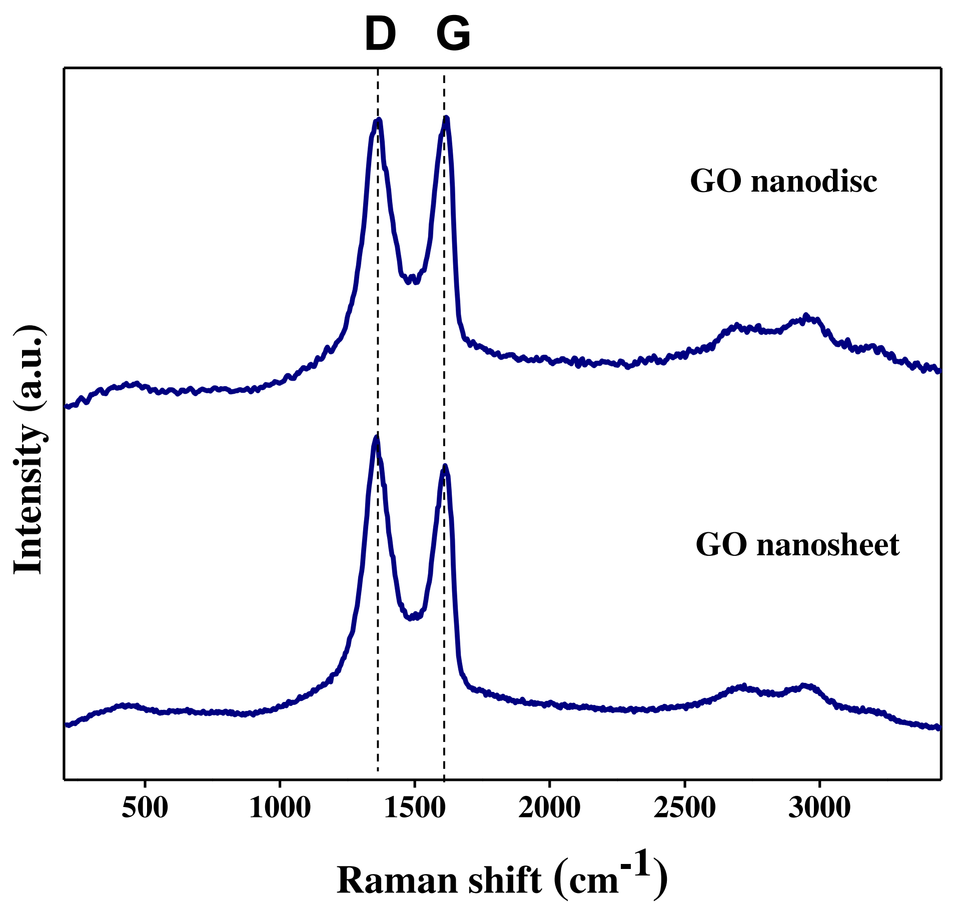

	E^1_{2g} (cm^{-1})	A^1_g (cm^{-1})
Bulk	381.34	407.67
NS	382.88	402.95
ND	386.01	406.67

Relative peak intensity

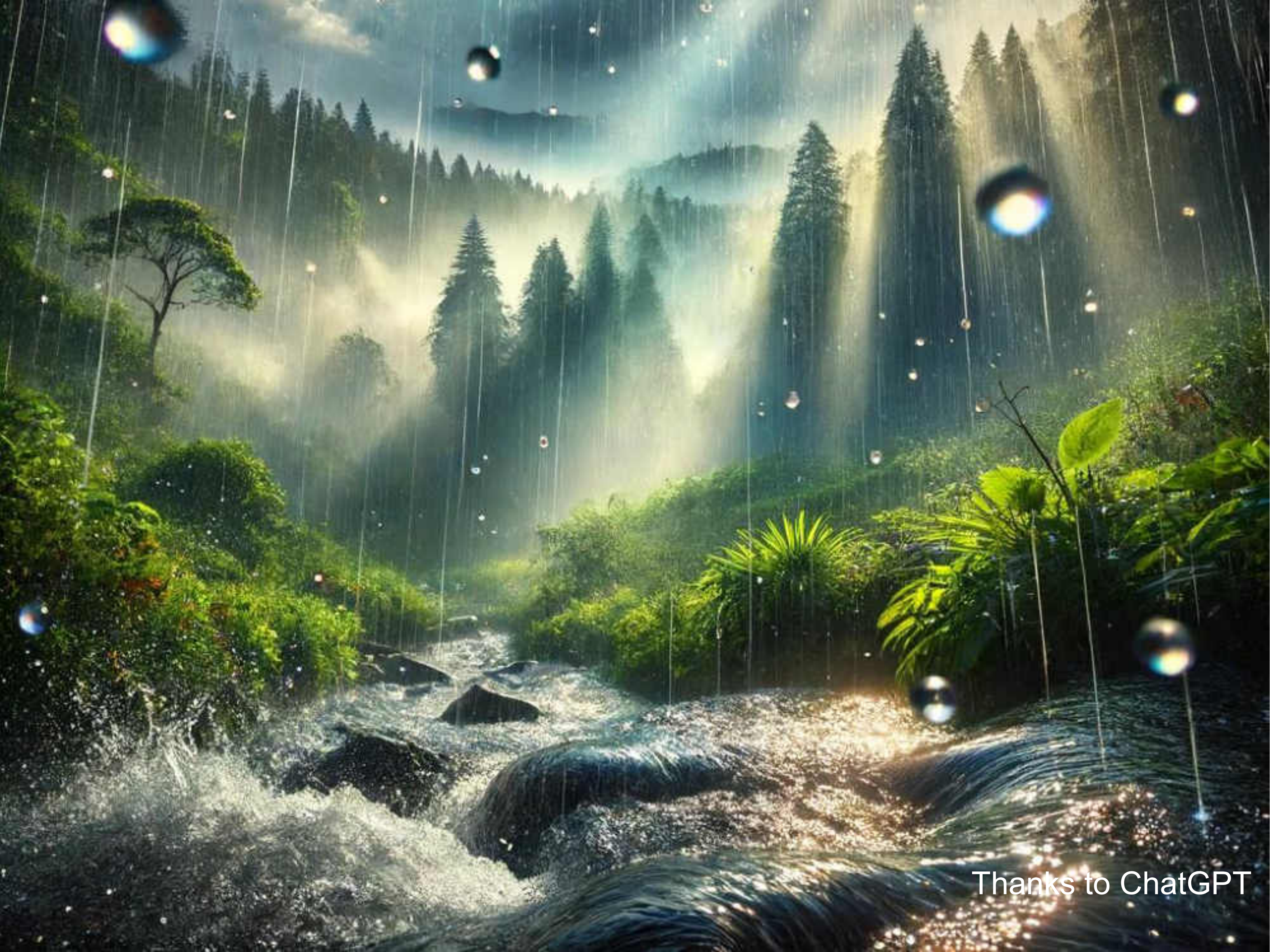
Thanks to ChatGPT

Vision

Make soil using processed wastewater and make deserts bloom.

Thanks to ChatGPT

ESI-MS of $Au_{144}(HT)_{60}$

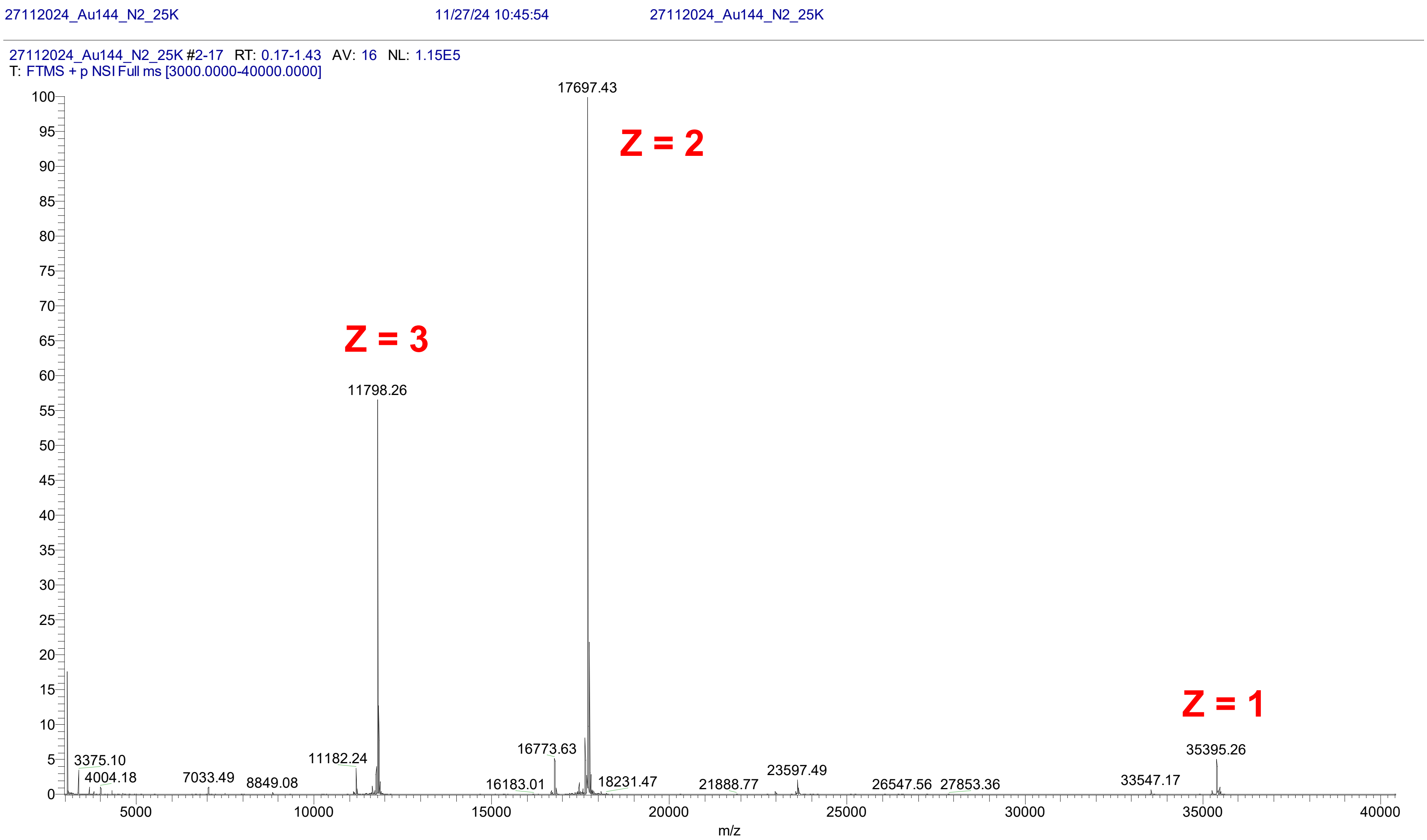

2D classification images

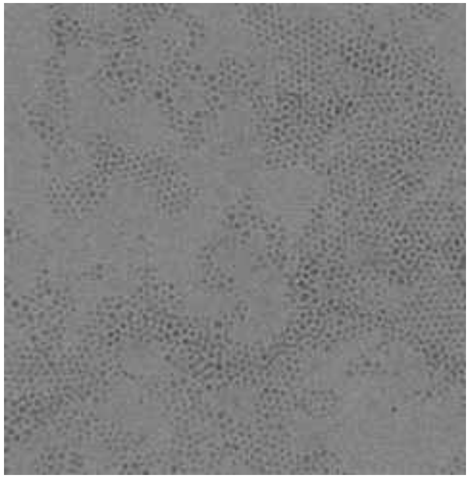

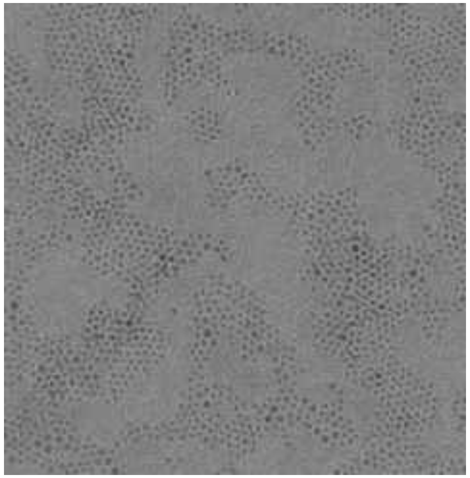

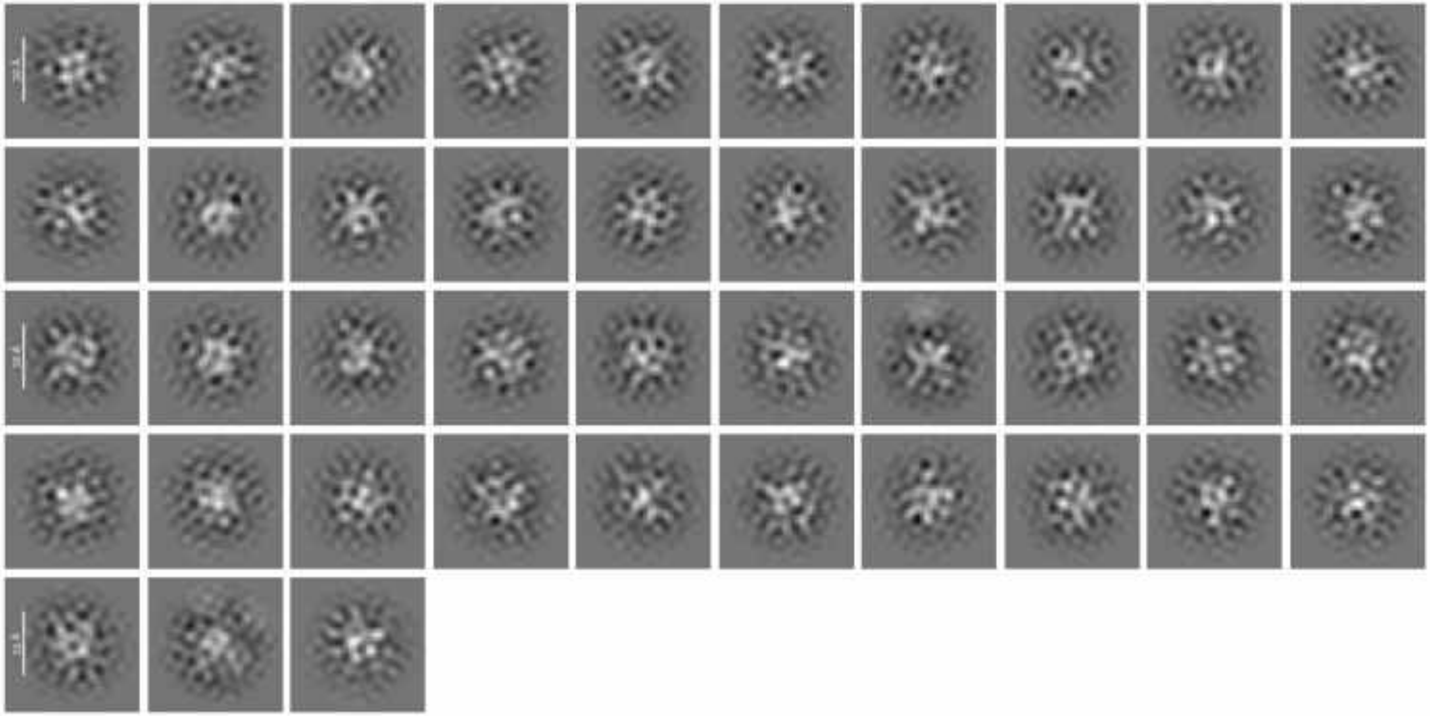


https://www.youtube.com/watch?v=fiJyptbXBtM

International Centre for Clean Water


IIT Madras Research Park

Collaborators

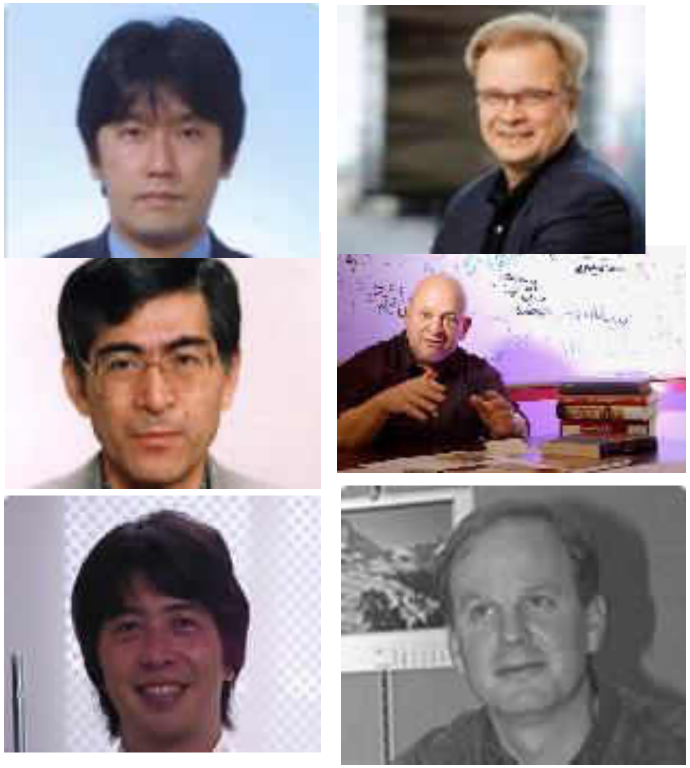

Tatsuya Tsukuda
Keisaku Kimura
Yuichi Negishi
Hannu Hakkinen
Uzi Landman
Rob Whetten
K. Vijayamohanan, Reji Philip, Shiv Khanna

Robin Ras

Nonappa

Tomas Base

Manfred Kappes

Olli Ikkala

Horst Hahn

Biswarup Pathak

K. V. Adarsh

G. U. Kulkarni

Vivek Polshettiwar

Indian Institute of Technology Madras

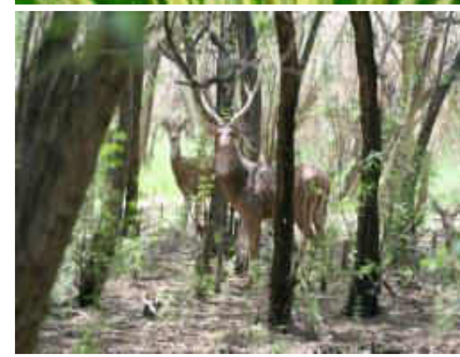

Bhaskar Ramamurthi/V. Kamakoti

Associate Editor

ACS Sustainable Chemistry & Engineering

Pradeep Research Group

Thematic Unit of Excellence